Modeling the Hydrology of the Black Sea Basin and Assessing the Impacts of Climate Change and Land use Change on Water Resources

Elham Rouholahnejad

Diss. ETH No. 21603

Diss. ETH No. 21603

Modeling the Hydrology of the Black Sea Basin and Assessing the Impacts of Climate Change and Land use Change on Water Resources

A thesis submitted to attain the degree of

DOCTOR of SCIENCES of ETH ZURICH

(Dr. sc. ETH Zurich)

presented by

ELHAM ROUHOLAHNEJAD

M.Sc., Civil Engineering - Environment, K.N Toosi University of Technology, Tehran, Iran

Born on 11.09.1983

citizen of Iran

accepted on the recommendation of

Prof. Dr. Rainer Schulin, examiner

Prof. Dr Martin Volk, co-examiner

Prof. Dr Anthony Lehmann, co-examiner

Dr. Karim Abbaspour, co-examiner

2013

SUMMARY

The Black Sea Basin (BSB) is internationally recognized for its ecologically unsustainable development and inadequate resource management leading to severe environmental, social and economical problems. The Black Sea itself is also affected by severe environmental degradation. In 1995, it was rated as being of the highest concern in five out of seven environmental categories, making it the worst of any of the European seas. On the other hand as water resources become further stressed due to increasing levels of societal demand, understanding the effect of climate change on various components of the water cycle is of strategic importance. According to the last IPCC report, there is medium confidence that droughts will intensify in the 21st century in some seasons and areas, due to reduced precipitation and/or increased evapotranspiration. This applies to regions including southern Europe, the Mediterranean region, and central Europe.

The Black Sea Basin lies in a transition zone between the Mediterranean region in an arid climate of North Africa and the temperate and rainy climate of central Europe and it is affected by interactions between mid-latitude and tropical processes. Because of these features, even relatively minor modifications of the general circulation can lead to substantial changes in the Mediterranean climate. This makes the BSB a potentially vulnerable region to climatic changes as induced, for example, by increasing concentrations of greenhouse gases. Indeed, the Mediterranean region has shown large climate shifts in the past and it has been identified as one of the most prominent "hot spots" in future climate change projections.

Land use changes are altering hydrologic systems, which may have potentially large impacts on water resources. Land use change also influences water quality. Hydrologic processes such as evapotranspiration, infiltration, surface runoff and groundwater flow are altered substantially by land use changes. Rapid socio-economic development drives land use changes especially in regions with long land use histories. This is particularly true in Eastern Europe, where the BSB lies, and where the land cover has changed substantially since the breakdown of the USSR in 1990.

The general goal of this study is to assess the impacts of land use and climate change on water resources of BSB at high spatial and temporal resolution. To attain this goal, the specific objectives were: i) to build a high-resolution hydrologic model of the Basin using the Soil Water Assessment Tool (SWAT), ii) design a parallel processing scheme that makes the calibration of such high-resolution model possible, iii) analyze the historic spatio-temporal availability of water resources components, mainly blue water flow, green water flow, and green water storage; iv) assess the severity of impacts of land use change on water balance components using historical information, and v) assess the impact of combined climate and land use changes on future water resources of the BSB.

To obtain the first objective, we used SWAT to model the hydrology of the BSB coupling water quantity, water quality, and crop yield components. The hydrological model was calibrated and validated with sensitivity and uncertainty analysis using SUFI-2. River discharges, nitrate concentrations, and crop yields were used to calibrate the model. A parallel processing scheme was developed to improve calibration computation time as described below. The calibration and validation results were quite satisfactory for a large number of observation stations for both discharge and nitrate loads. We also included crop growth processes for maize, barley, and wheat in the hydrological model with relatively good simulation results. We calculated all components of water resources including river discharge, infiltration, aquifer recharge, soil moisture, and actual and potential evapotranspiration. Furthermore, available water resources were calculated at sub-basin spatial and monthly temporal levels. Based on the results of this study, we showed that given the present technologies, it is possible to build a high resolution model of a large basin and effectively calibrate such detail model. A comprehensive database of the BSB created within the framework of the current study and the meta database became available in the Global Earth Observation (GEO) platform to contribute to fill the existing gaps in water resources data in the region. In the study, we discussed the challenges of building a large-scale model in fine spatial and temporal detail and highlight hotspots of water scarcity and nitrate pollution. The study provided the basis for further research on the impact of climate and land use change on water resources in the BSB.

Distributed hydrologic models are particularly difficult to calibrate because of reasons such as time constraints, difficulties in parameterization, non-uniqueness (having more than one acceptable solution), uncertainties in the conceptual model, and model inputs. In the second part of this study we address the problem of computation time and describe a system where the optimization algorithm, SUFI-2 (Sequential Uncertainty FItting ver. 2) is used in a parallel processing scheme to run on Windows-based computers for higher performance. SUFI-2 is a tool for sensitivity analysis, multi-site calibration, and uncertainty analysis. It lends itself easily to parallelization, and is capable of analyzing a large number of parameters and measured data from many gauging stations simultaneously. The parallel processing scheme developed here utilizes the existing capabilities of the available systems and is ideal for performing hydrologic model calibration and uncertainty analysis. We tested the program with large, medium, and small-size hydrologic models on several computer systems, including PCs, laptops, and servers with up to 24 CPUs. The performance was judged by calculating speedup, efficiency, and CPU usage. Performance results with both small and large size SWAT projects showed that parallel SUFI-2 achieves good speedup and reasonable scalability in most cases. Although the parallel SUFI-2 is designed to be used on any system, larger time savings can be achieved with multiple CPUs and larger RAM memory.

To achieve the third objective, we investigated the impact of historical land use changes on hydrology and water resources components of the BSB. For this purpose, the changes in land cover between the years 2001 and 2008 were identified using MODIS land cover data. There was an increase in forested areas from 19 to 21.3%, and in crop land from 47.2 to 47.4%, in addition to a decrease in crop and natural vegetation from 15.1 to 13.3%, and in shrub lands from 2 to 1.5% of the catchment area during the 7 years period. SWAT was used to assess the impacts of these land use changes between 2001 and 2008. The calibrated hydrologic model using MODIS land use data for 2008 was taken as the reference model. We modified this model by a land use from 2001 using the dynamic land use change module in SWAT where we updated the land use half way through simulation. Our analysis suggested that land use change had minor impacts on long-term averages of water balance components at the watershed or large basins within the BSB. This is due to compensating effects in catchment scale in large complex watersheds. At smaller subbasin scales and at Hydrologic Response Units (HRU) level, however, the impacts of land use change were quantified using delta method and were found to be more significant. To see the differences in water balance component we correlated between land use changes and water cycle components. But as there were multiple land use changes occurring in a subbasin, the changes in water balance could not be directly attributed to specific changes in land use. To overcome this, we analyzed the problem at the HRU level. Our results showed more pronounced changes directly attributable to land use change alone. However, these results could not be upscaled to the subbasin or watershed level. At the HRU level, the results showed that afforestation leads to an increase of evapotranspiration up to 3%, while runoff and water yield do not change significantly. The increase in cropland resulted in an increase in evapotranspiration by up to 5%. Given that these are only a 7 years land use change impacts and the fact that land use considered not to be changing in most hydrologic models, the present study shows the importance of land use update on the accuracy of modeling results. In addition, the study indicates that at the HRU scale, land use change may have important implications for developing better water management practices through a better understanding of system vulnerabilities to change.

In the last part of this study, future climate scenarios for periods of 2013–2050 were generated from the Danish Regional Climate Model (RCM) (HIRHAM) for IPCC's SRES A2 and B2 scenarios. The future climate data were downscaled for 1147 climate stations across the BSB using Delta Method. The two climate scenarios were then applied to the historically calibrated hydrologic model to analyze the effect of future climate on precipitation, blue water, and green water across the BSB for the period of 2013- 2050. Furthermore, four regionalized scenarios were defined for the changes of land use in the BSB based on the IPCC's special report on emissions scenarios (SRES). The land use change scenarios correspond to four marker scenarios representing different global socio-economic development pathways. The combination of future land use and climate change scenarios were then applied in the hydrological model one at the time and their impacts on the hydrology were investigated. While the combination of all scenarios showed decreases in water resources in wet areas in general, analysis of daily rainfall intensities in A2 scenario indicated more frequent and larger-intensity rainfalls in these regions. On average, water resources tend to increase in dry areas and decrease in wet areas as predicted by climate change scenarios. Land use changes showed less significant impact on water resources than climate change.

Overall, this study provides significant insights into Black Sea's freshwater availability and water quality on a subbasin level with a monthly time step. This information is very useful for developing an overview of the actual water resources status and helps to spot regions where an in-depth analysis may be necessary. We show that inherent uncertainties need to be considered, before general conclusions are drawn. Next to land use and climate change analyses, many more applications of the hydrologic model developed in this study could be foreseen such as calculating cross-boundary water transfers as well as transfer of pollutant loads from upstream, and calculation of nitrogen load entering the Sea, etc. Finally, we demonstrated that given the available technology on model building and calibration tools, and the availability of data it is possible to build a large-scale model at high spatial and temporal resolution. Better data availability of course, would help to make model predictions more accurate and uncertainties smaller.

ZUSAMMENFASSUNG

Das Schwarzmeerbecken (BSB, Black Sea Basin) ist international bekannt für seine ökologisch unnachhaltige Entwicklung und sein inadäquates Ressourcenmanagement, welches schwerwiegende ökologische, soziale und ökonomische Probleme verursacht. Das Schwarze Meer ist ebenfalls von einer starken Degradation der Umwelt betroffen. Im Jahr 1995 wurde es in fünf von sieben Umweltkategorien als höchstbedenklich eingestuft, der schlechtesten Bewertung unter den europäischen Meeren.

Durch zunehmenden Druck auf die Wasserressourcen infolge steigender gesellschaftlicher Nachfrage ist das Verständnis der Auswirkungen des Klimawandels auf verschiedene Komponenten des Wasserzyklus von strategischer Bedeutung. Gemäss des letzten IPCC Reports besteht mittlere Zuversicht, dass Dürren im 21. Jahrhundert in einigen Jahreszeiten und Regionen intensiver werden, bedingt durch verringerte Niederschlagsmengen und/oder verstärkte Evapotranspiration. Dies betrifft Regionen in Südeuropa, dem Mittelmeerraum und Zentraleuropa.

Das Schwarzmeerbecken liegt in einer Übergangszone zwischen der Mittelmeerregion und dem ariden Klima Nordafrikas, sowie dem regnerischen Klima Zentraleuropas, welche von Interaktionen zwischen dem Klima der mittleren Breiten und tropischen Klimaprozessen geprägt ist. Aufgrund dieser Gegebenheit können sogar relativ geringe Änderungen in der generellen Zirkulation zu substanziellen Änderungen des mediterranen Klimas führen. Dies macht das BSB zu einer im Bezug auf den Klimawandel potenziell vulnerablen Region, herbeigeführt zum

Beispiel durch steigende Konzentrationen an Klimagasen. Die Mittelmeerregion hat in der Vergangenheit in der Tat grosse klimatische Verschiebungen gezeigt und wurde als einer der prominentesten "Hot-Spots" zukünftiger Klimaprojektionen identifiziert.

Landnutzungänderungen verändern die hydrologischen Systeme mit möglicherweise grossen Auswirkungen auf die Wasserressourcen. Landnutzungänderungen beeinflussen ebenso die Wasserqualität. Hydrologische Prozesse wie Evapotranspiration, Versickerung, Oberflächenabfluss und Grundwasserfluss werden substanziell von Landnutzungsänderungen verändert. Eine schnelle sozio-ökonomische Entwicklung treibt Landnutzungsänderungen vor allem in Regionen mit historischer Landnutzung voran. Dieses ist besonders zutreffend in Osteuropa, wo das Schwarzmeerbecken (BSB) liegt und die Landüberdeckung seit dem Zusammenbruch der UdSSR 1990 substanziell verändert wurde.

Das übergeordnete Ziel dieser Studie ist es, den Einfluss von Landnutzungs- und Klimaänderungen auf die Wasserressourcen des Schwarzmeerbeckens in hoher zeitlicher und räumlicher Auflösung zu beurteilen. Um dieses Ziel zu erreichen, waren die spezifischen Ziele: i) Aufstellen eines hochaufgelösten hydrologischen Modells des Beckens unter Verwendung des Soil Water Assessment Tool (SWAT); ii) Entwickeln einer Herangehensweise zur Parallelverarbeitung und -berechnung, welches die Kalibrierung eines solchen hochaufgelösten Modells ermöglicht; iii) Analysieren der historischen, räumlich-zeitlichen Verfügbarkeit von Wasserressourcenkomponenten, vornehmlich der Menge an blauem und grünem Wasser und der Speicherung grünen Wassers; iv) Beurteilen des Schweregrads der Auswirkungen von Landnutzungsänderungen auf Komponenten der Wasserbilanz unter Verwendung historischer Information und v) Beurteilen der Auswirkungen kombinierter Landnutzungs- und Klimaänderungen auf die zukünftigen Wasserressourcen des BSB.

Um das erste Ziel zu erreichen, verwandten wir das Soil and Water Assessment Tool (SWAT) um die Hydrologie des BSB unter Kopplung von Wasserquantitäts-, Wasserqualitäts- und Ernteertragskomponenten zu modellieren. Das hydrologische Modell des BSB wurde mittels einer Sensitivitäts- und Unsicherheitenanalyse unter Verwendung von SUFI-2 kalibirert und validiert. Gewässerabfluss, Nitratkonzentrationen und Ernteerträge wurden für die Modellkalibrierung verwendet. Eine Herangehensweise zur Parallelverarbeitung und -berechnung wurde entwickelt um die Rechenzeit wie unten beschrieben zu verbessern. Die Kalibrierungs- und Validierungsergebnisse waren recht zufriedenstellend im Falle einer hohen Zahl von Messpunkten, sowohl für den Abfluss als auch für die Stickstofffrachten. Wir berücksichtigten im hydrologischen Modell auch die Wachstumsprozesse für Mais, Gerste und Weizen mit relativ guten Simulationsergebnissen. Wir berechneten alle Komponenten der Wasserrressourcen einschliesslich Gewässerabfluss, Versickerung, Grundwasserneubildung, Bodenfeuchte und die aktuelle und potenzielle Evapotranspiration. Weiterhin wurden die verfügbaren Wasserressourcen räumlich auf Ebene von Teilbecken und monatlicher Zeitauflösung berechnet. Basierend auf den Ergebnissen dieser Studie haben wir gezeigt, dass es mittels vorhandener Technologie möglich ist, ein hochaufgelöstes Model eines großen Beckens aufzustellen und erfolgreich zu kalibrieren. Innerhalb dieser Grundstruktur wurde eine umfassende Datenbank des BSB erstellt und die Metadatenbank wird auf der Global Earth Observation (GEO) Plattform bereitgestellt werden, um bestehende Datenlücken zu Wasserressourcendaten in der Region zu schliessen. In dieser Arbeit diskutieren wir die Herausforderungen beim Aufstellen eines grossskaligen Models mit hohem räumlichen und zeitlichen Detaillierungsgrad und heben Hotspots von Wassermangel und Nitratverschmutzung hervor. Die Studie bildet die Basis für weitere Forschung im Bezug auf Auswirkungen des Klima- und Landnutzungswandels auf die Wasserressourcen im BSB.

Flächendifferenzierte hydrologische Modelle sind aufgrund von Zeitbeschränkungen, Parameterisierungsschwierigkeiten, Uneindeutigkeit (mehr als eine akzeptable Lösung) sowie Unsicherheiten des konzeptuellen Models und der Modelleingangsgrössen besonders schwierig zu kalibrieren. Im ersten Teil dieser Studie gehen wir das Problem der Rechenzeit an und beschreiben ein System, in dem ein Optimierungsalgorithmus, SUFI-2 (Sequential Uncertainty Fitting version 2), in einer parallelen Berechnungsroutine für eine höhere Leistung bei Windows-basierten Computern verwendet wird. SUFI-2 ist ein Werkzeug für die Sensitivitätsanalyse, gleichzeitige Kalibrierung verschiedener Gebiete und die Unsicherheitenanalyse. Es bietet sich für die Parallelisierung an und ist in der Lage eine grosse Zahl von

Parametern und Messdaten von vielen Messstationen gleichzeitig zu analysieren. Die hierin entwickelte Herangehensweise für die Parallelverarbeitung verwendet bestehende Fähigkeiten vorhandener Systeme und ist ideal für die Kalibrierung und Unsicherheitenanalyse hydrologischer Modelle. Wir haben das Programm für grosse, mittelgrosse und kleine hydrologische Modelle auf verschiedenen Computersystemen inklusive PCs, Laptops und Servers mit bis zu 24 CPUs getestet. Die Leistung wurde anhand der Beschleunigung der Berechnung, Effizienz und CPU-Auslastung bewertet. Ergebnisse mit sowohl kleinen und grossen SWAT-Projekten zeigen, dass ein parallelisiertes SUFI-2 in den meisten Fällen eine gute Beschleunigung und sinnvolle Skalierbarkeit bewirkt. Obwohl das parallelisierte SUFI-2 für jegliche Art Computersystem vorgesehen ist, konnten grössere Zeitersparnisse auf Rechnern mit mehreren CPUs und grösserem Arbeitsspeicher erzielt werden.

Für die Erreichung des dritten Ziels erforschten wir den Einfluss historischer Landnutzungsänderungen auf die Hydrologie und Wasserressourcenkomponenten des BSB. Hierfür wurden die Änderungen in der Landbedeckung zwischen den Jahren 2001 und 2008 anhand von MODIS Landnutzungsdaten identifiziert. Während der Siebenjahresperiode wurde im Einzugsgebiet ein schrittweiser Anstieg bewaldeter Flächen von 19 auf 21.3% und von Ackerflächen von 47.2 auf 47.4% beobachtet, zusammen mit einem schrittweisen Rückgang an Feldern und natürlicher Vegetation von 15.1 auf 13.3% sowie von 2 auf 1.5% des Buschlands. SWAT wurde verwendet um die Auswirkungen von Landnutzungsänderungen zwischen 2001 und 2008 zu bewerten. Insbesondere haben wir das Ausmass der Einwirkungen einer dynamischen Umsetzung der Landnutzung auf die bessere Berücksichtigung der beobachteten Abflüsse in einer grossskaligen Anwendung erforscht. Das kalibrierte hydrologische Modell unter Verwendung von MODIS Land use 2008 wurde als Referenzmodell genutzt. Dieses Modell wurde mittels des dynamischen Landnutzungsänderungs-Models in SWAT hin zu einer Landnutzung von 2001 modifiziert, in dem die Landnutzung innerhalb des Simulationszeitraums angepasst wurde. Unsere Analyse zeigte, dass die Landnutzungsänderung geringe Auswirkungen auf die langfristigen Mittel der Wasserbilanzkomponenten innerhalb von Einzugsgebieten oder grossen Becken innerhalb des BSB haben. Dieses ist bedingt durch sich kompensierende Effekte auf Einzugsbereichsebene innerhalb eines grossen und komplexen Einzugsgebiets. Auf kleinerer Einzugsgebietsebene und auf HRU (hydrologic response unit)- Ebene hingegen waren die mittels der Delta-Methode quantifizierten Auswirkungen der Landnutzungsänderungen signifikanter. Um Unterschiede zwischen den Wasserbilanzkomponenten zu erkennen, korrelierten wir Landnutzungsänderungen und Wasserbilanzkomponenten. Aufgrund vieler Landnutzungsänderungen auf Teileinzugsgebietsebene konnten die Wasserbilanzänderungen nicht direkt einzelnen Landnutzungsänderungen zugeordnet werden. Um dies zu überwinden analysierten wir das Problem auf HRU-Ebene. Unsere Resultate zeigen deutlichere Änderungen, die direkt den Landnutzungsänderungen zugeordnet werden können. Trotzdem konnten diese Ergebnisse nicht auf den Einzugsbereich oder auf Teileinzugsgebietebene hochskaliert werden. Auf HRU-Ebene zeigten die Resultate, dass Aufforstung zu einer erhöhten Evapotranspiration von bis zu 3% führt, während der Abfluss und das Wasserdargebot sich nicht signifikant verändern. Die Zunahme an Ackerland führte zu einem Anstieg der Evapotranspiration bis zu 5%. In Anbetracht dieser Auswirkungen von Landnutzungsänderungen während lediglich 7 Jahren und der Tatsache, dass Landnutzungsänderungen in den meisten hydrologischen Modellen als unveränderlich angenommen werden, zeigt die vorliegende Studie die Bedeutung der Anpassung der Landnutzung für die Genauigkeit der Ergebnisse. Zusätzlich zeigt die Studie, dass Landnutzungsänderungen auf HRU-Ebene und ein verbessertes Verständnis der Systemvulnerabilitäten hinsichtlich Änderungen eine wichtige Bedeutung für die Entwicklung besserer Wassermanagementpraktiken haben.

Im letzten Teil dieser Arbeit wurden zukünftige Klimaszenarien für die Periode 2013-2050 des Dänischen Regionalen Klimamodells (Danish Regional Climate Model, RCM) (HIRHAM) für die IPCC-SRES A2 und B2 Szenarien entwickelt. Das zukünftige Klima wurde auf Ebene von 1147 Klimastationen innerhalb des BSB unter Verwendung der Delta-Methode herabskaliert. Die beiden Klimaszenarien wurden dann in den historisch kalibrierten hydrologischen Modellen verwendet, um den Effekt des zukünftigen Klimas auf den Niederschlag, blaues Wasser und grünes Wasser innerhalb des BSB für die Periode 2013-2050 zu analysieren. Die vier regionalisierten Szenarien wurden weiterhin speziell für die Landnutzungsänderungen im BSB basierend auf dem IPCC SRES (special report on emissions scenarios) definiert. Die Landnutzungsszenarien stehen für vier verschiedene Wege der globalen, sozio-ökonomischen Entwicklung. Die Verbindung zukünftiger Landnutzungs- und Klimaszenarien und deren Auswirkungen wurden daraufhin nacheinander im hydrologischen Modell untersucht. Während die Kombination aller Szenarien allgemein abnehmende Wasserressourcen in Feuchtgebieten aufzeigen, deutet die Analyse täglicher Regenintensitäten im HS1-Szenario auf häufigere und intensivere Regenereignisse in diesen Regionen hin. Im Durchschnitt nehmen die Wasserressourcen in Trockengebieten tendenziell zu und in Trockengebieten ab, wie von den Klimaszenarien vorhergesagt. Landnutzungsänderungen zeigten weniger signifikante Auswirkungen auf die Wasserressourcen im Vergleich zu Klimaänderungen.

Insgesamt gibt diese Arbeit signifikante Einblicke in die Süsswasservorkommnisse und Wasserqualität des Schwarzen Meers auf Teileinzugsgebietsebene bei monatlicher zeitlicher Auflösung. Diese Information ist sehr nützlich für die Entwicklung einer Übersicht des aktuellen Zustands der Wasserressourcen und hilft Regionen zu erkennen, in denen eine vertiefte Analyse nötig wäre. Wir zeigen, dass inhärente Unsicherheiten berücksichtigt werden müssen bevor generelle Schlüsse gezogen werden können. Zusätzlich zu den Analysen über Landnutzungs- und Klimaänderungen könnten viele weitere Anwendungen des in dieser Arbeit entwickelten hydrologischen Modells vorgesehen werden, wie zum Beispiel die Berechnung grenzüberschreitender Wassertransfers ebenso wie der Transfer von Schadstofffrachten vom Oberlauf und die Berechnung der zufliessenden **Stickstofffrachten** im Schwarzen Meer usw. Wir zeigten schliesslich, dass es mittels der vorhandenen Technologie an Modellentwicklungs- und Kalibrierungswerkzeugen und der vorhandenen Daten möglich ist, grosskalige Modelle in hoher räumlicher und zeitlicher Auflösung zu erstellen. Eine bessere Datenverfügbarkeit wäre selbstverständlich hilfreich zur Verbesserung der Genauigkeit der Modellvorhersagen und zur Verringerung der Unsicherheiten.

Acknowledgements

During my stay in Switzerland in the last four years, I had the luxury to study at the world class university ETH, work in a stimulating scientific working group at Eawag, meet a lot of interesting people from around the world and have the chance to enjoy the beautiful unique nature of Switzerland. I am grateful to the chance given to me and for the things I've learned during this time. I take this opportunity to sincerely thank people who made an enormous difference in my life, each of whom were a part of this experience and without them it would have been impossible to finish this work successfully.

First and foremost I would like to express my sincerest gratitude to my supervisor, Dr. Karim Abbaspour, for providing me with the opportunity of doing this research, sharing his knowledge along the way and his trust in allowing me the room to work on my own. He has not only been my greatest teacher, but also an spiritual support shedding light into my life journey. I can't be thankful enough to his time and patience walking me through some of the most amazing times of my life.

My sincere thanks goes to my ETH supervisor, Prof. Dr. Rainer Schulin, and to the Soil Protection group at Environmental Science Department, for all the scientific supports during my PhD. I will also never forget all the fun we had in the group excursions, skiing, hiking, running in the beautiful Switzerland.

I would like to thank Dr. Martin Volk as my PhD examination committee member for his constructive reviews on my thesis. In addition I am grateful to Dr. Bernhard Wehrli for chairing the examination session.

I would like to thank Dr. Anthony Lehmann and the management team in EnvirGrids project for offering financial supports, and organizing inspiring meetings in the last four years. I would like to thank enviroGrids partners for data collection, data sharing and feedbacks on my work.

I want to specially thank Dr. Srinivasan for his unique instant way of support and for hosting me as an exchange scientist at Texas A&M university in US and Eco Lab in Toulouse, France. Without his technical support, it would have been impossible to tackle the difficulties of this modeling work.

I would like to show my appreciation to the administration team, Karin Gilardi, Jadranka Vögelin, and Sandra Egler who enhanced my stay in Switzerland.

This dissertation is a computationally demanding modeling work, and I was fortunate enough to have the support of helpful and knowledgeable people at Eawag IT Department. Many thanks to Canan, Franz, and Raoul.

I thank Siam group head, Peter Reichert and my fellow labmates in Siam for the stimulating scientific and personal discussions, for the sleepless nights we were working together before deadlines, and for all the fun we have had in the last four years: Lisa, Anne, Nele, Carlo, Bahare, Jacqueline, Emaanuelle, Mira, David, Cedric, Amael, Hong, Saeed, Jose, Christian, Christine, Marco, Alexandre, Jenifer, Sören, Ruth, Hans Peter, Judit, Jaffet among others. Special thanks to Rosi for GIS technical support and Marrio Schirmer at W+T.

I would like to thank Lisa once more for being a true friend all these years. I appreciate a lot all we went through from our personal follow ups, meetings, and travels to her assistance in translating the summary of this work among many other things. Thank you Lisa!

I am lucky that I have met many people from all over the world and develop some valuable friendships. I would like to thank my international friends: Jose, Phillippe, Roger, Jaffet, Anouh, Inno, Cristoffel, Florian, Anja, Anna, Behnam, Stefano, Tim, Bas, Vidhya, Jana, and Fabian for all being a part of my life during these four years.

Many thanks goes to my friends outside work who I enjoyed most spending time with Abdolah, Saeed, Saba, Ehsan, Fereshte, Rezvan, Mohamad, Zahra, and Davood. I appreciate a lot the in depth discussions with Samira, Mahmoud, Peyman, Farzane, Haniye, and Farhad. You can't imagine how much I've learned from you. Thank you for the unique moments you made!

I would like to thank my family: my parents for what they are, the trust they have in my dreams and the love and support they always endow. I am grateful to my elder sister, Fereshteh as a pioneer in many aspects of my life and my twin sisters Fatemeh & Hanieh as their presence is my true reason of encouragement.

Last but not the least, I would like to thank a person whose companionship, and endless kindness and love was inspiring in pursuing my goals and advocating in the gloomy obscure days. Maysam is truly the one who reads every bit of me! I can never thank you enough Maysam!

Contents

1. Introduction

1.1 Background and motivation

According to the German Advisory Council on Global Change (WBGU), the Black Sea is likely to experience (i) degradation of freshwater resources; (ii) increase in storm and flood disasters; (iii) decline in food production; and (iv) environmentally-induced migration [WBGU, 2007]. In addition, transboundary pollution effects (TPE) can be expected with respect to all economic sectors [Paleari, 2005].

Previous researches, that addressed water quantity and water quality in the Black Sea Basin (BSB) include a few global and regional studies. WaterGAP2 [Alcamo et al., 2003; Döll et al., 2003] is a global model for water availability and water use. This model focuses on global hydrology at grid scale (30 arc min) considering 3,565 major basins in the world with drainage areas greater than 2,500 km^2. The model was initially used to estimate the water availability and demand and provides relatively limited water cycle-related components. In WaterGAP3 [Aus der Beek et al., 2012], a regional version of the WaterGAP2, hydrological fluxes draining into Mediterranean and Black Sea were modeled with improved spatial resolution (5 arc min) and inclusion of snow melt and water use components. However, results using WaterGAP3 and WaterGAP2 were not significantly different in the BSB [Aus der Beek et al., 2012]. Furthermore, discharges of water and nutrients to the Mediterranean and Black Sea are reported in a study by Ludwig et al. [2009] for major rivers. Next to the above mentioned studies, there are a few other investigations on the status of major river basins in the BSB [Sukhodolov et al., 2009; Sommerwerk et al., 2009; Wolfram and Bach, 2009]. However, often average loads entering the Sea are reported without adequate spatial and temporal resolution on the current and future freshwater availability for the entire BSB. General shortcomings of the previous studies are: missing details on model inputs and outputs, coarse spatial resolution and scale of the models, and missing model calibration/validation and uncertainty analysis. Another major limitations of available estimations are their focus on the countries directly bordering the Black Sea rather than the entire BSB while new modeling tools allow high resolution and more accurate estimations of all water components on very large areas.

There are a number of commonly used hydrologic models in the literature. CropWat and CropSyst [Confalonieri and Bocchi, 2005] simulate crop growth related processes. WaterGAP 2 [Alcamo et al., 2003; Döll et al., 2003] consists of two independent components for hydrology and water use, but does not include crop growth and agricultural management practices. The GIS-based Erosion Productivity Impact Calculator (GEPIC) [Liu et al., 2007] addresses spatial variability of crop yields and evapotranspiration, but lacks an explicit component for hydrology. The Soil and Water Integrated Model (SWIM) [Krysanova et al., 2005] was developed for use in mesoscale and large river basins (>100,000 km^2) mainly for climate change and land use change impact studies, and the Simulation of Production and Utilization of Rangelands (SPUR) is an ecosystem simulation model developed primarily for rangeland hydrology and crops [Foy et al., 1999]. The main shortcomings of the above models are: weak hydrology, missing calibration and validation against long-term annual discharges, application of correction factors to the modeled discharges leading to an inconsistent water balance, and lack of quantification of model prediction uncertainty, which could be quite large in distributed models.

The current modeling philosophy requires that models are transparently described; and that calibration, validation, sensitivity and uncertainty analysis are routinely performed as part of modeling work. As calibration is "conditional" (i.e., on the model structure, model inputs, analyst's assumptions, calibration algorithm, calibration data, etc.) and not uniquely determined, uncertainty analysis is essential to evaluate the strength of a calibrated model.

Given the above background, the main goal of this study is to assess the state of water quantity and quality in the BSB and to analyze the possible impacts of climate and land use change on the water resources of the region. To attain this goal, the specific objectives were: i) build a high-resolution hydrologic model of the Basin using the Soil Water Assessment Tool (SWAT), ii) design a parallel processing scheme that makes calibration and uncertainty analysis of such high-resolution model possible, iii) analyze the historic spatio-temporal availability of water resources components, mainly blue water flow, green water flow, and green water storage; iv) assess the severity of impacts of recent land use change on water balance components using historical data, and v) predict the impacts of combined climate and land use changes on future water resources of the BSB.

To achieve the first objective of this research we used the large scale hydrology simulator, Soil Water Assessment Tool (SWAT) [Arnold et al., 1998], to model the hydrology of the BSB. SWAT is a process-based, semi-distributed hydrologic model. The model was developed to quantify the impact of land management practices on water, sediment and agricultural chemical yields in large complex watersheds with varying soils, land uses and management conditions over long periods of time. SWAT was chosen because of the close linkage between its development purposes and the objectives of this research, open source code, and its successful application in a wide range of scales and environmental conditions [Guo et al. 2008; He et al. 2008; Ouyang et al. 2008; Wang et al. 2008, Gassman et al, 2007]. SWAT accounts for processes such as water quantity and quality, soil, climate, land use, agricultural managements, and nutrient cycling in a coupled single package. There is a great advantage in having such comprehensive overview of the basin.

Model calibration and uncertainty analysis are intimately linked and quite time consuming to perform. Several techniques are in popular use with different degrees of efficiency. The Monte Carlo Markov Chain (MCMC) [Vrugt et al., 2003], Generalized Likelihood Uncertainty Estimation (GLUE) [Beven and Binley, 1992], Parameter Solution (ParaSol) [van Griensven and Meixner, 2006], and Sequential Uncertainty Fitting ver.2 (SUFI-2) [Abbaspour et al., 2004, 2010] routines were compared in a study by Yang et al. [2008]. They found that SUFI-2 required much fewer simulations than other methods to achieve the same calibration results. This efficiency is of great importance when dealing with computationally intensive models. In this study we used

SUFI-2 as it is also already linked with SWAT in the software package SWAT-CUP [Abbaspour, 2007].

Distributed hydrologic models are especially difficult to calibrate because of time constraints, difficulties in parameterization, non-uniqueness, and uncertainties in the conceptual model, model inputs, and lack of knowledge on parameters [Abbaspour et al., 2010]. For this reason, the use of distributed computing in the form of grid and cloud computing has become more and more prevalent in the last years. In this thesis we addressed the problem of computation time by developing a procedure to run the high resolution BSB model on a grid system. Furthermore, we describe a system where the optimization algorithm, SUFI-2, is used in a parallel processing scheme running on Windows-based PCs or laptops.

The BSB lies in a transition zone between the Mediterranean region in an arid climate of North Africa and the temperate and rainy climate of central Europe. Because of its features, even relatively minor modifications of the general circulation can lead to substantial changes in the Mediterranean climate [Giorgi and Lionello, 2008]. This makes the BSB a potentially vulnerable region to climatic changes [e.g. Lionello et al., 2006; Ulbrich et al., 2006]. Indeed, the Mediterranean region has shown large climatic shifts in the past [Luterbacher et al., 2006] and it has been identified as one of the most prominent "Hot-Spots" in future climate change projections [Giorgi 2006].

Despite the importance of this region within the global change context, assessments of water resources under different climate change projections are relatively sparse in the literature. In the current study, the Danish Regional Climate Model (RCM) HIRHAM, was used under the scope of the PRUDENCE project to generate the future climate change projections over the BSB.

Hydrologic processes such as evapotranspiration, infiltration, surface runoff and groundwater flow are altered substantially by land use changes [Bultot et al. 1990; Sahin and Hall 1996; Fohrer et al. 2001; Lin et al. 2007; Tong and Chen 2002]. The evaluation of the impacts of land use change on water quantity and quality is fundamental to the development of sustainable land use alternatives [Lenhart et al. 2003; Lin et al. 2007] and is an integral component of river basin and water resources management [Eckhardt et al. 2003; Huisman et al. 2004].

In this study, the quantification of future land use scenarios was based on the framework provided by the Integrated Model to Assess the Global Environment [IMAGE, version 2.2: IMAGE team, 2001]. The four land use change scenarios used in the current study comprise a number of plausible alternatives (storylines) based on the IPCC-SRES [Nakicenovic et al., 2000] following four marker scenarios, represent different global socio-economic development pathways.

1.2 Content and structure of the thesis

This thesis consists of six chapters as follows:

Chapter 1 contains the introduction.

Chapter 2 describes building and calibrating a hydrologic model of the BSB using SWAT. We calibrated SWAT based on river discharge across BSB, river nitrate loads mainly in the Danube Basin, and yield of wheat, barley and maize across the countries.

Chapter 3 is devoted to the development of a Windows-based parallel processing scheme using the SUFI-2 calibration program. This technology helped with preliminary calibration of the model. We also assisted with the development of gSWAT [Gorgan et al., 2012; Mihon et al., 2013] by some project partners where final calibration runs of the model were made.

Chapter 4 quantifies the impact of historical land use changes on water resources components. We thought this was necessary in order to have some ideas about the significance for future land use changes on water resources. Similar to crop yield models, most studies of the impact of land use change is focused on the future where there are no data to agree or dispute the results.

In **Chapter 5**, we perform a comprehensive study on the coupled impact of climate and land use change on the water resources component for the near future years of 2013-2050.

Finally in **Chapter 6**, general conclusion concerning water resources in the Black Sea Basin are drawn. A number of shortcomings encountered in modeling are pointed out. Finally and outlook is provided to look at the potential applicability of the model developed in this study and further needed investigations.

References

Abbaspour KC, Yang J, Maximov I, Siber R, Bogner K, Mieleitner J, Zobrist J, Srinivasan R. 2007. Modelling hydrology and water quality in the pre-Alpine/Alpine Thur watershed using SWAT. Journal of Hydrology 333: 413–430.

Abbaspour KC. 2010. User Manual for SWAT-CUP, SWAT Calibration and Uncertainty Analysis Programs. Swiss Federal Institute of Aquatic Science and Technology, Eawag, Duebendorf, Switzerland. 93 pp.

Abbaspour, K.C., Johnson, C.A., van Genuchten, M.T., 2004. Estimating uncertain flow and transport parameters using a sequential uncertainty fitting procedure. Vadose Zone J. 3, 1340–1352.

Alcamo, J., P. Döll, T. Henrichs, F. Kaspar, B. Lehner, T. Rösch, and S. Siebert (2003), Development and testing of the WaterGAP 2 global model of water use and availability, Hydrological Sciences Journal, 48(3), 317-338.

Arnold JG, Srinivasan R, Muttiah RS, Williams JR. 1998. Large area hydrologic modeling and assessment–Part 1: Model development. Journal of the American Water Resources Association 34: 73–89.

Aus der Beek, T., L. Menzel, R. Rietbroek, L. Fenoglio-Marc, S. Grayekd, M. Becker, J. Kusche, and E. V. Stanev (2012), Modeling the water resources of the Black and Mediterranean Sea river basins and their impact on regional mass changes, J. Geodynamics, 59–60, 157–167.

Beven, K., Binley, A., 1992. The future of distributed models – model calibration and uncertainty prediction. Hydrol. Process. 6 (3), 279–298.

Bultot F, G. L. Dupriez, and D. Gellens (1990), Simulation of land use changes and impacts on the water balance—a case study for Belgium. J Hydrol 114:327–348. doi:10.1016/0022 1694(90) 90064-5

Confalonieri R, Bocchi S. 2005. Evaluation of CropSyst for simulating the yield of flooded rice in northern Italy. European Journal of Agronomy 23: 315–326.

Döll, P., F. Kaspar, and B. Lehner (2003), A global hydrological model for deriving water availability indicators: model tuning and validation, J. Hydrology, 270 (1-2), 105-134.

Eckhardt K, L. Breuer, and H. G. Frede (2003), Parameter uncertainty and the significance of simulated land use change effects. J Hydrol 273:164–176. doi:10.1016/S0022-1694(02)00395-5

Fohrer N, S. Haverkamp, K. Eckhardt, and H. G. Frede (2001), Hydrologic response to land use changes on the catchment scale. Phys Chem Earth 26(7–8):577–582. doi:10.1016/S1464-1909(01)00052-1.

Foy JK, Teague WR, Hanson JD. 1999. Evaluation of the upgraded SPUR model (SPUR2.4). Ecological Modelling 118: 149–165.

Gassman, P. W., M. Reyes, C. H. Green, and J. G. Arnold (2007), The Soil and Water Assessment Tool: Historical development, applications, and future directions, T. ASABE, 50, 1211–1250.

Giorgi, F. (2006), Climate change Hot-spots. Geophys. Res. Lett. 33, L08707.

Giorgi, F. and P. Lionello (2008), Climate change projections for the Mediterranean region, Global and Planetary Change, 63 (2008) 90–104.

Gorgan D., Bacu V., Mihon D., Rodila D., Abbaspour K.C., Rouholahnejad E. 2012. Grid based calibration of SWAT hydrological models. Natural Hazards and Earth System Sciences, 12:2411-2423.

Guo H., Q. Hu, T. Jiang (2008), Annual and seasonal streamflow responses to climate and land-cover changes in the Poyang Lake basin, China, J. Hyrol 355:106–122. doi:10.1016/j.jhydrol.2008.03.020.

He H., J. Zhou, W. Zhang (2008), Modelling the impacts of environmental changes on hydrological regimes in the Hei River Watershed, China. Global Planet Change 61:175–193. doi: 10.1016/j.gloplacha.2007.08.012

http://www.eawag.ch/organisation/abteilungen/siam/software/swat/index_EN

Huisman J.A., L. Breuer, and H. G. Frede (2004), Sensitivity of simulated hydrological fluxes towards changes in soil properties in response to land use change. Phys Chem Earth 29:749–758. doi:10.1016/j.pce.2004.05.012

Krysanova V, Hattermann F, Wechsung F. 2005. Development of the ecohydrological model SWIM for regional impact studies and vulnerability assessment. Hydrological Processes 19: 763–783.

Lenhart T, N. Fohrer, and H. G. Frede (2003), Effects of land use changes on the nutrient balance in mesoscale catchments. Phys Chem Earth 28:1301–1309. doi:10.1016/j.pce.2003.09.006.

Lin Y. P., N. M. Hong, P. J. Wu, C. F. Wu, and P. H. Verburg (2007), Impacts of land use change scenarios on hydrology and land use patterns in the Wu-Tu watershed in Northern Taiwan. Landsc Urban Plan 80:111–126.doi:10.1016/j.landurbplan.2006.06.007

Lionello, P., P. Malanotte-Rizzoli, and R. Boscolo (2006), The Mediterranean climate: an overview of the main characteristics and issues, Mediterranean Climate Variability, Elsevier, Amsterdam, pp. 1–26.

Liu, J.G., Williams, J.R., Zehnder, A.J.B., Yang, H., 2007. GEPIC – modelling wheat yield and crop water productivity with high resolution on a global scale. Agric. Syst. 94, 478-493.

Ludwig, W., E. Dumont, M. Meybeck, and S. Heussner (2009), River discharges of water and nutrients to the Mediterranean and Black Sea: Major drivers for ecosystem changes during past and future decades?, J. Progress in Oceanography, 80, 199-217.

Luterbacher, J., et al., 2006. Mediterranean climate variability over the last centuries. A review. In: Lionello, P., Malanotte-Rizzoli, P., Boscolo, R. (Eds.), Mediterranean Climate Variability. Elsevier, Amsterdam, pp. 27–148.

Mihon, D., Bacu, V., Rodila, D., Stefanut, T., Abbaspour, K., Rouholahnejad, E., Gorgan, D. 2013. Grid based hydrologic model calibration and execution**,** Advances in Intelligent Systems and Computing 187 AISC , pp. 279-293.

Nakicenovic, N., Alcamo, J., Davis, G., de Vries, B., Fenhann, J., Gaffin, S., Gregory, K., Grübler, A., Jung, T.Y., Kram, T., La Rovere, E., Michaelis, L., Mori, S., Morita, T., Pepper, W., Pitcher, H., Price, L., Riahi, K., Roehrl, A., Rogner, H.H., Sankovski, A., Schlesinger, M., Shukla, P., Smith, S., Swart, R., van Rooyen, S., Victor, N. and Dadi, Z. (2000). Special Report on emissions scenarios. Cambridge: Cambridge University Press.

Ouyang W, Skidmore AK, Hao F, Wang T (2010) Soil erosion dynamics response to landscape pattern. Sci Total Environ 408:1358–1366. doi:10.1016/j.scitotenv.2009.10.062.

Paleari, S., P. Heinonen, E. Rautalahti-Miettinen, and D. Daler (2005), Transboundary Waters in the Black Sea-Danube region; Legal and financial implications. University of Kalmar, Kalmar, Sweden.

Sahin V, and M. J. Hall (1996), The effects of afforestation and deforestation on water yields. J Hydrol 178:293–309, doi:10.1016/0022-1694 (95)02825-0

Sommerwerk, N., C. Baumgartner, J. Bloesch, T. Hein, A. Ostojić, M. Paunović, M. Schneider-Jacoby, R. Siber, and K. Tockner (2009), Rivers of Europe, Chapter 3 – The Danube River Basin, 59- 112, Elsevier, doi: http://dx.doi.org/10.1016/B978-0-12-369449-2.00003-5.

Sukhodolov, A. N., N. S. Loboda, V. M. Katolikov, N. A. Arnaut, V. V. Bekh, M. A. Usatii, L. A. Kudersky, and B. G. Skakalsky (2009), Rivers of Europe, Chapter 13 – Western Steppic Rivers, 497–523, Esevier, doi: http://dx.doi.org/10.1016/B978-0-12-369449-2.00013-8.

Tong S. T. Y., and W. Chen (2002), Modeling the relationship between land use and surface water quality. J Environ Manag 66:377–393. doi: 10.1006/jema.2002.0593

Ulbrich, U., et al., 2006. The Mediterranean climate change under global warming. In: Lionello, P., Malanotte-Rizzoli, P., Boscolo, R. (Eds.), Mediterranean Climate Variability. Elsevier, Amsterdam, pp. 398–415.

Van Griensven, A., Meixner, T., 2006. Methods to quantify and identify the sources of uncertainty for river basin water quality models. Water Sci. Technol. 53 (1), 51–59.

Vrugt, J.A., Gupta, H.V., Bouten, W., Sorooshian, S., 2003. A shuffled complex evolution metropolis algorithm for optimization and uncertainty assessment of hydrologic model parameters. Water Resour. Res. 39 (8), 1201.

Wang S., S. Kang , L. Zhang, F. Li (2008), Modelling hydrological response to different land-use and climate change scenarios in the Zamu River basin of northwest China, Hydrol Process 22:2502–2510. doi:10.1002/hyp.6846.

Wissenschaftlicher Beirat Globale Umweltveränderung (WBGU) (2007), World in Transition: Climate Change as Security Risk, German edition published in 2007 entitled Welt im Wandel: Sicherheitsrisiko Klimawandel, Springer-Verlag Berlin, Heidelberg, New York, 2008 ISBN 978-3-540-73247-1.

Wolfram, M., and H. Bach (2009), PROMET – Large scale distributed hydrological modelling to study the impact of climate change on the water flows of mountain watersheds, J. Hydrology, 376 (3-4), 362-377, doi: http://dx.doi.org/10.1016/j.jhydrol.2009.07.046.

Yang J, Reichert P, Abbaspour KC, Xia J, Yang H. 2008. Comparing uncertainty analysis techniques for a SWAT application to Chaohe Basin in China. Journal of Hydrology 358: 1–23.

Water Resources Research, Nov 2013, accepted

2. Water resources of the Black Sea Basin at high spatial and temporal resolution

Elham Rouholahnejad[1, 2], Karim C. Abbaspour[1], Raghvan Srinivasan[3], Victor Bacu[4], Anthony Lehmann[5]

[1] Eawag, Swiss Federal Institute of Aquatic Science and Technology, Ueberlandstrasse 133, 8600 Duebendorf, Switzerland

[2] ETH Zürich Institute of Terrestrial Ecosystem, Universitätstr. 16, 8092 Zürich, Switzerland

[3] Texas A&M University, Texas Agricultural Experimental Station, Spatial Science Lab, College Station, TX 77845, USA

4 Computer Science Department, Technical University of Cluje - Napoca, Romania

[5] University of Geneva, Climatic Change and Climate Impacts, 7 Route de Drize, CH-1227 Carouge, Switzerland

Abstract

The pressure on water resources, deteriorating water quality, and uncertainties associated with the climate change create an environment of conflict in large and complex river system. The Black Sea Basin (BSB), in particular, suffers from ecological unsustainability and inadequate resource management leading to severe environmental, social, and economical problems. To better tackle the future challenges, we used the Soil and Water Assessment Tool (SWAT) to model the hydrology of the BSB coupling water quantity, water quality, and crop yield components. The hydrological model of the BSB was calibrated and validated considering sensitivity and uncertainty analysis. River discharges, nitrate loads, and crop yields were used to calibrate the model. Employing grid technology improved calibration computation time by more than an order of magnitude. We calculated components of water resources such as river discharge, infiltration, aquifer recharge, soil moisture, and actual and potential evapotranspiration. Furthermore, available water resources were calculated at sub-basin spatial and monthly temporal levels. Within this framework, a comprehensive database of the BSB was created to fill the existing gaps in water resources data in the region. In this paper, we discuss the challenges of building a large-scale model in fine spatial and temporal detail. This study provides the basis for further research on the impacts of climate and land use change on water resources in the BSB.

KEYWORDS: Calibration; Uncertainty analysis; SUFI-2; Blue water; Green water

2.1 Introduction

The pressures on water resources and increasing conflict of interest present a huge water management challenge in the Black Sea Basin (BSB) [GIWA, 2005]. The small-scale sectoral structure of water management is now reaching its limits. The integrated management of water in the Basin requires a new level of consideration where water bodies are to be viewed in the context of the whole river system and managed as a unit within their basins. This is of key interest for efficient and targeted water management through regional coordination, transparent balancing of interests, and clear priority setting [Water Agenda 21, 2011]. A frequently advocated approach is to have adequate knowledge of temporal and spatial variability of the fresh water availability and water quality [UNEP, 2006].

The BSB is internationally recognized for its ecologically unsustainable development and inadequate resource management leading to severe environmental, social, and economical problems. In 1995, it was rated as being of the highest concern in five out of seven environmental categories, making it the worst of any of the European seas [Stanners and Boudreau, 1995]. In another study, the German Advisory Council on Global Change (WBGU) states that the Black Sea is likely to experience (i) a degradation of freshwater resources; (ii) an increase of storm and flood disasters; (iii) a decline in food production; and (iv) environmentally-induced migration [WBGU, 2007]. In addition, transboundary pollution effects (TPE) can be seen with respect to all economic sectors. Transboundary pollution is the pollution that originates in one country but cause damage in another country's environment, by crossing borders in the rivers [Paleari, 2005].

Furthermore, the Intergovernmental Panel on Climate Change [IPCC 2007] predicts important changes in the coming decades that will not only modify climate patterns in terms of temperature and rainfall, but will also drastically change freshwater resources qualitatively and quantitatively. This is expected to lead to more floods or droughts in different regions, lowering of drinking water quality, increased risk of water-borne diseases, and irrigation problems. These changes may trigger socio-economic crises that need to be addressed well in advance of the events in order to reduce the associated risks.

Previous research, which addressed water quantity and water quality in the BSB include a few global and regional studies. WaterGAP2 [Alcamo et al., 2003; Döll et al., 2003] is a global model for water availability and water use. This model focuses on the global hydrology at grid scale (30 arc min) considering 3,565 major basins in the world with the drainage areas greater than 2500 km^2. The model was initially used to estimate the water availability and demand and provides relatively limited water cycle-related components. In WaterGAP3 [Aus der Beek et al., 2012], a regional version of WaterGAP2, the hydrological fluxes draining into Mediterranean and Black Sea were modeled with improved spatial resolution (5 arc min), snow melt, and water use. However, results using WaterGAP3 and WaterGAP2 are not significantly different in the BSB [Aus der Beek et al., 2012]. In a different approach, Meigh et al., [1999] developed a grid-based model Global Water Availability Assessment (GWAVA) to predict water resources scarcity at continental and global scales. This model has recently been further developed to include water quality [Dumont et al., 2012]. Using a statistical approach, Grizzetti et al. [2008] assessed nitrogen content of surface water for major European river basins. Furthermore, discharges of water and nutrient to the Mediterranean and Black Sea are reported in a study by Ludwig et al. [2009] for major rivers.

Next to the above mentioned studies, there are a few other investigations on the status of river basins in the BSB [Sukhodolov et al., 2009; Sommerwerk et al., 2009; Wolfram and Bach, 2009]. However, often average loads entering the Sea are reported without adequate spatial and temporal resolution on the current and future freshwater availability for the entire BSB. General shortcomings of the previous studies are: missing detail information on model inputs and outputs, unavailability of their input data, coarse spatial resolution and scale of the models, and missing model calibration/validation and uncertainty analysis components.

In recent years, improvements in integrated hydrological modeling, advancements in calibration and uncertainty analysis tools, and availability of grid technology for model execution, allows building more detailed and holistic models. These models account for processes such as: water quantity and quality, soil, climate, land use, agricultural managements, and nutrient cycling in a coupled single package. The aim of the project is to build a high-resolution model of the entire BSB, and to look at the impact of land use and climate change on the water resources. The reason for building a single model of the BSB is to have a uniformly calibrated model of the region rather than several disparately calibrated models. A high-resolution large-scale model has the advantages of allowing a holistic look at the Basin while retaining the small-scale system variabilities. The objectives of the current study are to: i) gather and share a comprehensive database of the BSB, ii) model the hydrology of the entire BSB by including agricultural management and crop yield to better quantify water quantity and water quality at daily time step and sub-basin level, iii) calibrate and validate the model with uncertainty analysis using grid technology, iv) produce a relatively accurate picture of water resources availability, reliability, and pressures in the Basin.

To achieve the objectives of this research, we used the program Soil and Water Assessment Tool (SWAT) [Arnold, et al., 1998]. SWAT was used because it is a continuous time and spatially distributed watershed model, in which hydrological processes and water quality are coupled with crop growth and agricultural management practices. The program was successfully applied in a wide range of scales and environmental conditions [Gassman et. al., 2007]. Another advantage of SWAT is its modular implementation where different processes can be selected.

For calibration and uncertainty analysis in this study, we used the Sequential Uncertainty Fitting program SUFI-2 [Abbaspour et al., 2004, 2007]. SUFI-2 is a tool for sensitivity analysis, multi-site calibration, and uncertainty analysis. It lends itself easily to parallelization, and is capable of analyzing a large number of parameters and measured data from many gauging stations (outlets) simultaneously. SUFI-2 is linked to SWAT in the SWAT-CUP software [Abbaspour, 2011]. Yang et al. [2008] found that SUFI-2 needed the smallest number of model runs to achieve a similarly good calibration and prediction uncertainty results in comparison with four other techniques. This efficiency is of great importance when dealing with computationally intensive, complex large-scale models. We ran parallelized SUFI-2 on grid system described by Rouholahnejad et. al. [2012] and Gorgan et al. [2012].

2.2. Material and Methods

2.2.1. Study area

The Black Sea Basin (Figure 2.1) with a total area of 2.3 million km^2 drains rivers of 23 European and Asian countries (Austria, Belarus, Bosnia, Bulgaria, Croatia, Czech Republic, Georgia, Germany, Hungary, Moldova, Montenegro, Romania, Russia, Serbia, Slovakia, Slovenia, Turkey, Ukraine, Italy, Switzerland, Poland, Albania and Macedonia) to the Black Sea. The Basin is inhabited by a total population of around 160 million people [BSEI, 2005]. It is mountainous in the east and south, in the Caucasus and in Anatolia, and to the northwest with the Carpathians in the Ukraine and Romania. Most of the rest of the Black Sea's western and northern neighborhood is low lying. Mean annual air temperature shows a distinct north-south gradient from < -3 °C to > 15 °C. The precipitation pattern is characterized by a west-east gradient from a high of > 3000 mm yr $^{-1}$ to a low of < 190 mm yr^{-1} [Tockner et al., 2009]. The dominant land use in the basin is agricultural with 65% of coverage according to MODIS Land Cover [NASA, 2001]. Major rivers draining into the Black Sea include Danube, Dnieper and Don. The greatest sources of diffuse pollution are agricultural and households not connected to sewer systems [EEA, 2010].

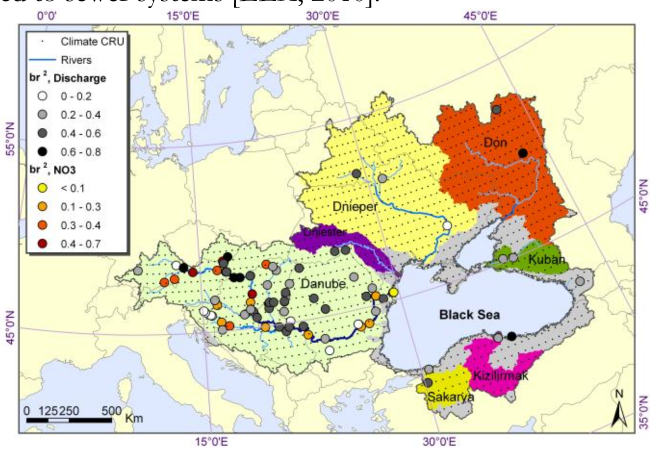

Figure 2.1. Illustration of Black Sea Basin showing, major rivers, and measured stations of climate, discharge, and nitrate. Also shown are the comparison of observed and simulated discharge and nitrate using the efficiency criterion bR^2. The six large river basins of Danube, Dnieper, Don, Kuban, Kizilirmak, and Sakarya are highlighted.

2.2.2. Soil Water Assessment Tool (SWAT)

SWAT was used to simulate hydrology, water quality, and vegetation growth in BSB. SWAT is a process-based, semi-distributed hydrologic model. The model has been developed to quantify the impact of land management practices on water, sediment and agricultural chemical yields in large complex watersheds with varying soils, land uses and management conditions over long periods of time. SWAT was chosen because of the close linkage between its development purposes and the objectives of this project, open access to the source code, and its successful application in a wide range of scales and environmental conditions.

The main components of SWAT are hydrology, climate, nutrient cycling, soil temperature, sediment movement, crop growth, agricultural management, and pesticide dynamics. SWAT is a continuous simulation model operating on a daily time step. The spatial heterogeneity of the watershed is preserved by topographically dividing the basin into multiple sub-basins. These are further subdivided into hydrologic response units (HRU) based on soil, land use, and slope characteristics. These subdivisions enable the model to reflect differences in evapotranspiration for various crops and soils. In each HRU and on each time step the hydrologic and vegetation-growth processes are simulated based on the curve number rainfall-runoff partitioning and the heat unit phenological development method [Neitsch et al., 2009].

Runoff is predicted separately for each HRU and routed to obtain the total model runoff for the watershed. The routing phase of the hydrologic cycle in SWAT is the movement of water, nitrate, etc. through the channel network of the watershed. Once SWAT determines the loadings of water, sediment, nutrients, and pesticides to the main channel, the loadings are routed through the stream network of the watershed. In addition to keeping track of mass flow in the channel, SWAT models the transformation of chemicals in the stream and streambed.

Energy availability governs vegetation phenology. At each point in the growth cycle, biomass production is derived from the interception of solar radiation by leaves, plant-specific radiation-use-efficiency and leaf area index (LAI). Crop yield is calculated at harvest by multiplying the above-ground biomass with the harvest index. The harvest index is a fraction of the above-ground plant dry biomass removed as dry yield. Plant growth is limited by temperature, water, and nutrient availability in the soil; and is influenced by agricultural management (e.g. fertilization, irrigation, and timing of operations). A detailed description of SWAT's theory can be obtained in Neitsch et al. [2009].

2.2.3. Input data and model outputs

BSB Digital Elevation Model (DEM) at 90 m spatial resolution was extracted from SRTM [Jarvis et al, 2008]. The river network dataset was from European Catchments and RIvers Network System [ECRINS, 2012]. The ECRINS river map was corrected in the areas where there was a mismatch with DEM to achieve a correct flow direction.

The soil data was obtained from the FAO-UNESCO global soil map [FAO, 1995], which provides data for 5000 soil types comprising two layers (0–30 cm and 30–100 cm depth) at a spatial resolution of 5 km.

Four different land uses were available for the region: (i) Global Land Cover Characterization (GLCC) at 1 km spatial resolution [USGS, 2008], (ii) MODIS land cover with spatial resolution of 500 m [NASA, 2001], (iii) GlobCover with spatial resolution of 300 m [ESA, 2008], (iv) Global Corine at 300 m spatial resolution [ESA, 2010].

Two different climate databases were available: Measured and gridded data. Measured climate included 456 rainfall and 678 temperature stations mainly collected from National Climatic Data Centre [NCDC], the European Climate Assessment & Dataset (ECAD) [Haylock et al., 2008], Turkish Ministry of Forest and Water Affairs (MEF), Romanian National Institute of Hydrology and Water Management (INHGA) for the period of 1970 to 2008. Only stations with < 20% missing data were included in the model. Gridded data are constructed from measured climate stations and interpolated to grid resolution. We used data from Climate Research Units [CRU, 2008; Mitchell and Jones, 2005] at 0.5o resolution amounting to 1147 grid points. The daily global solar radiation data was obtained from 6,110 virtual stations at 0.5o resolution for the duration of 1960-2001 [Weedon et al., 2011].

Monthly river discharge data for model calibration and validation was obtained from Global Runoff Data Center [GRDC, 2011], National Institute of Hydrology and Water Management (INHGA) and Danube Delta National Institute for Research and Development (DDNI) in Romania, and Turkish Ministry of Forest and Water Affairs (MEF) for the period 1970–2008. Only stations with < 20% missing data and minimum length of 5 years were included in calibration-validation process. This led to 144 discharge outlets where 37 of them also contained nitrate data form International Commission for the Protection of the Danube River (ICPDR). These outlets had differing beginning and ending time periods.

Point sources were also assigned to each subbasin in the model. The nutrient loads of subbasins were calculated based on the population of the subbasins, the percentage of population connected to wastewater treatment plant, and the average rate of nitrogen per population equivalent. Population percentage connected to any kind of sewage treatment was derived from Eurostat for the period of 2000 to 2009. This share was above 80% in approximately half of the European Union countries for which data are available, rising to 95% in Germany. At the other end, less than one in two households were connected to urban wastewater treatment in Bulgaria and Romania. In terms of treatment levels, tertiary wastewater treatment was most common in Germany, Austria and Italy where at least four in every five persons were connected to this type of wastewater treatment. In contrast, no more than 1% of the population was connected to tertiary wastewater treatment in Romania and Bulgaria. We assumed the treatment efficiency to be 80% in all countries with 20% loading directly into surface waters and hence considered as point sources.

To account for industrial and household releases, Zessner et al., [2005] calculated the nitrogen load to be 8.8 g N Pe^{-1} day-1, where Pe is population equivalent, which is the number expressing the ratio of the sum of the pollution load produced during 24 hours by industrial facilities and household to the individual pollution load in household sewage produced by one person in the same time. The ratio of population and Pe varies in a way that 80% of the treatment plants lie in the range of 0.4 to 0.9. The average value of this ratio is assumed to be 0.63 [Zessner et al, 2005]. The nutrient load is calculated as:

$$L_N = P_e l_N \left[\left(1 - S_{rate}\right) + \left(1 - T_{eff}\right) S_{rate} \right] \quad (1)$$

Where L_N is the nitrogen load entering rivers in subbasins (g day^{-1}), T_{eff} is the wastewater treatment efficiency, l_N is the average input of nitrogen from household to wastewater (g N Pe^{-1} day^{-1}), S_{rate} is the percentage of the population connected to any kind of sewage treatment. We used population map of year 2005 from the Center for International Earth Science Information Network in 2.5 arc min resolution [CIESIN, 2005] and extrapolated to other years based on the national population growth rate provided by the World Bank.

Cropping area and the start and end month of cropping periods in the BSB countries were derived from MIRCA2000 database on global monthly irrigated and rainfed cropping areas around the year 2000 (5-year average), at a spatial resolution of 5 arc min [Portmann et al, 2010]. This database represents multi-cropping systems and maximizes consistency with census-based national and sub-national statistics. Crop yield data was obtained from McGill University [Monfreda et al., 2008] at 5 minute resolution. This data was five-year averages around the year 2000, and was used to calculate per subbasin crop yields for maize, barley and wheat. Country-based crop yield was obtained from FAOSTA database [FAO, 2013].

SWAT produces a large amount of output variables. In this study we look at the water cycle components, crop yield, and nitrate concentration in rivers. Using the water cycle constituents calculated in SWAT, we could also calculate water resources components such as "blue water", "green water flow", and "green water storage". Currently, the definition of blue water is generally accepted as the sum of the river discharge and the deep groundwater recharge. This is in essence the water resources by the traditional hydrological and engineering definition. There exist slightly different definitions for the term green water. Falkenmark and Rockstrom [2006] differentiate between the green water "resource" and the green water "flow". According to their definition, green water resource is the moisture in the soil, which is a renewable resource and can potentially generate economic returns, as it is the source for rain-fed agriculture. The green water flow is composed of the actual evaporation (the nonproductive part) and the actual transpiration (the productive part), commonly referred to together as the actual evapotranspiration.

2.2.4. Model setup

The sub-basins were delineated with a threshold area of 100 km^2 yielding 12,982 sub-basin. This was the smallest threshold that could be used to build the ArcSWAT project on a 64 bit laptop with 2.7 GHz processors, 4 cores, 8 GB of RAM and Windows7 operating system. This is because of memory limitation and inefficiency of ArcGIS in handling large raster calculation. In addition, the personal geodatabase of ArcSWAT created by ArcGIS 9 has a limitation of 2 GB on the file size. Fourteen different land cover classes of MODIS were assigned to land uses in the SWAT database. Subsequently, each of the 12,982 sub-basins was spilt into unique combinations of slope, land use classes, and soil types resulting in 89,202 Hydrologic Response Unit (HRU). Three classes of slope (0-3%, 3-6%, and >6%) were used in the subbasin discretization. We also used 5 elevation bands in each subbasin to adjust for orographic change in temperature (-6°C km^{-1}) and precipitation (670 mm km^{-1}) after some initial fitting.

Twenty five different management plans were designed based on the crop types, cropping dates, winter or summer crops, irrigated or rain-fed applications. Each HRU then corresponded to a management plan. Exclusive agricultural classes were assigned to each country so that desired management could be defined at the national level. Subsequently, agricultural areas within these classes were subdivided proportional to the cropping areas of irrigated/rainfed, winter/spring types for wheat, maize and barely. The three major crops were allocated to agricultural lands in MODIS proportional to their contribution in each country's harvested areas as reported by MIRACA2000 [Portmann et al., 2010].

The option of automatic fertilization in SWAT was employed to meet crop need and the annual maximum application amount was set to 300 kg N ha^{-1}. This assumption leads to underestimation of nitrogen in areas where application is more than crop need. Elemental nitrogen and elemental phosphors were applied to the agricultural lands in each subbasin as the main fertilizer in BSB. An additional nitrogen input of

1.2 mg N l^{-1} was assumed in the rainfall. It is notable that in the MODIS classification agricultural land does not include permanent grassland.

We invoked automatic irrigation based on plant water demand in such a way as to minimize crop water stress in irrigated lands. In this study, potential evapotranspiration (PET) was estimated using the Hargreaves method [Hargreaves et al., 1985] while actual evapotranspiration (ET) was estimated based on Ritchie [1972].

The simulation period was 1970–2006 using 3 years of initialization (1970-1972) as warm up period. As each station had a different beginning and ending time periods, the model was calibrated from 1973 to 1996 and validated from 1997 to 2006 for discharge, and because of fewer data in the early years; the nitrate loads were calibrated from 1973 to 2000 and validated from 2001 to 2006. Within these general years different stations had different data availability periods. Given the disparity in data lengths and timing, this was the most sensible division of data between calibration and validation time period. SWAT always runs on daily time step, but we used monthly outputs for calibration and validation of the model. Using SWAT 2009, it took 42 hours for a single model run on the laptop where ArcSWAT project was built.

2.2.5. Model calibration procedure

Sensitivity, calibration, validation, and uncertainty analysis were performed for water quantity, water quality, and crop yield using river discharges, nitrate loads in rivers, and yields of wheat, barley, and maize. SUFI-2 was used for calibration and uncertainty analysis. In SUFI-2 all sources of uncertainties are mapped to a set of parameter ranges. They are calibrated with the dual aim of bracketing most of the observed data with as narrow as possible uncertainty band. Initially, a set of meaningful parameter ranges are assigned to calibrating parameters based on literature, knowledge of site processes, and sensitivity analyses. Then a set of Latin hypercube samples are drawn from the parameter ranges and the objective function is calculated for each parameter set. The uncertainty is quantified at the 2.5% and 97.5% levels of the cumulative frequency distribution of all simulated output values and it is referred to as the 95% prediction uncertainty (95PPU). The lower, middle, and upper boundaries of the 95PPU (L95PPU, M95PPU, U95PPU) reflect the 2.5, 50, and 97.5 percentiles of the distribution, respectively. Values at the 50% probability level are used for drawing average long-term maps of different variables. The goodness of model performance in terms of calibration and uncertainty level is evaluated using the *P-factor* and the *R-factor* indices. The *P-factor* is the percentage of measured data bracketed by the 95PPU band. It ranges from 0 to 1 where 1 is ideal and means all of the measured data are within the uncertainty band (i.e., model prediction). The *R-factor* is the average width of the band divided by the standard deviation of the measured variable. It ranges from 0 to ∞ where 0 reflects a perfect match with the observation. Based on the experience, an *R-factor* of around 1 is usually desirable [Abbaspour et al., 2007] where the thickness of the uncertainty band does not exceed the measured standard deviation. SUFI-2 allows for a measurement error of about 10% to be assigned to all observed variables, which are accounted for in the 95PPU calculations.

Coefficient of determination r^2 is a measure of dispersion around the mean of the observed and predicted values and can be used as an efficiency criteria. The range of r^2 lies between 0 and 1 which describes how much of the observed dispersion is explained by the prediction. A value of zero means no correlation at all whereas a value of 1 means that the dispersion of the prediction is equal to that of the observation. The fact that only the dispersion is quantified is one of the major drawbacks of r^2 if it is considered alone. A model which systematically over- or under predicts all the time will still result in good r^2 values close to 1.0 even if all predictions were wrong. By weighting r^2 by the slope of regression line between observed and predicted, under- or over predictions are quantified together with the dynamics which results in a more comprehensive reflection of model results. We used the following weighted r^2 introduced by Krause et al. [2005] as efficiency criterion for discharge and nitrate :

$$\phi = \begin{cases} br^2 & \text{for} \quad b \le 1 \\ b^{-1}r^2 & \text{for} \quad b > 1 \end{cases} \tag{2}$$

where r^2 is the coefficient of determination and b is the slope of the regression line between the simulated and measured data. For a good agreement the interception of the regression line should be close to zero which means that an observed runoff of zero would also result in a prediction near zero and the gradient b should be close to one. For multiple outlets and attributes, the objective function Φ was expressed as:

$$\Theta = \frac{1}{w_{v1} + w_{v2}} \left[\frac{w_{v1}}{\sum_{i=1}^{n_1} w_i} \sum_{i=1}^{n_1} w_i \phi_i + \frac{w_{v2}}{\sum_{i=1}^{n_2} w_i} \sum_{i=1}^{n_2} w_i \phi_i \right] \qquad (3)$$

where w_{v1} and w_{v2} are weights of the two variables, n_1 and n_2 are the number of discharge and nitrate stations, respectively, and w_i's are the weights of variables at each station. The function ϕ, and consequently Θ vary between 0 and 1. The best simulation is considered the one with the highest Θ value. A major advantage of br^2 efficiency criterion is that it ranges from 0 to 1, which compared to Nasch-Sutcliff Efficiency coefficient, ensures that in a multi-site multi-attribute calibration, the objective function is not dominated by a few bad results. Weights in Eq. (3) would be critical if an objective function such as mean square error was used, but because of using br^2 they did not make any significant difference to model calibration results. For this reason we set them to 1. For crop yield we used mean square error as the objective function after an initial calibration of model for discharge and nitrate:

$$\phi_3 = \frac{1}{n_3} \sum_{i=1}^{n3} \left(Y_i^o - Y_i^s \right)^2 \qquad (4)$$

where n_3 is the number of sites with wheat, barley, and corn yield data, Y^o (t ha $^{-1}$) is the observed yield, and Y^s (t ha $^{-1}$) is the simulated yield.

A few iterations are then carried out seeking to reach an optimal *P-factor* and *R-factor* until a further improvement in the objective function is not found. As mentioned before, the calibration runs were made using parallel SUFI-2 [Rouholahnejad, 2012] and the grid-based SWAT (gSWAT) [Gorgan, et al., 2012]. As SUFI-2 is a sequential procedure, several iterations of 200 simulations each were performed for calibration.

2.3. Results and discussion

The model response to various land uses and climate data was tested by comparing simulated river discharges against the observation. For land use, our analysis indicated that classification and resolution did not have a significant effect on river discharge simulation in the BSB model. MODIS land cover was used in the final SWAT project as it produced relatively better discharge results. As model calibration started far back in time, we also tested the model by changing the land use during SWAT simulation. We found that the impact of historic land use change on our large-scale model results was negligible and, hence, did not consider this change during calibration.

We also found that CRU-based simulated discharges performed significantly better in the project as compared to simulated discharges based on measured climate stations. This could be because the climate stations suffered from a large amount of missing data, different data qualities, and uneven distribution throughout the region. Subsequently, the CRU data set was selected to model the hydrology of the BSB.

SWAT calculates the rainfall and temperature of each subbasin using the nearest climate station to the centroid of that subbasin. As rainfall is the most important driving variable in a hydrological model, when comparing the results of this work with other works, it is important to have the distribution of the rainfall in mind (Figure 2.2). Differences are observed in the coefficients of variation (CV) of long-term annual precipitation and temperature averages (1973-2006) across the BSB. This indicates the degree of year to year variability during the simulation period. This variation has an influence on the prediction uncertainties of all water cycle components as we will see later for the case of Bulgaria and Turkey.

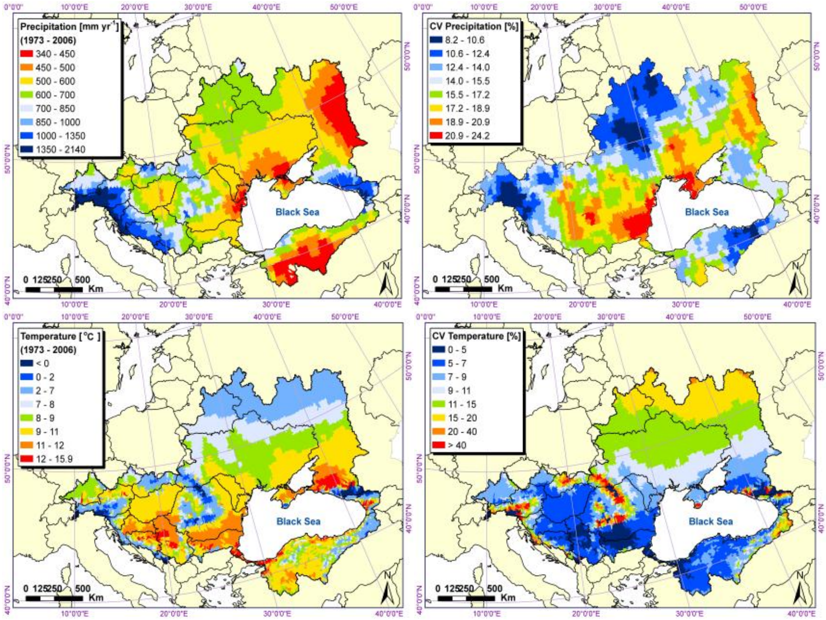

Figure 2.2. Long-term annual average (1973–2006) precipitation and average temperature distribution across Black Sea Basin based on the CRU data set. Also shown are the coefficients of variation indicating the temporal variability of precipitation and average temperature.

2.3.1. Calibration and uncertainty analysis

2.3.1.1. Examining model setup

Initially, a broad set of parameters were used for discharge calibration [Holvoet et al., 2005; Wang et al., 2005, Abbaspour et al., 2007; and Faramarzi et al., 2009]. Then a sensitivity analysis was performed to identify the key parameters across BSB, which led to selection of 20 parameters integrally related to stream flow (Table 2.1). Although the initial parameter ranges were as wide as physically meaningful, some outlets were still completely outside of the 95PPU range. These outlets would obviously not benefit from parameter calibration alone. We investigated the poorly simulated outlets one by one using the visualization module of SWAT-CUP. This involves projection of the study area on the Microsoft's BING map to identify the reasons for the inadequate simulations. In the visualization module, we observe the subbasins, outlet positions, simulated rivers, and climate stations from the SWAT project, as well as landcover and other layers of information in the BING map. Several problems were discovered, which are inevitable in a large-scale projects and needed careful attention.

Examples of these include positioning the outlets on a wrong rive (Figure 2.3a,b). As SWAT connects each measured outlet to the nearest rivers, any errors in the coordinates of outlets can cause a wrong placement. This perhaps leads to the biggest calibration problem. As shown in Figure 2.3b the outlet is placed on a tributary of the Danube called Tamis near Pancevo in Serbia. The black dashed line near the x-axis (Figure 2.3c) is simulated river discharge before correcting the location, and the red line shows simulated discharge after correcting the location.

Table 2.1. List of parameters and their initial ranges used for model calibration.

Parameter name	Definition	Initial range
r__CN2.mgt	SCS runoff curve number for moisture condition II	-0.35 - 0.35
r__ALPHA_BF.gw	Base flow alpha factor (days)	-0.8 – 0.8
r__GW_DELAY.gw	Groundwater delay time (days)	-0.8 – 0.8
r__GWQMN.gw	Threshold depth of water in shallow aquifer for return flow (mm)	-0.8 – 0.8
r__GW_REVAP.gw	Groundwater revap. coefficient	-0.4 – 0.4
r__REVAPMN.gw	Threshold depth of water in the shallow aquifer for 'revap' (mm)	-0.4 – 0.4
r__RCHRG_DP.gw	Deep aquifer percolation fraction	0.3 – 0.5
r__CH_N2.rte	Manning's n value for main channel	-0.8 – 0.8
r__CH_K2.rte	Effective hydraulic conductivity in the main channel (mm hr^{-1})	-0.8 – 0.8
r__ALPHA_BNK.rte	Baseflow alpha factor for bank storage (days)	-0.6 – 0.6
r__SOL_AWC().sol	Soil available water storage capacity (mm H2O/mm soil)	-0.5 – 0.5
r__SOL_K().sol	Soil conductivity (mm hr^{-1})	-0.8 – 0.8
r__SOL_BD().sol	Soil bulk density (g cm^{-3})	-0.4 – 0.4
r__SFTMP().sno	Snowfall temperature (°C)	-0.4 – 0.4
r__SMTMP().sno	Snow melt base temperature (°C)	-0.4 – 0.4
r__SMFMX().sno	Maximum melt rate for snow during the year (mm°C^{-1} day^{-1})	-0.4 – 0.4
r__SMFMN().sno	Minimum melt rate for snow during the year (mm°C^{-1} day^{-1})	-0.4 – 0.4
r__SLSUBBSN.hru	Average slope length (m)	-0.4 – 0.4
r__OV_N.hru	Manning's n value for overland flow	-0.4 – 0.4
r__HRU_SLP.hru	Average slope steepness (m m^{-1})	-0.4 – 0.4
r__CMN.bsn	Rate factor for humus mineralization of active organic nitrogen	-0.4 – 0.4
r__NPERCO.bsn	Nitrogen percolation coefficient	-0.4 – 0.4
r__N_UPDIS.bsn	Nitrogen uptake distribution parameter	-0.4 – 0.4
r__RCN.bsn	Concentration of nitrogen in rainfall (mg N L^{-1})	-0.4 – 0.4
r__SHALLST_N.gw	Concentration of nitrate in groundwater to streamflow (mg N L^{-1})	-0.4 – 0.4

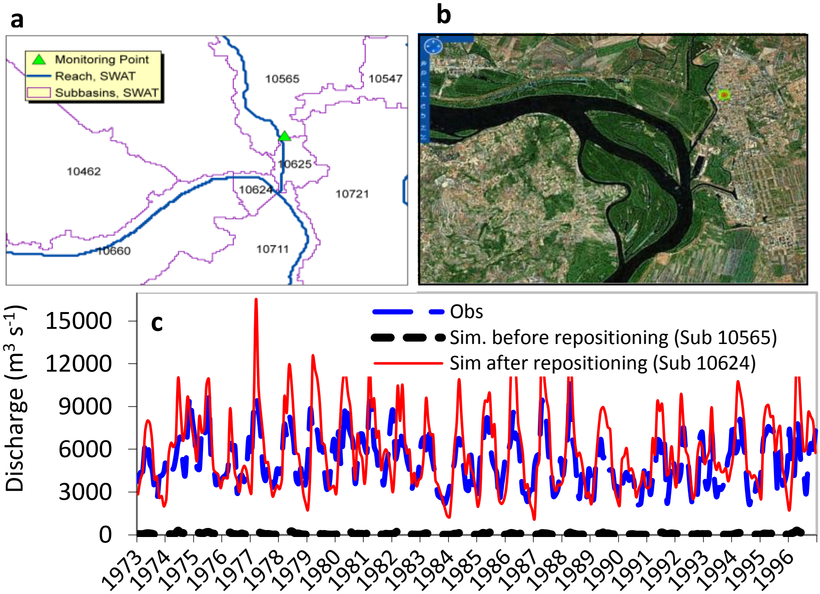

Figure 2.3. Example of a wrong positioning of the outlets due to errors in the reported coordinates of the measurement stations. The outlet's correct position is on the Danube River rather the Tamis River, a tributary of the Danube.

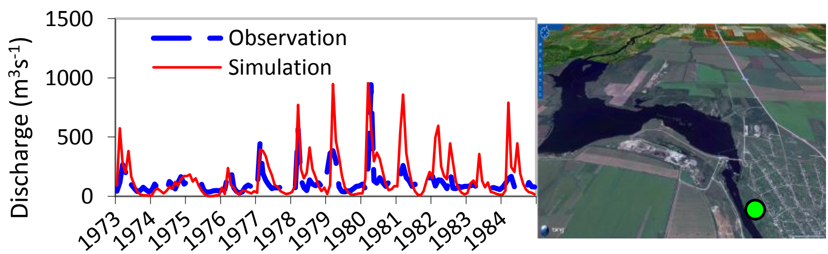

Figure 2.4. Example of an outlet being at the downstream of a reservoir. In the Southern Bug in Ukraine, Alexandra Reservoir came into operation in 1979. There is a clear change in the discharge pattern after the operation of the reservoir which could not be captured by the model.

Other major problems result from an outlet being positioned downstream of a reservoir. In particular, in Southern Bug in Ukraine, the simulated discharge and observations match quite well until the Alexandra Reservoir came into operation in 1979 (Figure 2.4). Clearly the dynamics of such outlets depend on the management of the reservoir and not natural processes. Other problematic situations may arise when outlets are in a highly populated or agricultural region where water management and water transfers are large. In these situations also, SWAT cannot be expected to produce proper results unless data is available. Constructions of dams for irrigation and power generation purposes as well as other water management practices such as water abstraction and diversion create major difficulties for model calibration. As management information are usually not available, proper cautions need to be taken during calibration. These include converting outlets to inlets, weighing those outlets under the influence of management less in the objective function, or removing the outlets downstream of reservoirs from the calibration process. Because of lack of water management data we excluded from calibration those outlets directly affected by infrastructures such as dams and reservoirs. After making appropriate corrections to badly simulated outlets, and obtaining relatively satisfactory discharge estimation, nitrate parameters (Table 2.1) were added to the parameter pool.

2.3.1.2. Parameterization

In subsequent iterations the model was parameterized. Parameterization refers to regionalization of parameters tailored to achieve the best response from the simulation program and individual outlets. Some examples are: if there is an early shift in the simulation (Figure 2.5a), then decreasing the overland flow (HRU_SLP) by 10-20%, increasing Manning's roughness coefficient (ON_N) by 10-30%, and increasing the flow length (SLSUBBSN) by 5-15 m in all the upstream subbasins of that outlet will improve the simulated discharge. Accordingly if the simulated base flow is too high (Figure 2.5b), then parameterization includes: increasing deep percolation loss (GWQMN), increasing groundwater revap coefficient (GW_REVAP) to a maximum of 0.4, and decreasing the threshold depth of water in shallow aquifer (REVAPMN) to a minimum of zero. In another example if the simulated peak flow is underestimated (Figure 2.5c), then the following adjustments to the upstream subbasins of that outlet should be made: increasing the curve number (CN2) by 10-15%, decreasing the soil available water storage capacity (SOL_AWC) by 5-10%, and decreasing the soil evaporation compensation factor (ESCO) by 20-30%. This will ensure a better simulation at the specified outlet. For every outlet, the upstream subbasins were parameterized as described above.

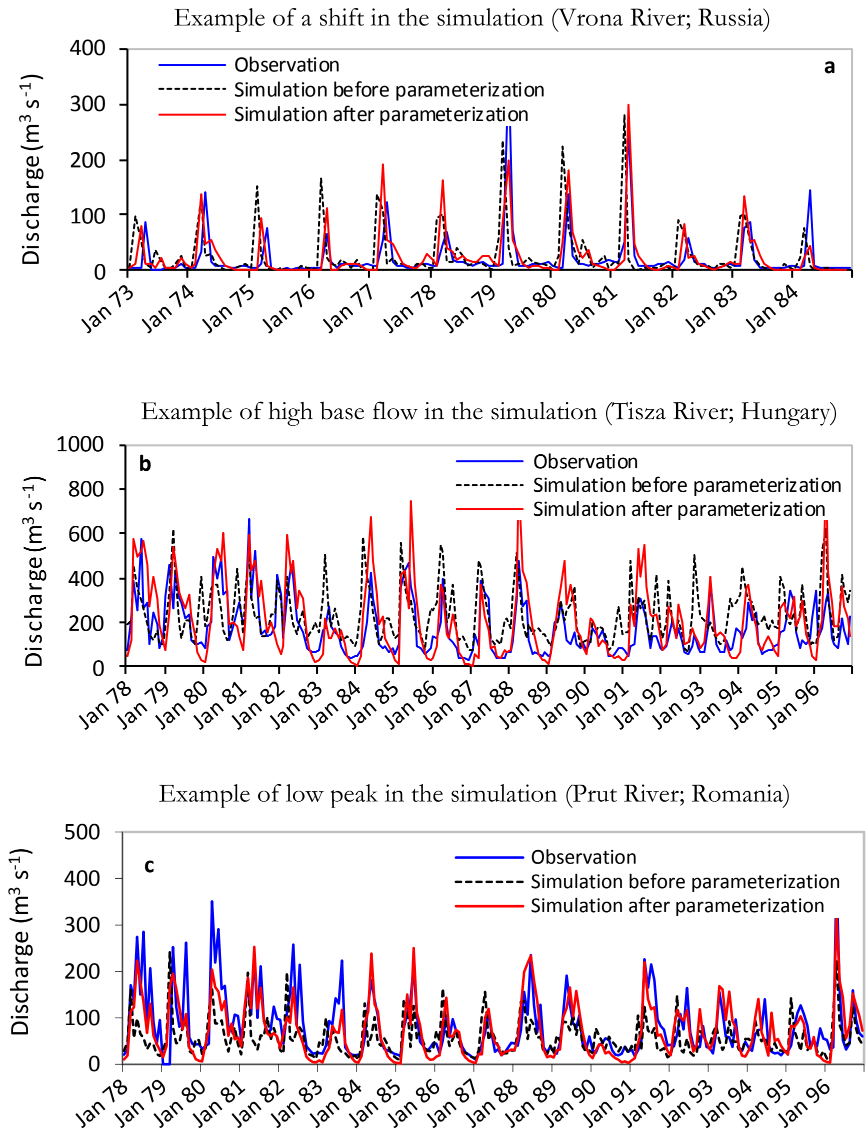

Figure 2.5. Examples of parameterization. Simulations are discrepant in terms of a shift, higher base flow, or lower peaks. In each case, relevant parameters are changed in all the upstream subbasins.

2.3.1.3. Calibration performance

The final calibration results for outlets that were used in model calibration range from very good to poor (Figure 2.1). The bR^2 statistic for discharge outlets range from 0.2 to 0.8, and for nitrate outlets from less than 0.1 to 0.7. The time series examples (Figure 2.6) for two outlets show good results in both calibration and validation periods.

It is important to note that the 95PPU represents model prediction and not the "best simulation". The latter is only provided for reference. Calibration is concerned with the problem of making inferences about physical systems from measured output variables of the model (e.g., river discharge, nitrate load, etc.). Because nearly all measurements are subject to some uncertainty, the inferences are usually statistical in nature. Furthermore, because one can only measure a limited number of (noisy) data and because physical systems are usually modeled by continuum equations, no calibration problem is really uniquely solvable [Abbaspour, et al. 2007]. In calibration, therefore, we characterize the set of models, mainly through assigning distributions (uncertainties) to the parameters that fit the data. We should also make the distinction here between uncertainty and error. Prediction uncertainty arises from the uncertainty in the parameters, in the model, and in the inputs. In the concept of SUFI-2, all these uncertainties are assigned to the parameter distributions. The uncertainty is expressed as the 95PPU, which as stated above is also the output of the model (Figure 2.6). Model error, however, is the degree in which the 95PPU does not account or does not bracket the observation. This, in SUFI-2, is indicated by (1 - *P-fcator*), which is around 20% for Daniper and 41% for Prut River (Figure 2.6). A closer examination of the Prut River simulation reveals that most of the error originates from the base flow simulation. Hence, the processes related to surface water-ground water interaction are not very well represented in the model in that region.

For a model to better represent a region of study we could introduce more attributes in the objective function. In this research, we used nitrate load as well as crop yield to achieve a model with more confidence in predicting the water balance components.

Water quality was simulated through nitrate loads in rivers. We were disappointed at the lack of more easily-available information in the BSB, especially with respect to water quality. Most of the information we gathered came from the Danube River Basin, therefore the water quality component of the Black Sea model should be considered as uncalibrated or at best partially calibrated for other river basins within the BSB. The simulations, however, were surprisingly satisfactory for most stations given that we had estimated the point sources and had only rough data with respect to diffuse sources of pollution in different countries (Figure 2.7). It is expected that nitrate simulation would be accompanied by much large prediction uncertainty due to larger uncertainty in the input data for point and diffuse sources. An interesting observation is the overestimation of the model at the stations near Danube Delta. As the river approaches the Delta, the concentration of nitrate decreases, but the model cannot account for this because deltas and wetlands are not represented in SWAT (Figure 2.8).

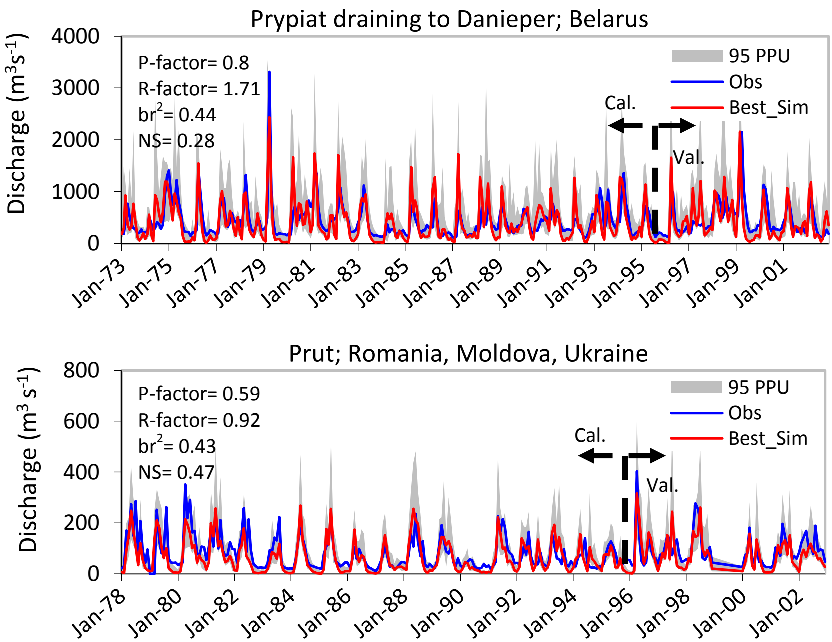

Figure 2.6. Comparison of simulated and observed discharges at Prypiat and Prut rivers for calibration and validation periods. The shaded region is 95% prediction uncertainty band. The best model simulation is also shown by the red line. The reported statistics are for the entire simulation period.

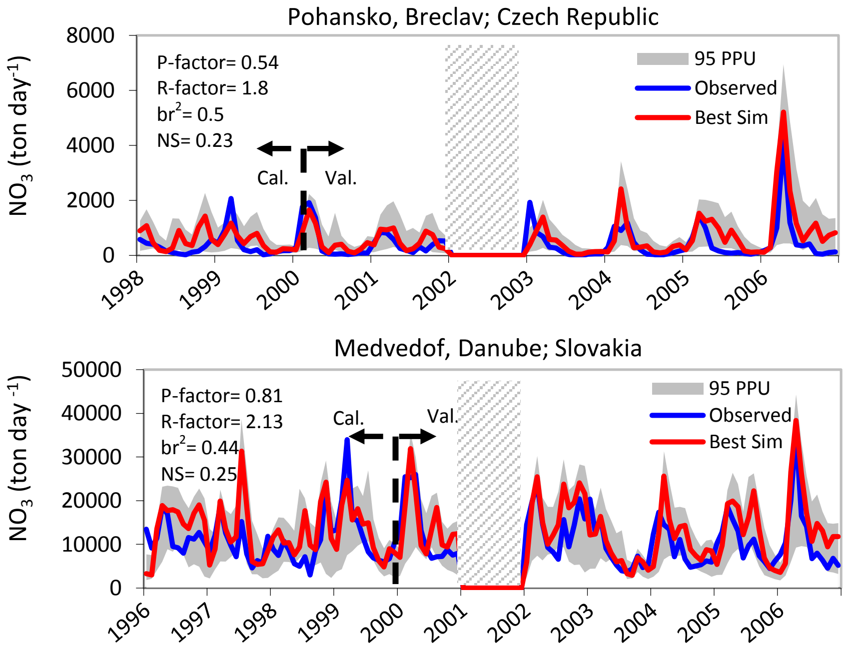

Figure 2.7. Comparison of simulated and observed nitrate loads in Dyje River in Czech Republic and Danube River in Slovakia for calibration and validation periods. The shaded region is 95% prediction uncertainty band. The best model simulation is also shown by the red line. The reported statistics are for the entire simulation period.

Because of a direct relationship between crop yield and evapotranspiration [Jensen, 1968; FAO, 1986], in addition to nitrate loads, we included yields of maize, barley, and wheat as extra target variables in the calibration process. With measured river discharges we can obtain a good knowledge of runoff, but cannot have any confidence with respect to soil moisture, evapotranspiration, or aquifer recharge. Knowledge of evapotranspiration through simulation of crop yield could, therefore, increase our confidence in soil moisture and aquifer recharge. Average annual yield of three major crops (barley, maize, and wheat) are simulated at subbasin level and aggregated per country for the duration of 1973-2006 and expressed as 95% prediction uncertainty

(Figure 2.9). The FAO yield data and the data from the McGill University fall inside or are close to the predicted bands. We note that the actual uncertainty should perhaps be larger than what we have reported here. In the final iteration some crop parameters (e.g., heat unit, harvest index, biomass target, etc.) were fixed to values obtained by manual calibration for the entire country and were not treated as uncertain. Crop parameters were parameterized based on crop type, management operation (e.g., planting time, harvest time, irrigation, fertilization, etc.), and region-specific operations, resulting in a large number of parameters. Their inclusion in the uncertainty analysis would require a large number of simulations, which was not feasible in the time span of the project. The discrepancies between the simulated and the reported yields could be due to a lack of knowledge of detailed agricultural management in different regions in our model, but also errors in the observed data, as there were also differences in the reported yields of FAO and McGill databases (Figure 2.9).

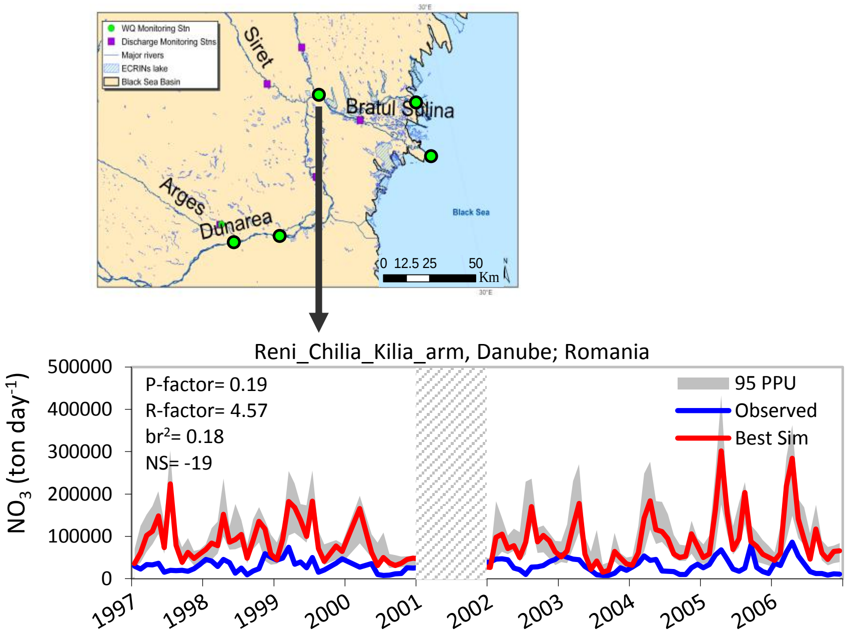

Figure 2.8. Decrease in river load as it enters the Danube Delta. Observation shows much lower load than model simulation since deltas and wetland processes are not accounted in the model.

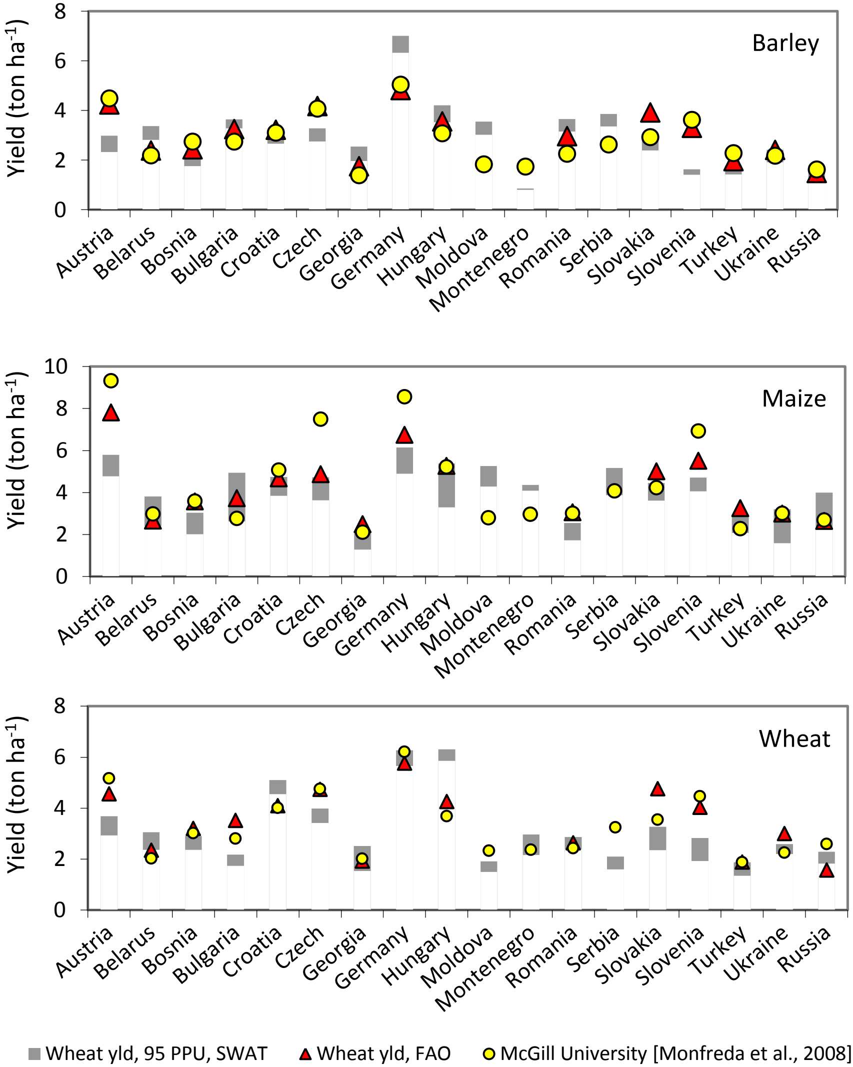

Figure 2.9. Subbasin yields are aggregated per country to compare with FAO's statistical reports and the report by McGill University. Some model discrepancies are due to lack of knowledge of detail management operations in different countries.

2.3.2. Quantification of water resources and their respective uncertainties

We used the calibrated BSB model to calculate water resources components: blue water, green water flow, and green water storage. These concepts give an overall picture of water resources, and bring the outputs of the BSB model closer to the needs of water resources researchers and policy makers. The upper and lower bounds of the 95% prediction uncertainties for the blue water (Figure 2.10a,b) show a wide range in some regions indicating the importance of uncertainty analysis in hydrological modeling. This uncertainty reflects primarily the prediction uncertainty (including model, parameters, and inputs) as well as the temporal climate variation as a secondary effect. The temporal variation is depicted by the coefficient of variation (CV) in Figure 2.10d. The simulated daily water fluxes have been accumulated on the annual basis and averaged for the years 1973-2006 at the subbasin level (Figure 2.10c). The latter map shows the distribution of the average annual freshwater availability. It is basically the water yield to stream flow from HRUs in the watershed (e.g., surface runoff, plus the lateral flow to the river, plus the shallow aquifer contribution to the rivers, minus pond abstraction and transmission losses) plus deep aquifer recharge. Transmission losses reflect the water lost from tributary channels in the HRUs via transmission through the bed.

Green water components are illustrated in Figure 2.11 along with their CVs. In each case, there are large spatial variations across the Basin. CV depicts the temporal variation and it is seen that green water storage or soil moisture is relatively less variable temporally in many regions. This indicates a higher reliability of this resource over time, and hence, a less risky opportunity for development of green, or rainfed agriculture.

The confidence on water resources estimates is relatively high because surface runoff as well as evapotranspiration (through crop yield) was satisfactorily calibrated in the model. For a further comparison with the reported literature we calculated the freshwater availability on country basis and compared them to the values of FAO (Figure 2.12). The simulation results are expressed as 95% prediction uncertainty bands. It is seen that the FAO-estimated water availability fall inside or are very close to the simulation 95PPU band in all countries. Summary of water resources for major BS countries are presented in Table 2.2.

Georgia is shown to have the largest blue water in mm yr^{-1}, and Bulgaria the smallest.

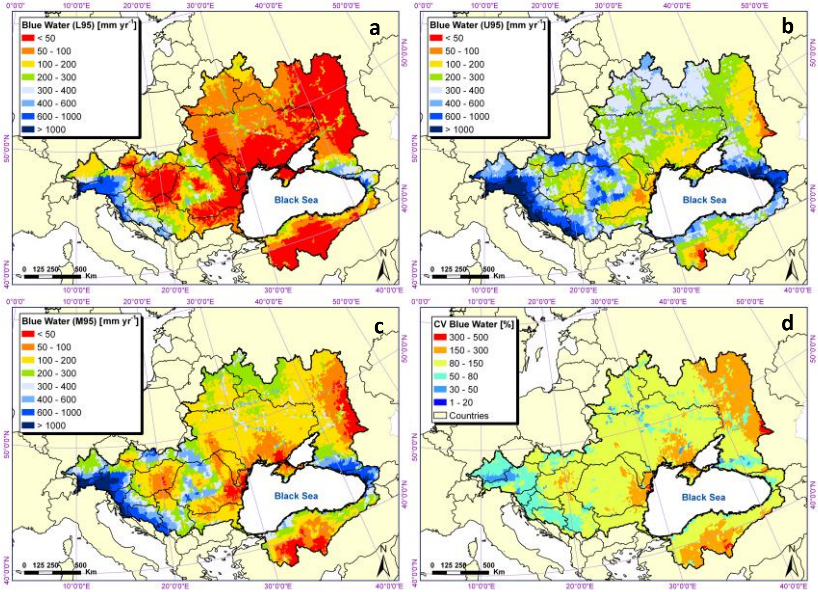

Figure 2.10. Annual averages of blue water at 12,982 modelled subbasins of Black Sea Basin expressed as: (a) lower (L95), (b) upper (U95), and (c) median (M95) of the 95% prediction uncertainty range, (d) coefficient of variation indicating temporal flocculation calculated for the period of 1973-2006.

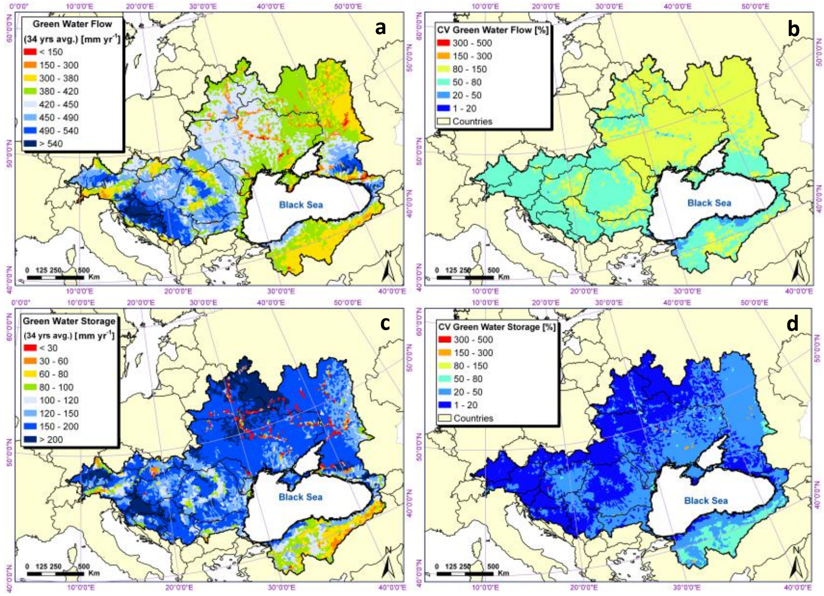

Figure 2.11. Long-term annual averages (1973-2006) of green water flow and green water storage at subbasin level in the Black Sea Basin (a,c). The coefficients of variation (CV) on the right (b,d) show the temporal variability in each component (1973-2006). A low CV indicates a higher reliability of that resource.

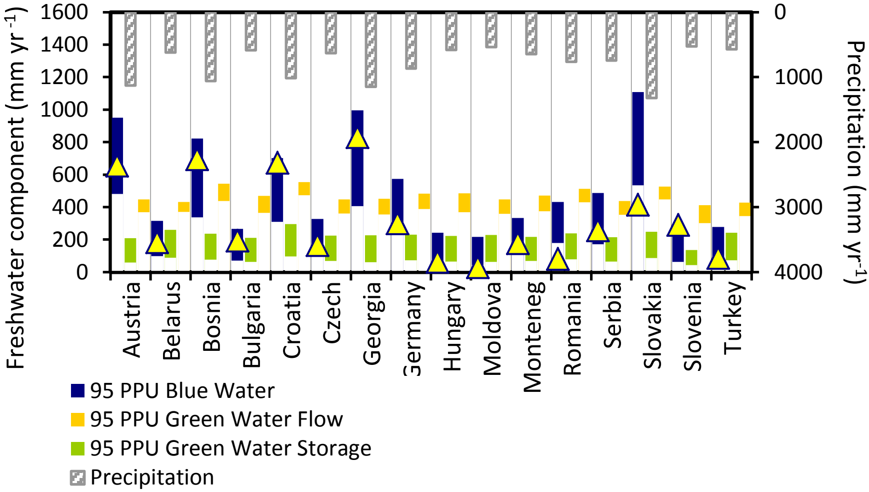

Figure 2.12. Comparison of simulated average annual freshwater availability (blue water, green water flow, and green water storage) per country for the duration of 1973-2006 expressed as 95% prediction uncertainties and precipitation. FAO estimates on internal renewable water resources (blue water) are provided as a comparison.

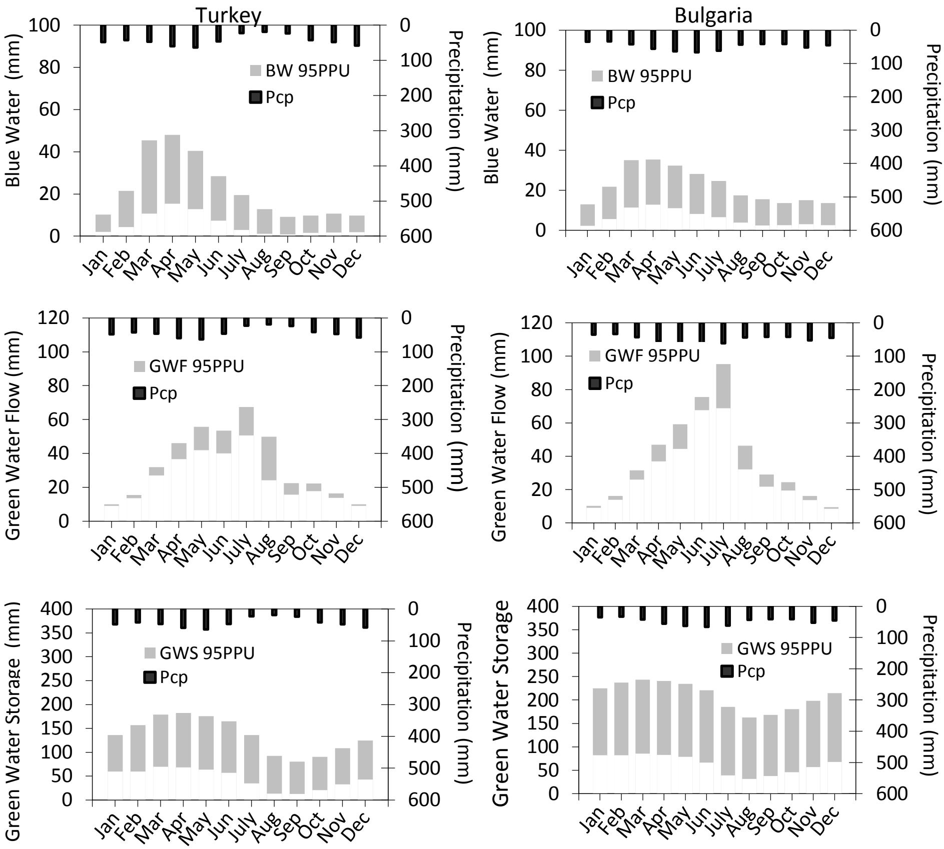

Figure 2.13. Average (1973-2006) monthly 95% prediction uncertainty distributions of fresh water availability components (blue water, green water flow, and green water storage) in Turkey and Bulgaria.

Knowledge of the long-term time series of water availability is very important in water management and planning studies, water transfers, reservoir operation, and conjunctive water analyses. Many countries have large monthly variabilities in the blue and green water components as illustrated, for example, by the long-term monthly variations in Turkey and Bulgaria (Figure 2.13). It is interesting to note that soil moisture (green water storage) is larger in Bulgaria than in

Turkey; while Turkey's blue water is larger. We could conclude that as a whole, runoff is larger in Turkey, while the share of infiltration is greater in Bulgaria. The large uncertainty in green water storage in Bulgaria appears to be dominated by large annual variation in precipitation (Figure 2.2b).

Table 2.2. Fresh water availability and per capita water resources of Black Sea Basin countries. Precipitation is presented as the average rainfall in the simulation period. The 95% prediction uncertainty ranges are shown for water resources components. The lower and upper bounds are averaged over the period of 1973-2006.

Country	**Area (km^2)**	**Pcp ($mm\ yr^{-1}$)**	**Blue Water ($mm\ yr^{-1}$)**	**Green Water Flow ($mm\ yr^{-1}$)**	**Green Water Storage (mm)**	**Per Capita Blue Water Availability ($m^3\ capita^{-1} yr^{-1}$)**
Austria	83870	1124	481 - 951	369 - 448	60 - 208	5331 - 10544
Belarus	202900	617	99 - 315	371 - 432	89 - 260	3292 - 10455
Bosnia	51129	1059	338 - 823	438 - 545	77 - 236	5686 - 13865
Bulgaria	108489	585	72 - 265	364 - 469	63 - 212	1667 - 6167
Croatia	55974	1015	309 - 702	473 - 555	96 - 295	5967 - 13549
Czech	79000	627	96 - 327	360 - 448	68 - 224	2833 - 9589
Georgia	70000	1144	406 - 995	355 - 452	61 - 226	13683 - 33572
Germany	357022	862	242 - 574	389 - 483	72 - 231	9012 - 21388
Hungary	93030	579	46 - 242	368 - 486	64 - 223	443 - 2337
Moldova	33843	536	44 - 218	358 - 448	63 - 228	358 - 1769
Romania	238300	643	106 - 333	375 - 470	68 - 217	1168 - 3648
Serbia	102350	760	180 - 433	431 - 513	78 - 238	2114 - 5093
Slovakia	48845	739	172 - 487	352 - 438	65 - 214	1638 - 4643
Slovenia	20253	1319	534 - 1109	448 - 527	86 - 249	5427 - 11267
Turkey	780000	526	63 - 269	302 - 412	44 - 137	1850 - 7883
Ukraine	603000	568	73 - 279	344 - 427	72 - 242	959 - 3676
Russia	1719712	564	74 - 306	326 -407	71 - 241	5654 - 23271

2.3.3 Transboundary rivers

As measurements cannot be made at all transboundary points and for all variables, models can play an important role. We use the example of Dniester River to show the ability of the model to address some transboundary issues. Dniester (1,380 km) has its source in the Carpathian Mountains in Ukraine, flowing south and east along the territory of Moldova, and re-entering Ukraine near the Black Sea coast (Figure 2.14a). The Dniester is the main source of drinking water in Moldova and is no less important for a significant part of Ukraine, particularly the Odessa Region. Hydropower is one of the major sectors affecting the ecological status of the Dniester Basin. The Dniester flow in its middle section was dammed to fill a chain of reservoirs, the largest of them being the Dubossary (1954) and Dniestrovsky (1983) reservoirs. Large areas of intensive irrigated agriculture, both in Ukraine and Moldova, and soil erosion contribute significantly to the contamination of water bodies by nutrients and chemical fertilizers [OSCE/UNECE, 2005].

The simulation of discharge and nitrate loads just before the Dniester River enters Moldova and right after it leaves the country (Figure 2.14b,c) shows an increase in the discharge with larger peaks as well as a significant increase in nitrate load as the river leaves Moldova. Such analyses can serve as important instruments in resolving transboundary conflicts and lead to a better management of the transboundary rivers.

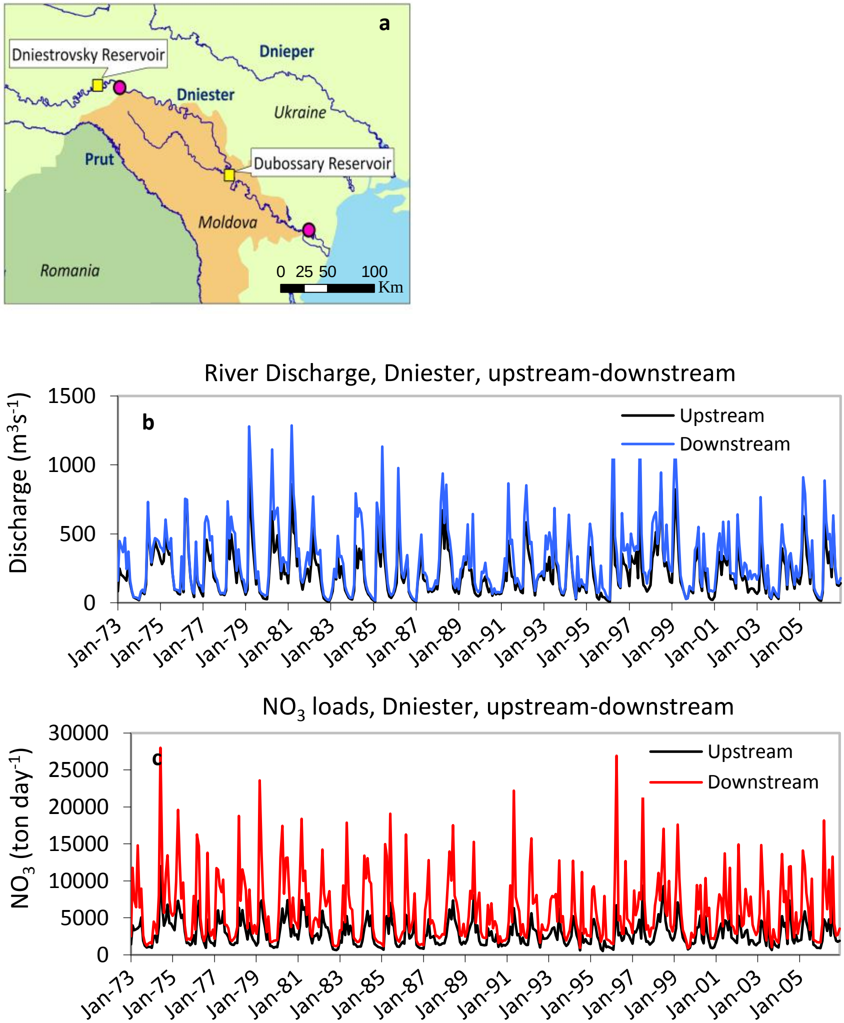

Figure 2.14. Dnieper Transboundary River crossing Ukraine-Moldova boarder and entering Ukraine again. Discharges and nitrate loads are shown at the entry (upstream) and exit (downstream) points in Moldova.

2.4. Summary and Conclusion

In this study, we aimed for building a high-resolution hydrological model for the Black Sea Basin. The objective was to quantify water resources availability and water quality in terms of nitrate load at subbasin spatial and monthly temporal level. We used the SWAT model for this purpose and calibrated the model using SUFI-2 algorithm, which ran on a grid network. The calibration was based on river discharge, crop growth, and river nitrate load at multiple sites. As there are often no data on soil moisture, evapotranspiration, or aquifer recharge, we used crop yield as a surrogate to add confidence on the distribution of the components of the infiltrated water. The calibration and validation results were quite satisfactory for a large number of outlets for both discharge and nitrate loads. As a consequence, our confidence on the estimated water resources is high. However, as nitrate data was only available for the Danube Basin, nitrate load estimation at other areas should be considered as less reliable.

The model output included blue water flow, green water flow, and green water storage as well as nitrate load, and crop yields. We identified water scarce regions, and showed how the model could provide information on transboundary water issues such as natural flows and pollution loads. Regions in Ukraine and Romania bordering the Black Sea and parts of Turkey and Russia in the Basin experience the highest water deficit. Model outputs could be used to establish environmental goals, planning of remedial measures and development of monitoring strategies. Much more results and analysis could be obtained with the model developed in this study, such as calculation of freshwater and nutrient fluxes in to the Sea. In the next phase of the study, we will use results of land use and climate change models to describe variability in hydrological water balance and nutrient load for future conditions.

Based on the results of this study, we conclude that given the present technologies it is possible to build a high resolution model of a large basin. What could provide more confidence in the model result is more discharge and water quality data (nitrate, phosphate, sediment, etc.) and higher resolution crop yield data for model calibration.

Acknowledgment

This project has been funded by the European Commission's Seventh Research Framework through the enviroGRIDS project (Grant Agreement n 226740). The authors are especially grateful to Envirogrid partners for contributing data to this project: Alex Hebort from International Commission for the Protection of the Danube River (ICPDR), Gencay Serter from Turkish Ministry of Forest and Water Affairs (MEF), Romanian National Institute of Hydrology and Water Management (INHGA), Danube Delta National Institute for Research and Development (DDNI) in Romania. Special thanks to Dr. Dorian Gorgan and his team in Cluje Technical University for their support on calibration execution on grids. We are also grateful to Prof. Dr. Rainer Schulin from ETH Zurich University for their valuable comments and discussions for this work.

References

Abbaspour, K. C. (2011), User manual for SWAT-CUP, SWAT calibration and uncertainty analysis programs, 103 pp., Eawag: Swiss Federal Institute of Aquatic Science and Technology, Duebendorf, Switzerland, http://www.eawag.ch/forschung/siam/software/swat/index.

Abbaspour, K. C., C. A. Johnson, and M. Th. van Genuchten (2004), Estimating Uncertain Flow and Transport Parameters Using a Sequential Uncertainty Fitting Procedure, J. Vadouse Zone, 3 (4), 1340-1352.

Abbaspour, K. C., J. Yang, I. Maximov, R. Siber, K. Bogner, J. Mieleitner, J. Zobrist, and R. Srinivasan (2007), Modelling hydrology and water quality in the pre-Alpine/Alpine Thur watershed using SWAT. J. Hydrology, 333, 413-430, doi: http://dx.doi.org/10.1016/j.jhydrol.2006.09.014.

Alcamo, J., P. Döll, T. Henrichs, F. Kaspar, B. Lehner, T. Rösch, and S. Siebert (2003), Development and testing of the WaterGAP 2 global model of water use and availability, Hydrological Sciences Journal, 48(3), 317-338.

Arnold, J. G., R. Srinivasan., R. S. Muttiah., and J. R. Williams (1998), Large area hydrologic modeling and assessment part I: model development. Journal of American Water Resources Association, 34 (1), 73-89.

Aus der Beek, T., L. Menzel, R. Rietbroek, L. Fenoglio-Marc, S. Grayekd, M. Becker, J. Kusche, and E. V. Stanev (2012), Modeling the water resources of the Black and Mediterranean Sea river basins and their impact on regional mass changes, J. Geodynamics, 59–60, 157–167.

Black Sea Investment Facility (BSEI) (2005), 'Review of the Black Sea Environmental Protection Activities. General review', Black Sea Investment Facility.

Center for International Earth Science Information Network (CIESIN), Columbia University; United Nations Food and Agriculture Programme (FAO); and Centro Internacional de Agricultura Tropical (CIAT) (2005), Gridded Population of the World: Future Estimates (GPWFE). Palisades, NY: Socioeconomic Data and Applications Center (SEDAC), Columbia University. Available at http://sedac.ciesin.columbia.edu/gpw

Climatic Research Unit (CRU) (2008), CRU Time Series (TS) high resolution gridded datasets, University of East Anglia Climatic Research Unit (CRU), NCAS British Atmospheric Data Centre, Available from: http://badc.nerc.ac.uk/view/badc.nerc.ac.uk__ATOM__dataent_1256223773328276.

Döll, P., F. Kaspar, and B. Lehner (2003), A global hydrological model for deriving water availability indicators: model tuning and validation, J. Hydrology, 270 (1-2), 105-134.

Dumont, E., R. Williams, V. Keller, A. Voss, and S. Tattari, (2012), Modelling indicators of water security, water pollution and aquatic biodiversity in Europe, Hydrol Sci J 57:1378-1403.

EEA Catchments and Rivers Network System (ECRINS) v1.1 (2012), Rationales, building and improving for widening uses to Water Accounts and WISE applications, Luxembourg: Publications Office of the European Union, ISBN 978-92-9213-320-7, ISSN 1725-2237, doi:10.2800/51667.

European Environmental Agency (EEA) (2010), The European environment — state and outlook 2010: synthesis. European Environment Agency, Copenhagen.

Environmental Space Agency (ESA) (2008), ESA GlobCover Project, led by MEDIAS-France/POSTEL, Data access: ESA GCAT web site: http://www.esa.int/due/ionia/globcover.

Environmental Space Agency (ESA) (2010), ESA GlobCorine Project, Led by Université Catholique de Louvain, Data access: http://dup.esrin.esa.int/ionia/globcorine/products.asp.

Falkenmark, M., J. Rockström (2006), The new blue and green water paradigm: Breaking new ground for water resources planning and management. J. Water Resour. Plann. Manage.: ASCE 132 (3), 129–132.

Faramarzi, M., K. C. Abbaspour, R. Schulin, and H. Yang (2009), Modelling blue and green water resources availability in Iran, J. Hydrol. Process., 23, 486–501, doi: 10.1002/hyp.7160.

Food and Agricultural Organization Statistics (FAOSTAT) (2013), http://faostat3.fao.org/faostat-gateway/go/to/home/E

Food and Agricultural Organization (FAO) (1995), The digital soil map of the world and derived soil properties, CD-ROM, Version 3.5, Rome, Italy.

Food and Agricultural Organization (FAO) (1986), Early Agrometeorological crop yield forecasting. FAO Plant Production and Protection paper No. 73, by M. Frère and G.F. Popov. FAO, Rome, Italy.

Gassman, P.W., M. R. Reyes, C. H. Green, and J. G. Arnold (2007), The soil and water assessment tool: Historical development, applications, and future research directions, J. American Society of Agricultural and Bio Engineering (Asabe), 50, 1211–1250.

Global International Waters Assessment (GIWA), (2005), Global International Waters Assessment Transboundary Waters in the Black Sea-Danube region, 53pp.

Global Runoff Data Centre (GRDC) (2011), Long-Term Mean Monthly Discharges and Annual Characteristics of GRDC Station / Global Runoff Data Centre. Koblenz, Germany: Federal Institute of Hydrology (BfG), http://grdc.bafg.de.

Gorgan, D., V. Bacu, D. Mihon, D. Rodila, K. Abbaspour, and E. Rouholahnejad (2012), Grid based calibration of SWAT hydrological models, J. Nat. Hazards Earth Syst. Sci., 12, 2411–2423, doi:10.5194/nhess-12-2411-20.

Grizzetti, B., F. Bouraoui, and G. De Marsily (2008), Assessing nitrogen pressures on European surface water, Global Biogeochem. Cycles, 22, GB4023, doi:10.1029/2007GB003085.

Hargreaves G. L., G. H. Hargreaves, J. P. Riley (1985). Agricultural benefits for Senegal River Basin. J. Irrigation and Drainage Engineering, 111, 113–124.

Haylock, M. R., N. Hofstra, A. M. G. Klein Tank, E. J. Klok, P. D. Jones and M. New (2008), A European daily high-resolution gridded dataset of surface temperature and precipitation. J. Geophys. Res (Atmospheres), 113, D20119, doi:10.1029/2008JD10201.

Holvoet, K., A. van Griensven, P. Seuntjens, and P. A. Vanrolleghem (2005), Sensitivity analysis for hydrology and pesticide supply towards the river in SWAT, J. Phys. Chem. Earth, 30, 518–526, doi:10.1016/j.pce.2005.07.006.

IPCC (2007), Climate Change 2007 - Impacts, Adaptation and Vulnerability - Contribution of Working Group II to the Fourth Assessment Report of the IPCC, ISBN 978 0521 88010-7.

Jarvis, A., H. I. Reuter, A. Nelson, and E. Guevara (2008), Hole-filled SRTM for the globe Version 4, Data access: The CGIAR-CSI SRTM 90m Database: http://srtm.csi.cgiar.org.

Jensen, M. E. (1968), Water consumption by agricultural plants. In: Kozlowski TT (ed) Water deficits and plants growth, vol II. Academic Press, New York, 1–22.

Krause P., D. P. Boyle,and F. Bäse (2005), Comparison of different efficiency criteria for hydrological model assessment, J. Advanced Geosciences, 5, 89–97.

Ludwig, W., E. Dumont, M. Meybeck, and S. Heussner (2009), River discharges of water and nutrients to the Mediterranean and Black Sea: Major drivers for ecosystem changes during past and future decades?, J. Progress in Oceanography, 80, 199-217.

Meigh, J. R., A. A. McKenzie, and K. J. Sene, (1999), A grid-based approach to water scarcity estimates for eastern and southern Africa. Water Resources Management, 13, 85–115.

Mitchell, T. D. and P. D. Jones (2005), An improved method of constructing a database of monthly climate observations and associated high-resolution grids, Int. J. Climatology, 25, 693-712, doi: 10.1002/joc.1181.

Monfreda, C., N. Ramankutty, and J. A. Foley (2008), Farming the planet: 2. Geographic distribution of crop areas, yields, physiological types, and net primary production in the year 2000, J. Global Biogeochemical Cycles, 22, GB1022, doi:10.1029/2007GB002947.

NASA (2001), Land Processes Distributed Active Archive Center (LP DAAC), ASTER L1B, USGS/Earth Resources Observation and Science (EROS) Center, Sioux Falls, South Dakota, Data access: http://lpdaac.usgs.gov.

National Climate Data Center (NCDC) , http://www.climate.gov/#dataServices/dataLibrary.

Neitsch, S. L., J. G. Arnold, J. R. Kiniry, and J. R. Williams (2009), Soil and Water Assessment Tool, Theoretical Documentation, Version 2009, Grassland, Soil and Water Research Laboratory, Agricultural Research Service and Blackland Research Center, Texas Agricultural Experiment Station, Temple, Texas, USA.

OSCE/UNECE (2005), Transboundary Co-operation and Sustainable Management of the Dniester River, Transboundary Diagnostic Study for the Dniester River Basin. Environment, Housing and Land Management Division United Nations Economic Commission for Europe and Office of the Co-ordinator of OSCE Economic and Environmental Activities, 76p.

Paleari, S., P. Heinonen, E. Rautalahti-Miettinen, and D. Daler (2005), Transboundary Waters in the Black Sea-Danube region; Legal and financial implications. University of Kalmar, Kalmar, Sweden.

Portmann, F. T., S. Siebert, and P. Döll, (2010), MIRCA2000 Global monthly irrigated and rainfed crop areas around the year 2000: A new high resolution data set for agricultural and hydrological modeling, J. GLOBAL BIOGEOCHEMICAL CYCLES, 24, GB1011, doi:10.1029/2008GB003435.

Ritchie, J. T., (1972), Model for Predicting Evaporation from a Row Crop with Incomplete Cover,Water Resour. Res., 8, 1204–1213.

Rouholahnejad, E., K. C. Abbaspour, M. Vejdani, R. Srinivasan, R. Schulin, and A. Lehmann (2012), A parallelization framework for calibration of hydrological models, J. Environmental Modelling & Software, 31, 28–36, doi:http://dx.doi.org/10.1016/j.envsoft.2011.12.001.

Sommerwerk, N., C. Baumgartner, J. Bloesch, T. Hein, A. Ostojić, M. Paunović, M. Schneider-Jacoby, R. Siber, and K. Tockner (2009), Rivers of Europe, Chapter 3 – The Danube River Basin, 59- 112, Elsevier, doi: http://dx.doi.org/10.1016/B978-0-12-369449-2.00003-5.

Stanners, D. and P. Bourdeau (1995), "Europe's Environment: The Dobris Assessment," European Environment Agency Task Force, European Environment Agency, Copenhagen, Denmark.

Sukhodolov, A. N., N. S. Loboda, V. M. Katolikov, N. A. Arnaut, V. V. Bekh, M. A. Usatii, L. A. Kudersky, and B. G. Skakalsky (2009), Rivers of Europe, Chapter 13 – Western Steppic Rivers, 497–523, Esevier, doi: http://dx.doi.org/10.1016/B978-0-12-369449-2.00013-8.

Tockner, K., U. Uehlinger, and C. T. Robinson (2009), Rivers of Europe, Academic Press, ISBN: 978-0-12-369449-2.

U. S. Geological Survey (USGS) (2008), Global Land Use Land Cover Characterization (GLCC) database, Data access: http://edc2.usgs.gov/glcc/globdoc2_0.php.

United Nations Environmental Program (UNEP) (2005), Eutrophication in the Black Sea Region: impact assessment and causal chain analysis, University of Kalmar, Sweden.

United Nation Environment Program (UNEP) (2006), Africa Environment Outlook 2, Our environment, our wealth. Division of early warning and assessment, Nairobi, Kenya.

Wang, X., X. He, J. R. Williams, R. C. Izaurralde, and J. D. Atwood (2005), Sensitivity and uncertainty analyses of crop yields and soil organic carbon simulated with EPIC, American Society of Agricultural Engineers (ASAE), 48, 1041–1054.

Water Agenda 21 (2011), Watershed Management. Guiding Principles for Integrated Management of Water in Switzerland. Bern, 20 pages.

Weedon, G. P., S. Gomes, P. Viterbo, W. J. Shuttleworth, E. Blyth, H. Österle, J. C. Adam, N. Bellouin, O. Bouche, and M. Best (2011), Creation of the WATCH Forcing Data and Its Use to Assess Global and Regional Reference Crop Evaporation over Land during the Twentieth Century, J. Water and Global change (WATCH), Special Collection, 823-848.

Wissenschaftlicher Beirat Globale Umweltveränderung (WBGU) (2007), World in Transition: Climate Change as Security Risk, German edition published in 2007 entitled Welt im Wandel: Sicherheitsrisiko Klimawandel, Springer-Verlag Berlin, Heidelberg, New York, 2008 ISBN 978-3-540-73247-1.

Wolfram, M., and H. Bach (2009), PROMET – Large scale distributed hydrological modelling to study the impact of climate change on the water flows of mountain watersheds, J. Hydrology, 376 (3-4), 362-377, doi: http://dx.doi.org/10.1016/j.jhydrol.2009.07.046.

Yang, J., P. Reichert, K. C. Abbaspour, J. Xia, and H. Yang (2008), Comparing uncertainty analysis techniques for a SWAT application to Chaohe Basin in China, J. of Hydrology, 358, 1–23, doi:10.1016/j.jhydrol.2008.05.012.

Zessner, M., and S. Lindtner (2005), Estimations of municipal point source pollution in the context of river basin management, J. Water Science & Technology, 52 (9), 175–182.

Environmental Modelling and Software, 31, (2012), 28-36

3. A parallelization framework for calibration of hydrological models

E. Rouholahnejad[a], K.C. Abbaspour[a], M. Vejdani[b], R. Srinivasan[c], R. Schulin[d], A. Lehmann[e]

[a] Eawag, Swiss Federal Institute of Aquatic Science and Technology, Ueberlandstrasse 133, CH-8600 Duebendorf, Switzerland

[b] Neprash Technology, 1625 Sundew Pl, Coquitlam, B.C., V3E 2Y4, Canada

[c.] Spatial Sciences Laboratory, Texas A&M University, Texas Agricultural, Experimental Station, College Station, Texas, USA

[d] ETH Zürich Institute of Terrestrial Ecosystem, Universitätstr. 16, 8092 Zürich, Switzerland

[e.] University of Geneva, Climatic Change and Climate Impacts, 7 Route de Drize, CH-1227 Carouge, Switzerland

Abstract

Large-scale hydrologic models are being used more and more in watershed management and decision making. Sometimes rapid modeling and analysis is needed to deal with emergency environmental disasters. However, time is often a major impediment in the calibration and application of these models. To overcome this, most projects are run with fewer simulations, resulting in less-than-optimum solutions. In recent years, running time-consuming projects on gridded networks or clouds in Linux systems has become more and more prevalent. But this technology, aside from being tedious to use, has not yet become fully available for common usage in research, teaching, and small to medium-size applications. In this paper we explain a methodology where a parallel processing scheme is constructed to work in the Windows platform. We have parallelized the calibration of the SWAT (Soil and Water Assessment Tool) hydrological model, where one could submit many simultaneous jobs taking advantage of the capabilities of modern PC and laptops. This offers a powerful alternative to the use of grid or cloud computing. Parallel processing is implemented in SWAT-CUP (SWAT Calibration and Uncertainty Procedures) using the optimization program SUFI2 (Sequential Uncertainty FItting ver. 2). We tested the program with large, medium, and small-size hydrologic models on several computer systems, including PCs, laptops, and servers with up to 24 CPUs. The performance was judged by calculating speedup, efficiency, and CPU usage. In each case, the parallelized version performed much faster than the non-parallelized version, resulting in substantial time saving in model calibration.

KEYWORDS: Parallel processing, SWAT-CUP, SUFI2, Hydrologic models

3.1. Introduction

Advances in GIS technology and interfacing of hydrological programs with advanced GIS systems allow the construction of high resolution large-scale models. However, the execution time of these models can be rather long, not allowing proper model calibration and uncertainty analysis. For this reason, in the last few years, the use of distributed computing in the form of grid and cloud computing has become increasingly prevalent. Distributed hydrologic models are especially difficult to calibrate because of reasons such as time constraints, difficulties in parameterization, non-uniqueness (having more than one acceptable solution), uncertainties in the conceptual model, and model inputs. In this paper we address the problem of computation time and describe a system where an optimization algorithm, SUFI2, is used in a parallel processing scheme to run on Windows-based computers. The parallel processing scheme developed here utilizes the existing capabilities of the available systems and is ideal for performing hydrologic model calibration and uncertainty analysis.

Distributed computing is an extension of the object-oriented programming concept of abstraction (Sundaram, 2010). Abstraction removes the complex working details from visibility. All that is visible is an interface which receives inputs and provides outputs. How these outputs are computed is completely hidden. Grid and cloud computing and parallel processing belong to the family of distributed computing. Currently, two different ways are pursuit in parallelizing hydrological models. One is parallelization of the code itself to be run as parallel threads (Neal et al., 2010; Li et al., 2011), and another is to submit model runs with different parameters to different CPUs (or GPUs) on the same or different computers (Lecca, 2011; Sing et al., 2011; Kalayanapu et al., 2011). Jobs submitted to a network of computers are run on grid and cloud. Below is a brief definition of these systems and their advantages and disadvantages.

A *grid network* is a computer network consisting of a number of computers connected in a grid topology. Some advantages of grid computing are: there is no need to buy expensive symmetric multiprocessing (SMP) servers for applications that can be split up and distributed to less powerful servers; much more efficient use of idle resources is made; grid environments are much more modular and don't have single points of failure; and jobs can be executed in parallel, speeding up the performance (Fernandez-Quiruelas, et al., 2011; Vassilios, 2008).

Some disadvantages of the grid are: memory intensive applications that can't take advantage of message passing interface (MPI) may not be able to take advantage of the grid system; a fast connection between computer resources (gigabit Ethernet at a minimum) is needed in intense MPI applications; some applications may need to be tweaked to take full advantage of a new model; licensing across many servers may make it prohibitively expensive for some applications; and political challenges associated with sharing resources across different administration domains may also prohibit the use of grids for many users (Taylor et al., 2004).

Cloud computing is Internet-based computing whereby shared resources, software, and information are provided to computers and other devices on demand, like the electricity grid. Similar to grid computing, some of the advantages offered by cloud computing are: lower computer costs, improved performance with less use of computer memory, virtually unlimited storage capacity, increased data reliability, universal document access, and easier group collaboration. There are also a number of disadvantages associated with cloud computing, which include: requiring a constant high-speed Internet connection, and not getting an instantaneous connection if the cloud servers are busy. It is the opinion of some experts that security may be a disadvantage of the cloud (Miller, 2009). Theoretically, data stored in the cloud should be safe because it is replicated across multiple machines. But in the case of missing data, there is no physical or local backup (unless data is methodically downloaded).

Parallel processing or *parallel computing* is the ability to carry out multiple operations or tasks simultaneously. In parallel processing more than one CPU or processor core is used to execute a program or multiple computational threads. Parallel processing makes programs run faster because there are more CPUs or cores running it. In practice, it is often difficult to divide a program in such a way that separate CPUs can execute different portions without interfering with each other. Older computers have just one CPU, but newer computers have multi-core processor chips and many CPUs. With single-CPU, or single-core computers, it is also possible to perform parallel processing by connecting the computers in a network. However, this type of parallel processing requires very sophisticated distributed processing software. The main advantages of the system we have developed is that: it does not have the disadvantages of the grid and cloud; but it has all the advantages of using a PC. These include: the user being in full control of the job being processed; the job can be stopped and restarted at any time; a PC is much simpler to use, not needing grid or cloud certificate and permission. For very large models, a powerful computer (e.g., 24-48 CPUs with >16 GB RAM) is, however, needed to take full advantage of parallel processing. With the advancement of new technologies, this is now available at a reasonable cost.

In the current paper we describe and test a parallel processing software that allows calibration of the hydrologic simulator Soil Water Assessment Tool (SWAT) (Arnold et al., 1998), which is linked to five different optimization schemes in the SWAT-CUP software package (Figure 3.1). SWAT-CUP is a standalone program that links to SWAT's output text files set. Theoretically, any other model or optimization algorithm could be added to this package. Currently, however, the program SWAT is linked with the Generalized Likelihood Uncertainty Estimation (GLUE) (Beven and Binley, 1992), Sequential Uncertainty Fitting (SUFI2) (Abbaspour et al., 2004; 2007), Parameter Solution (ParaSol) (Van Griensven and Meixner, 2006), Markov chain Monte Carlo (MCMC) (e.g., Kuczera and Parent, 1998; Marshall et al., 2004; Vrugt et al., 2003), and Particle Swarm Optimization (PSO) (Kennedy and Eberhart, 1995). The parallel processing currently only supports SUFI2, which lends itself easily to parallelization as the program runs with independent parameter sets. Support for PSO is under development.

The objective of this paper is to describe the SUFI2 parallel processing algorithm as implemented in the SWAT-CUP. We compare the computation time of parallel SUFI2 by applying it to a small, a medium, and a large size SWAT project using different computer systems. This study is designed to investigate parallel processing issues not to perform a meaningful calibration task. Finally, we summarize the performance of the parallelization and the gains in time obtained by parallel processing.

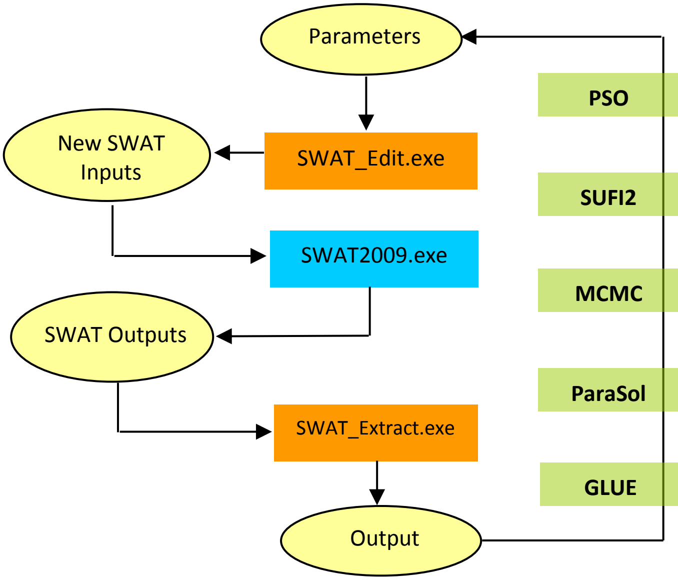

Figure 3.1. Structure of the SWAT-CUP and its linkage to five optimization algorithms.

3.2. Materials and Methods

3.2.1. The hydrologic simulator (SWAT)

SWAT is a process-based, river basin-scale, semi-distributed hydrologic model. The program has been developed to predict the impact of land management on water, sediment, and agricultural chemical yield in large, complex watersheds. SWAT is an integrated model including components such as weather, hydrology, soil, nutrients, pesticides, land management, bacteria and pathogens. The model is a computationally efficient simulator of hydrology and water quality at various scales which has been used in many international applications (Arnold and Allen, 1996; Abbaspour *et al.*, 2007; Yang *et al.*, 2007; Schuol *et al.*, 2008a, b). It includes procedures to describe how CO_2 concentration, precipitation, temperature, and humidity affect plant growth. It also simulates evapotranspiration, snow and runoff generation, and is used to investigate climate change impacts [Abbaspour et al., 2009; Eckhardt and Ulbrich, 2003; Fontaine et al., 2001].

SWAT is a continuous simulation model which operates on a daily time step. In SWAT the spatial heterogeneity of the watershed is taken into account, considering information from the Digitized Elevation Model, soils, and land use GIS data. Spatial parameterization of the SWAT model is performed by dividing the watershed into sub-basins based on topography. These are further subdivided into hydrologic response units (HRU) based on soil and land use characteristics. These data and related parameters are stored in text files. A high resolution project could easily result in thousands of input files, which would make it challenging to reconfigure or update model parameters. All SWAT's text input and output files reside in the TxtInOut directory. Initially, SWAT-CUP copies these files to a BACKUP directory, which remain unchanged throughout the calibration process.

3.2.2. SUFI2 Optimization Program

In Figure 3.2 a schematic diagram of the coupling between SUFI2 and SWAT is illustrated. Initially, a Latin hypercube (McKay et al., 1979) procedure draws samples from the spaces defined by user-supplied parameter ranges. This is the pre-processing stage executed by a batch file *SUFI2_pre.bat*, which runs the program *SUFI2_LH_sample.exe*. The parameter sets thus sampled are independent and for this reason parallel runs could be executed. Theoretically, all samples could be run at once, hence an entire iteration would require only the time that it takes to make one model run.

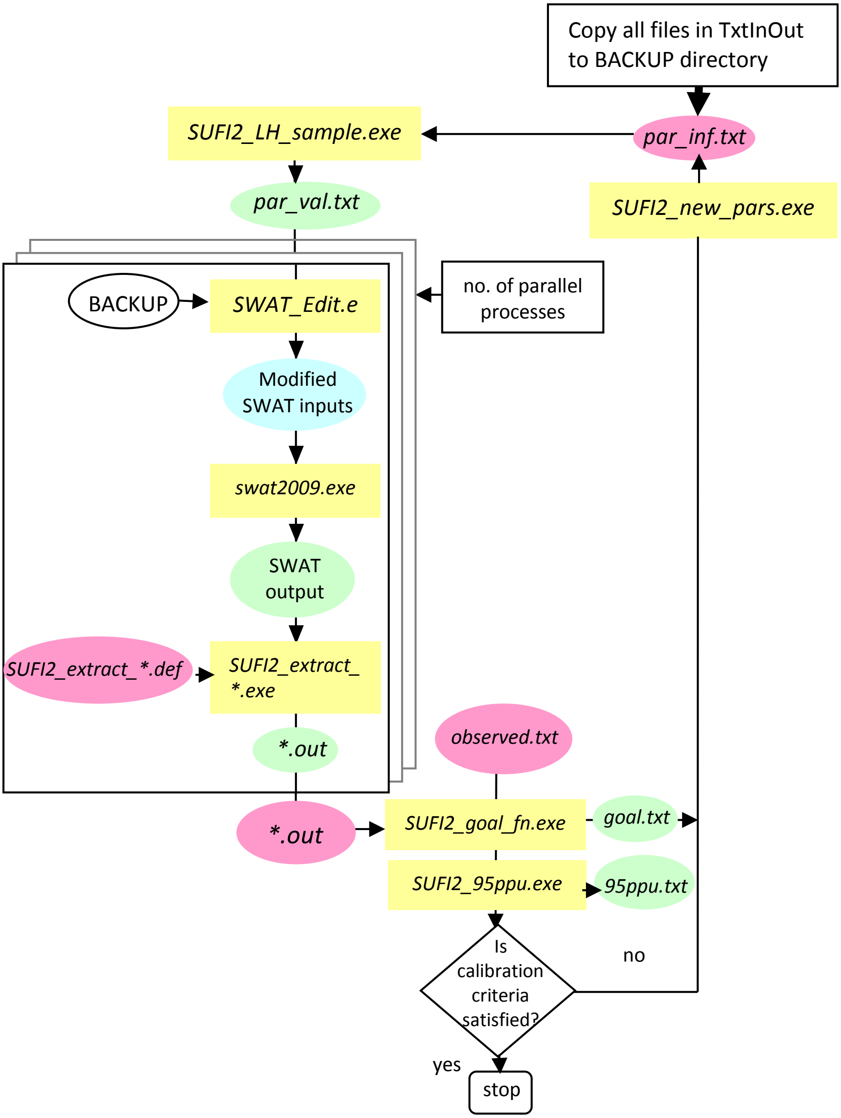

Figure 3.2. Schematic coupling of SWAT, and SUFI2. The entire algorithm is run by three batch files: SUFI2_pre.bat, which runs the SUFI2_LH_sample.exe; SUFI2_run.bat, which runs SWAT_Edit.exe, swat2009.exe, and SUFI2_extract_*.exe files, and SUFI2_post.bat, which executes the SUFI2_goal_fn.exe, SUFI2_95PPU.exe, and SUFI2_new_pars.exe programs. The symbol * stands for rch, hru, and sub files.

Table 3.1. Examples of parameterization in SWAT-CUP *

Parameter identifiers	Description
r__SOL_K(1).sol____FSL__PAST__1-3	Example of a parameter in .sol file. K of layer 1 of subbasin 1,2, and 3 with HRUs containing soil texture FSL and land use PAST will be modified
v__HEAT_UNITS{rotation no,operation no}.mgt	Example a parameter in .mgt file. Management parameters are subject to operation/rotation. Here, heat unit is modified for a certain rotation and operation
v__PLTNFR(1){3}.CROP.DAT	Example of a parameter in crop.dat file. Nitrogen uptake parameter #1 for crop number 3 is modified
v__precipitation(){1977001-1977361,1978001-1978365,1979003}.pcp	Example of data in a precipitation file. ( ) means all stations from day 1 to day 361 in 1977, and from day 1 to day 365 in 1978, and day 3 in 1979 are modified

* r__ indicates relative change, v__ indicates value change, SOL_K is soil hydraulic conductivity, HEAT_UNITS is the total heat units required for crops to reach maturity, PLTNFR is crop's nitrogen uptake parameter, precipitation is the mm of daily precipitation.

After pre-processing, another batch file, *SUFI2_run.bat*, executes the *SWAT_Edit.exe* program, which copies a set of sampled parameters from *par_val.txt* in their appropriate locations in the SWAT input files. Model parameterization is based on the physical characteristics of the parameters as described in the formulation below:

x__<parname>.<ext>__<hydrogrp>__<soltext>__<land use>__<subbsn>__<slope>

where x__ is a code to indicate the type of changes to be applied to a parameter, <parname> is a SWAT parameter name, <ext> is the SWAT file extension, <hydrogrp> is the soil hydrological group, <soltext> is soil texture, <land use> is the name of the land use category, <subbsn> is the subbasin number, and <slope> is the slope of an HRU.

Any combination of the above factors can be used to describe a parameter. If the change is made globally, the identifiers <hydrogrp>, <soltext>, <land use>, <subbsn>, and <slope> are omitted. Table 3.1 shows examples of parameterization in different SWAT files.

The encoding scheme allows the parameters to be kept regionally constant to modify a prior spatial pattern, or be changed globally. This gives the analyst greater freedom in depicting the spatial complexity of a distributed parameter. By using this flexibility, a calibration process can be started with a small number of parameters that only modify a given spatial pattern, with more complexity and regional resolution added in a stepwise learning process.

Next, the SWAT model is executed, and the outputs of interest are extracted from SWAT output files (*output.rch*, *output.hru*, *output.sub*). In the last step, post-processing begins, where *SUFI2_post.bat* executes a number of programs, which are briefly described below.

First, *SUFI2_goal_fn.exe* calculates the objective function. SUFI2 allows seven different functions including summation and multiplicative forms of mean square error, r^2, Chi square, Nash-Sutcliffe, weighted r^2, and ranked sum of square error aimed at fitting the frequency distributions. Each formulation may lead to a different result; hence, the final parameter ranges are always *conditioned* on the objective function used. The use of a "multi-objective" formulation (Duan et al. 2003; Gupta et al., 1998) where different variables are included in the objective function reduces the non-uniqueness problem. An option is now included in SWAT-CUP where variables from different SWAT output files can be included in the objective function. Furthermore, As SUFI2 is iterative; we also found advantages when different objective functions were used in different iterations.

Second, *SUFI2_95ppu.exe* is executed to calculate the 95% prediction uncertainty. SUFI2 describes parameter uncertainty by means of a multivariate uniform distribution in a parameter hypercube, while the output uncertainty is quantified by the 95% prediction uncertainty band (95PPU). SUFI2 maps uncertainties on the parameters in the hydrological model by bracketing all measurements in the 95PPU while minimizing the thickness of the uncertainty band (Figure 3.3) (Abbaspour et al., 2007). Although disaggregation of the errors into their source components is quite desirable, de-convolution of the interacting errors both in the simulated and measured signals is quite difficult, particularly in nonlinear models.

Third, *SUFI2_new_pars.exe* runs, which calculates updated parameters for the next iteration. For this step, the users must define physically meaningful absolute minimum and maximum ranges for the parameters being optimized. There is no theoretical basis for excluding any one particular distribution. However, because of the lack of information, we assume that all parameters are uniformly distributed within a region bounded by minimum and maximum values. Because the absolute parameter ranges play a constraining role, they should be as large as possible, yet physically meaningful. Parameter ranges should be based on ranges measured in the watershed and the field under study when possible. SWAT-CUP reads a file called *Absolute_SWAT_Values.txt* where the absolute ranges of all parameters are listed. These ranges can be set by the user. When these data are lacking, then the suggested values from the SWAT database could be used. The absolute parameter ranges in the SWAT database are mostly based on professional judgment and the experimental values taken from the literature (Winchell et al., 2010). Updated parameters are then calculated as:

$$b'_{j,\min} = b_{j,lower} - \mathrm{Max}\left(\frac{(b_{j,\mathrm{lower}} - b_{j,\min})}{2}, \frac{(b_{j,\max} - b_{j,\mathrm{upper}})}{2}\right) \qquad j = 1,\ldots, p \qquad (1)$$

$$b'_{j,\max} = b_{j,\mathrm{upper}} + \mathrm{Max}\left(\frac{(b_{j,\mathrm{lower}} - b_{j,\min})}{2}, \frac{(b_{j,\max} - b_{j,\mathrm{upper}})}{2}\right) \qquad j = 1,\ldots, p \qquad (2)$$

where b' indicate updated values, $b_{j,\mathrm{lower}}$ and $b_{j,\mathrm{upper}}$. are calculated using the best parameter values of the current iteration as well as the confidence intervals around them, $b_{j,\min}$, and $b_{j,\max}$ are the absolute parameter ranges, and p is the number of parameters. The above formulation, while producing narrower parameter ranges for the subsequent iteration; ensure that the updated parameter ranges are always centered on the best estimates of the current iteration. In the formulation of (1) and (2), the uncertainty in the sensitive parameters decrease faster than those of the insensitive parameters due to the inclusion of the confidence interval that is larger for less sensitive parameters.

After updating, the process repeats until a satisfactory value for the objective function or model evaluation parameters, *P-factor* and *R-factor,* are achieved. These indices are explained below.

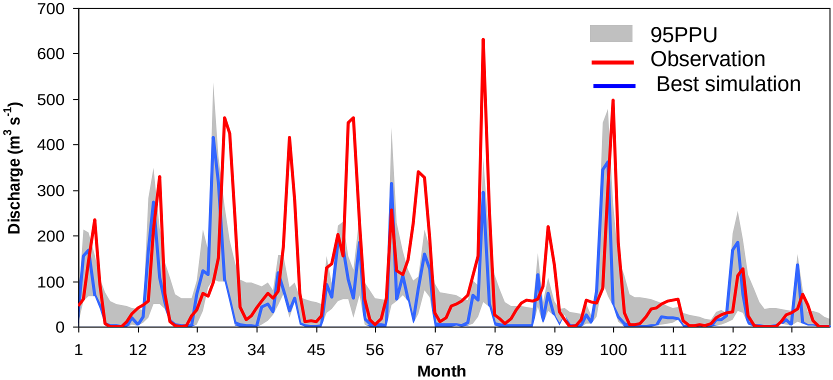

Figure 3.3. The 95PPU graph in the SWAT-CUP interface. Also shown are the observed signal and the best simulation. The 95PPU is given for every variable considered in the objective function.

3.2.3. Goodness of fit in SUFI2

As the simulation result is expressed by the 95PPU band, it cannot be compared with observation signals using the traditional indices such as r^2, Nash-Sutcliffe (*NS*) or mean square error (*MSE*). For this reason we used two measures referred to as the *P-factor* and the *R-factor* (Abbaspour et al., 2004, 2007). The *P-factor* is the percentage of the measured data bracketed by the 95PPU. This index provides a measure of the model's ability to capture uncertainties. As all the "true" processes are reflected in the measurements, the degree to which the 95PPU does not bracket the measured data, the predictions are in error. Ideally, *P-factor* should have a value of 1, indicating 100% bracketing of the measured data, hence capturing or accounting for all the correct processes. The *R-factor,* on the other hand, is a measure of the quality of calibration and indicates the thickness of the 95PPU. It is calculated as the average distance between the upper and the lower 95PPU divided by the standard deviation of the observed data:

$$R-factor=\frac{\frac{1}{m}\sum_{i=1}^{m}(X_{s,97.5\%}-X_{s,2.5\%})_i}{\sigma_{obs}} \quad (3)$$

where $X_{s,97.5\%}$ and $X_{s,2.5\%}$ represent the upper and lower boundary of the 95PPU for a simulated variable X_s, and σ_{obs} is the standard deviation of the measured data. *R-factor* should ideally be near zero, hence coinciding with the measured data.

The goodness of calibration and prediction uncertainty is judged on the basis of the closeness of the *P-factor* to 1 (i.e., all observations bracketed by the prediction uncertainty) and the *R-factor* to 0 (i.e., measured and simulated values coinciding). The combination of these two indices together indicates the strength of model calibration and uncertainty assessment as these are intimately linked.

3.2.4. Parallel Processing setup

The structure of parallel SUFI2 is also schematically shown in Figure 3.2. Although the parallelization is mostly hidden from the user, different processors are involved. The program initially calculates the number of parallel processes that can be submitted to a system by optimizing the number of CPUs against the required RAM to run a certain project.

Although the SUFI2 program has the potential to execute model tasks in parallel, using the full processing capacity of a computer was challenging. There are several hardware components which affect file read and write speed including CPU, RAM, and the hard disk. It was important to minimize communication to the hard disk by utilizing the RAM. All attempts were made to speed up the runs while using less memory by changing the SUFI2 algorithm, primarily in the following two areas:

1- Changes in the SWAT-edit.exe program: SWAT-edit is a program that incorporates updated calibration parameters into SWAT input files. Initially, the files in the BACKUP directory are cached, and held static during the calibration process. All relative changes in the parameters are made with respect to their initial values. The number of SWAT input/output files can vary from tens to hundreds of thousands of files, depending on the project, but each file is only a few KB in size. We took advantage of this characteristic and changed SWAT_edit so that it loads a number of input files on the system's RAM, makes the necessary changes using the cached BACKUP files and writes them to the hard disc. Then it deletes them from the RAM to load the next set of files. This reduces memory usage by up to 90%.

2- Changes in the SWAT-CUP: SWAT-CUP functions were split to apply simultaneously on several nodes or parallel jobs. The number of nodes can be the same or fewer than the number of CPUs. Depending on the project size and the available RAM of the system, the program calculates the maximum number of jobs that can be submitted to the system. For example, to have 48 simulations on a machine with 8 processors, 8 nodes can be made, each conducting 6 simulations if the RAM allows. The parallel processing program does not allow the number of nodes to exceed a certain limit if there is a lack of memory. Hence, having a large system RAM (≥ 16 GB) is an advantage.

The changes in the SWAT-CUP package include: a) changes in user interface to make the parallel option available to users, b) showing the status of each parallel node while the program is running, c) preventing system freezing by giving priorities to other jobs being simultaneously executed, and d) disallowing SWAT-CUP sub-processes to continue running in the background when the program is stopped for any reason. When the program is finished, or stopped unexpectedly, all systems resources are restored.

As parallel SUFI2 is being executed, the user sees the following tasks being performed:

1- *Collect and delete unused files*. These are cached files and files in the *ParallelProcessing* directory left over from previous runs in case of program failure or crash. It is necessary to delete these files to clear the RAM and establish the conditions necessary for step 4 below. This step is mostly used when a parallel processing job has already been run in the same directory.

2- *Collect source files*. It counts the number of files in the project directory.

3- *Validate memory usage*. It calculates the number of parallel processes that can be run on the system. In estimating the number of parallel processes, we consider the available RAM of the system, the amount of system cache memory per file, reserve memory for the system's other operations, and SWAT-edit memory usage. SWAT_edit checks that total parallel processing memory usage plus protected free memory for other operations on the system are less than the available memory. If this constraint is not fulfilled, the program reduces the maximum number of parallel processes.

4- *Synchronize files*. The program copies the necessary files to each parallel folder from the project folder (these files are pre-fetched so the copy operation is done quite fast) and makes them available for each node to read from the corresponding folder.

5- *Collect BACKUP files*. The program enumerates BACKUP files to make the condition ready for pre-fetching all the files in this directory to make them ready for faster read operation by parallel nodes. In this parallel version of SWAT-Edit there is no need to copy the BACKUP directory in every parallel process directory. All the parallel processors will read from the same BACKUP files.

After finishing the program set up, the simulations are divided between different processors and run in a synchronized manner along each other.

After the parallel runs are finished, parallel processing clean up starts to work by collecting output files from each parallel processing directory and concatenating them in the SUFI2.OUT of the main project directories. Then all unused files are deleted, and the RAM which was used during the parallel process, including the RAM which was used by caching the BACKUP files are released.

Now all is done with the parallel section. The rest is post processing, which is done in the same way as the single calibration run by executing *SUFI2_post.exe*.

3.2.5. Case studies and computer systems

To demonstrate the functionality of parallel SUFI2, we evaluated the program with six benchmarks, including three hydrological models tested on six different systems. We used one server, three personal computers, and two laptops. Table 3.2 has a summary of the attributes of these systems. For hydrological models, we built large, medium, and small projects using the SWAT2009 program. The period of simulation for all runs was set to 5 years.

The large-size project is the Danube River Basin, which covers an area of 801,093 km^2. Danube is Europe's second longest river, flows for a distance of 2,826 km and enters the Black Sea east of Izmail (Ukraine) and Tulcea (Romania). We simulate the Danube river basin using SWAT, where we divide the region into 1,224 smaller subbasins taking into account elevation, soil, land use and climatic information. This resulted in 69,875 HRUs. Running the calibration program SUFI2, 48 simulations took approximately 2 days to run on the server without using the parallel option. The medium-size project is the Alberta project that covers an area of 661,185 km^2. The region is divided into 938 subbasins for a total of 2,689 HRUs. The small-size project (Test project) is a small test example in the SWAT program with only 4 subbasins and 75 files. It should be mentioned that calibration of the hydrological models is not the focus of this study and we only tried to focus on the speed of the calibration process.

3.2.6. Performance measures

There are two performance measures that are commonly used to evaluate the performance of parallel computation: *speedup* and *efficiency* (Houstis et al., 1997, Mateos et al., 2010). Speedup for *n* parallel sessions is defined as the computed time of the task when only one processor is used to the computing time when *n* processors are used. The efficiency of a parallel system of *n* processor is defined as the ratio of actual speedup to ideal speedup, where the ideal speed up is equal to the number of processors.

Table 3.2. Description of the 6 computer systems used to test the parallel Sufi2.

Server 1 24 CPUs Processors: Intel(R) Xeon(R) CPU L5640@2.27GHz (2 processor) RAM = 24.0 GB System type = 64-bit OS Windows 7	**PC 1** 8 CPUs Process: Intel(R) Core(TM) i7 CPU 860@2.8 GHz RAM = 16.0 GB System type = 64-bit OS Windows 7
PC 2 2 CPUs Processor: Intel(R) Core(TM) 2 Duo CPU E8600@3.33GHz RAM = 3.46 GB System type = 32-bit OS Windows XP	**PC 3** 2 CPUs Processor: Intel(R) Pentium(R) D CPU 3.01 GHz RAM = 1.00 GB System type = 32-bit OS Windows XP
Laptop 1 2 CPUs Processor: Intel(R) Core(TM) 2Duo CPU T960000 @ 2.80 GHz RAM = 3.0 GB System type = 32-bit OS Windows XP	**Laptop 2** 2 CPUs Processor: Intel(R) Core(TM) 2 Duo CPU P8700 @ 2.53 GHz RAM = 4.0 GB System type = 64-bit OS Windows 7

3.3. Results and Discussion

Parallel SUFI2 was tested on different computers using three different projects. Calibration speedup, designed system efficiency, and peak CPU usage of each system versus the number of processors is shown in Figures 3.4, 3.5 and 3.6, respectively.

Figures 3.4a and 3.4b show the speedup of the Danube, the Alberta, and the Test project on machines with 24 and 8 processors, respectively. In the system with 24 CPUs, the speedup of parallel SUFI2 follows closely the ideal speedup up to 8 processors. As the number of the processors increases, the gap between the parallel SUFI2 and the ideal performance grows. As the number of jobs increases, the communication of each CPU with the hard disk increases. The loss of speed is, hence, mostly due to hard disk limitation. The use of Redundant Array of Independent Disks (RAID) or Solid State Drive

(SSD) should improve the performance. If the number of parallel jobs is set to 24, then in the Danube project (24 x 69,875) files are simultaneously read and written to the hard disk. So as the number of parallel processes increases, the speedup decreases for large projects. Hence, Danube shows a smaller speedup than the Alberta or Test project for 24 CPUs (Figure 3.4a).

Figures 3.4 (c,d,e,f) shows the speedup of running the same projects on 2 PCs with weaker capabilities than PC 1, and two laptops with only 2 CPUs. Because the machines only have 2 processors, we could only submit up to 2 parallel jobs. The speedup achieved using parallel SUFI2 is around 1.9 with 2 processors. This compares quite well to the ideal speedup, indicating that the running time was halved. The small deviations in different machines and projects have to do with the initial state of the computers. For the best result the computers should be re-started before each run to release the remaining occupied memories from previous computer use. It should be noted that the Danube project is missing from Figures 3.4 c,d,e. This is because the memory limitation, as the size of the project was too large for these machines to run two parallel processes.

Figure 3.5 illustrates the efficiency of parallel SUFI2. In general, the efficiency of a parallel system is less than unity because of the system overhead such as the resolution of conflicting demands between shared resources, the communication time between processors, and the inability to keep every processor fully busy. For the ideal case, when the number of processors allocated to a particular task increases, a higher speedup (reduction in computing time) can usually be obtained. The efficiency therefore decreases for the above reasons and the fact that the processors cannot be fully utilized. For small requests, such as the Test case in this study, the overhead introduced by the initial model set up is not compensated because the number of processors is too small. This can be seen in Figure 3.5a, which shows that for very small jobs the server becomes more efficient as the number of processors increase.

Figure 3.6 shows the peak CPU usage. In Server 1 and PC 1 a non-parallelized program used little of the CPU capacities. As the number of parallel jobs increases, more CPUs are used. In each machine, as the number of parallel jobs equals the number of CPUs, 100% of the CPU is used.

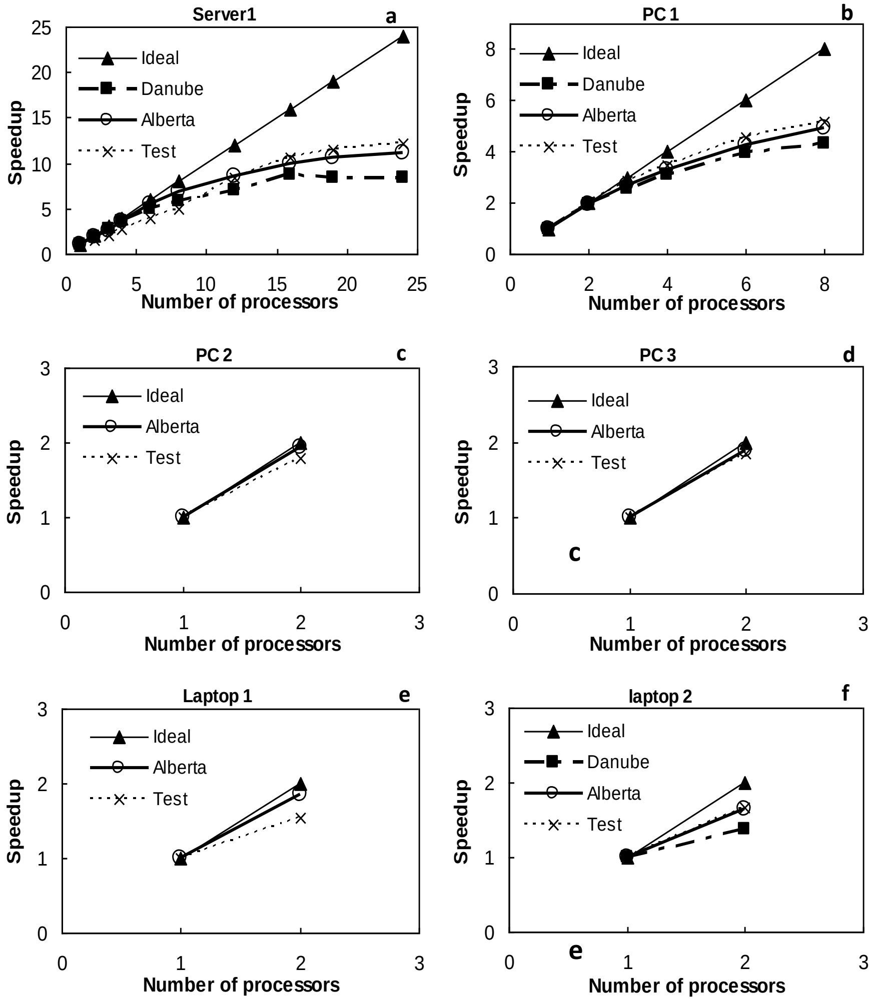

Figure 3.4. The speedup achieved for different computer systems and SWAT projects. Number of processors on the horizontal axis indicates the number of parallel jobs submitted. The Figure shows that most projects could be run 10 times faster with about 16 processors. Note that PC 2, PC 3, and Laptop 1 could not handle the size of the Danube project for two parallel runs.

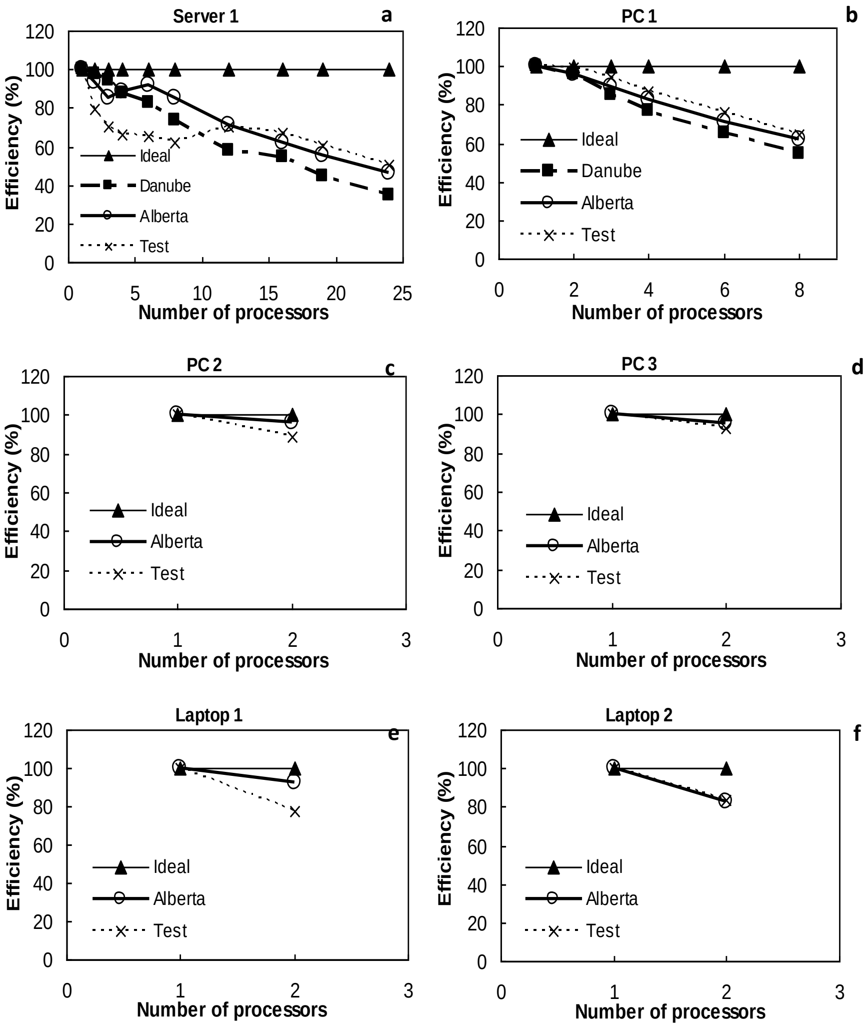

Figure 3.5. Percentage efficiency calculated for different computer systems and SWAT projects. The decrease in efficiency is a function of the size of the project and the characteristics of the hard disk.

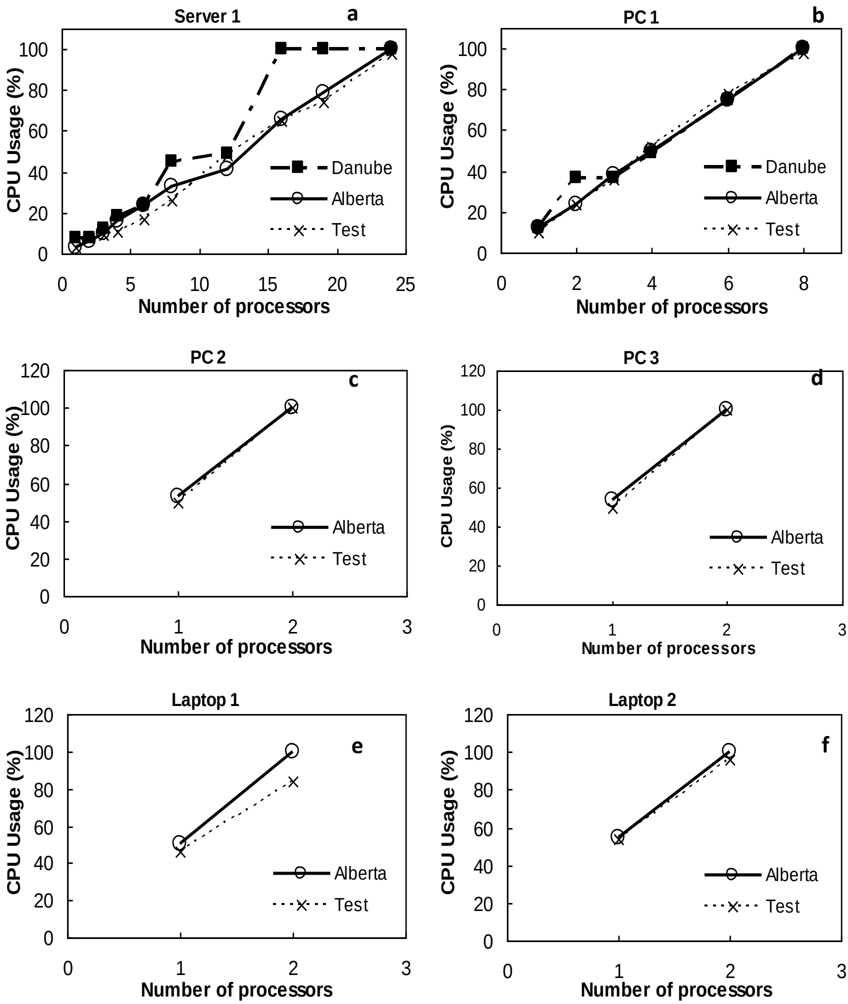

Figure 3.6. Peak CPU usage in different computer systems and SWAT projects. As the number of parallel jobs increase, the efficiency in using CPU also increases.

A few recommendations should be followed when running SUFI2 in parallel mode. 1) Do not run multiple SWAT-CUP projects on a single system using the parallel process. 2) It is recommended to restart the computers before starting the parallel calibration project to access the full memory available on the computer although the program itself will clean up the unused files related to the SWAT-CUP project. As the number of parameters increase, SWAT_edit requires more RAM to cache the files. 3) No other memory consuming programs along the parallel SWAT-CUP should be run simultaneously. 4) The number of simulations should be (but not absolutely necessary) a multiple of the number of parallel processing jobs. 5) It is very important to switch off any antivirus program during the parallel program run or exclude the corresponding directory from the virus scan. The antivirus scan decreases the speed of parallel SUFI2 substantially.

3.4. Conclusion

In this paper, we presented parallel SUFI2, a framework that automatically and transparently parallelizes the SUFI2 optimization program for higher performance calibration purposes. Performance results with both small and large size projects show that parallel SUFI2 achieves good speedup and reasonable scalability in most cases.

Although the parallel SUFI2 is designed to be used on any system, larger time savings can be achieved with multiple CPUs and larger RAM memory. Note that the emphasis of this research was not on achieving the highest possible speedup and that our current implementation is an early proof-of-concept prototype that does not contain optimization or refinement. Computations based on GPU technology hold the promise of achieving greater speed ups in execution of hydrologic models (Kalyanapu, et al., 2011; Singh, et al., 2011). However, we show that parallel SUFI2 is able to achieve reasonable speedup on real-world computation-intensive calibration applications, while significantly exceeding the performance of non parallelized packages.

Acknowledgments

This project has been funded by the European Commission's Seventh Research Framework through the enviroGRIDS project (Grant Agreement n 226740).

References

Abbaspour, K.C., Faramarzi, M., Ghasemi, S.S., Yang, H., 2009. Assessing the impact of climate change on water resources in Iran, Water Resour. Res., 45, W10434, doi:10.1029/2008WR007615.

Abbaspour, K.C., Yang, J., Maximov, I., Siber, R., Bogner, K., Mieleitner, J., Zobrist, J., Srinivasan, R., 2007. Modelling hydrology and water quality in the pre alpine/alpine Thur watershed using SWAT. Journal of Hydrology 333, 413-430.

Abbaspour, K.C., Johnson, A., van Genuchten, M.Th, 2004. Estimating uncertain flow and transport parameters using a sequential uncertainty fitting procedure. Vadose Zone Journal 3(4), 1340-1352.

Arnold, J.G., Srinivasan, R., Muttiah, R.S., Williams, J.R., 1998. Large area hydrologic modeling and assessment - Part 1: Model development. Journal of the American Water Res. Association 34(1), 73-89.

Arnold, J.G., Allen, P.M., 1996. Estimating hydrologic budgets for three Illinois watersheds. Journal of Hydrology 176, 57–77.

Beven, K., Binley, A., 1992. The future of distributed models - model calibration and uncertainty prediction. Hydrol. Process 6(3), 279-298.

Duan, Q., 2003. Global Optimization for Watershed Model Calibration, in Calibration of Watershed Models, edited by Duan, Q., Gupta, H.V., Sorooshian, S., Rousseau, A. N., Turcotte, R., pp. 89-104, AGU, Washington, DC.

Eckhardt, K., Ulbrich, U., 2003. Potential impacts of climate change on groundwater recharge and streamflow in a central European low mountain range, J. Hydrol. 284, 244–252.

Fernandez-Quiruelas, V., Fernandez, J., Cofino, A. S., Fita, L., Gutierrez, J. M., 2011. Benefits and requirements of grid computing for climate applications. An example with the community atmospheric model. Environmental Modelling and Softwaree, 26, 1057-1069.

Fontaine, T.A., Klassen, J.F., Cruickshank, T.S., Hotchkiss, R.H., 2001. Hydrological response to climate change in the Black Hills of South Dakota, USA, Hydrol. Sci. J. 46, 27– 40.

Gupta, H.V., Sorooshian, S., Yapo, P.O., 1998. Toward improved calibration of hydrologic models: multiple and non-commensurable measures of information, Water. Resour. Res. 34,751-763.

Houstis, C.; Kapidakis, S., Markatos, E. P., Gelenbe, E., 1997. Execution of computer-intensive applications into parallel machines. Information Sciences, 97, 83-124.

Kalyanapu, A. J., Shankar, S., Pardyjak, E. R., Judi, D. R., Burian, S. J., 2011. Assessment of GPU computational enhancement to a 2D flood model. Environmental Modelling and Software, 26, 1009-1016.

Kennedy, J., Eberhart, R., 1995. IEEE International Conference on Neural Networks (ICNN 95), Nov 27-Dec 01, 1995 UNIV W Australia, Perth, Australia, Source: 1995 IEEE International Conference on Neural Networks Proceedings 1-6, 1942-1948.

Kuczera, G., Parent, E., 1998. Monte Carlo assessment of parameter uncertainty in conceptual catchment models: the Metropolis algorithm. Journal of Hydrology, 211(1-4), 69-85.

Lecca, G., Petitdidier, M., Hluchy, L., Ivanovic, M., Kussul, N., Ray, N., Thieron, V., 2011. Grid computing technology for hydrological applications. Journal of Hydrology, 403, 186-199.

Li, T., Wang. G., Chen, J., Wang, H. 2011. Dynamic parallelization of hydrological model simulation. Environmental Modelling and Software, 26, 1736-1746.

Marshall, L., Nott, D., Sharma, A., 2004. A comparative study of Markov chain Monte Carlo methods for conceptual rainfall-runoff modeling. Water Resour. Res., 40, W02501, doi:10.1029/2003WR002378.

Mateos, C., Zunino, A., Campo, M., 2010. On the evaluation of gridification effort and runtime aspects of JGRIM applications. Future Generation Computer Systems, 26, 797-819.

McKay, M.D., Beckman, R.J., Conover, W.J., 1979. A comparison of three methods for selecting values of input variables in the analysis of output from a computer code. Technometrics 21, 239-245.

Miller, M., 2009. Cloud computing pros and cons for end users. Article on Internet. http://www.informit.com/articles/article.aspx?p=1324280

Neal, J. C., Fewtrell, T. J., Bates, P. D., Wright, N. G. 2010. A comparison of three parallelization methods for 2D flood inundation models. Environmental Modelling and Software, 25, 398-411.

Schuol, J., Abbaspour, K.C., Sarinivasan, R., Yang, H., 2008a. Estimation of freshwater availability in the West African Sub-continent using the SWAT hydrologic model.

Schuol, J., Abbaspour, K.C., Srinivasan, R., Yang, H., 2008b. Modelling Blue and Green Water Availability in Africa at monthly intervals and subbasin level. Water Resources Research. 44, W07406, doi:10.1029/2007WR006609.

Singh, B., Pardyjak, E. R., Norgren, A., Willemsen, P., 2011. Accelerating urban fast response Lagrangian dispersion simulation using inexpensive graphics processor parallelism. Environmental Modelling and Software, 26, 739-750.

Sundaram, K., 2010. Cloud Computing vs. Grid Computing. Article on Internet. http://www.brighthub.com/environment/green-computing/articles/68785.aspx

Taylor, S.J.E., Popescu, G.V., Pullen, J.M., Turner, S.J. 2004. Panel on distributed simulation and the grid. Proceeding of 8th IEEE International Symposium on Distributed Simulation and Real-Time Applications (DS-RT 2004), Budapest, Hungary October 21-23, 2004. IEEE Comp Soc Tech Comm Parallel Process; IEEE Comp Soc Tech Comm Simulat; IEEE Comp Soc Tech Comm Comp Architecture; Pages: 144-149 DOI: 10.1109/DS-RT.2004.14.

Van Griensven, A., Meixner, T., 2006. Methods to quantify and identify the sources of uncertainty for river basin water quality models. *Water Sci.* Technol. 53(1), 51-59.

Vassilios, P., 2008. Computing, virtualization, configuration management. Article on Internet. http://it.toolbox.com/people/outervillage/

Vrugt, J.A., Gupta, H.V., Bouten, W., Sorooshian, S., 2003. A Shuffled Complex Evolution Metropolis algorithm for optimization and uncertainty assessment of hydrologic model parameters. Water Resour. Res. 39(8), 1201.

Winchell, M., Srinivasan, R., Di Luzio, M., Arnold, J. 2010. ArcSWAT interface for SWAT2009, User's Guid. Blackland Research and Extension Center Texas AgriLife Research.Temple, Texas 76502. pp.495.

Yang, J., Reichert, P., Abbaspour, K.C., Yang, H., 2007. Hydrological modelling of the Chaohe basin in China: Statistical model formulation and Bayesian inference. Journal of Hydrology 340, 167–182.

Hydrological Processes, to be submitted

4. Does land use update matter in large scale hydrologic models?

[1,2]Elham Rouholahnejad, [1]Karim C. Abbaspour, [3]Emanuele Mancosu, [2]Rainer Schulin, [4]Anthony Lehmann

[1] Eawag, Swiss Federal Institute of Aquatic Science and Technology, Ueberlandstrasse 133, 8600 Duebendorf, Switzerland.

[2] ETH Zürich Institute of Terrestrial Ecosystem, Universitätstr. 16, 8092 Zürich, Switzerland.

[3] UMA - ETCSIA, University of Malaga, European Topic Centre for Spatial Information and Analysis, 29071, Malaga, Spain

[4] University of Geneva, Climatic Change and Climate Impacts, 7 Route de Drize, CH-1227 Carouge, Switzerland.

Abstract

Land use changes are altering hydrologic systems, which may have potentially large impacts on water resources. However, this is not investigated in any systematic manner in hydrologic models that use land use as input. In Europe, land cover has changed substantially in recent decades. In this article, we investigate the impact of these changes on hydrology and water resources components of the Black Sea Basin (BSB). Soil and Water Assessment Tool (SWAT) was used for this purpose considering the changes between 2001 and 2008. A previously calibrated hydrologic model using MODIS Land use 2008 was taken as the reference model. We modified this model by a land use from 2001 using the dynamic land use change module in SWAT where we updated the land use half way through simulation. There was an incremental change in forested areas from 19 to 21.3%, and in crop land from 47.2 to 47.4%, in addition to a decremental change in crop and natural vegetation from 15.1 to 13.3%, and in shrublands from 2 to 1.5% of the catchment area during the 7 years period. At the catchment scale, we found no net significant change on water balance when looking at the long term averages. However, at the HRU scale, the results showed that afforestation leads to an increase of evapotranspiration up to 3%, while runoff and water yield did not change significantly. The increase in cropland resulted in an increase in evapotranspiration by up to 5%. This research indicates that at the HRU scale, land use change may have important implications for developing better water management practices through a better understanding of system vulnerabilities to change.

KEYWORDS: hydrology, land use change, SWAT, water cycle, Black Sea Basin

4.1. Introduction

Land use changes have potentially large impacts on water resources [Stonestrom et al., 2009]. Rapid socio-economic development drives land use changes especially in regions with long land use histories. This is particularly true in Eastern Europe, where the Black Sea Basin (BSB) lies, and where the land cover has changed substantially since the breakdown of the USSR in 1990 [Ref.]. Land use change may have a great impact in regions where water availability is limited. This could result in an increase of water scarcity and thus contribute to a deterioration of living conditions [Wagner et al., 2013]. In a previous study, BSB showed to experience water stress periods in the last three decades [Rouholahnejad et al., 2003].

Land use change also influences water quality. Hydrologic processes such as evapotranspiration, infiltration, surface runoff and groundwater flow are altered substantially by land use changes [Bultot et al. 1990; Sahin and Hall 1996; Fohrer et al. 2001; Lin et al. 2007; Tong and Chen 2002]. The evaluation of the impacts of land use change on water quantity and quality is fundamental to the development of sustainable land use alternatives [Lenhart et al. 2003; Lin et al. 2007] and an integral component of river basin and water resources management [Eckhardt et al. 2003; Huisman et al. 2004].

Given the ability to account for the spatial variability of land surface characteristics, physically based and distributed hydrologic models are great tools for the prediction of land use change effects [Klöcking and Haberlandt 2002; Legesse et al. 2003]. The use of eco-hydrologic models provides an insight into the consequences of changes in policies or other land use determinants [Van Rompaey et al. 2001; Verburg and Veldkamp 2001; Fohrer et al. 2002, 2005] and can contribute to decision making in the fields of land use planning and integrated watershed management [Leh et al. 2011].

Models often used to assess the impacts of land use change on water resources among many others include: HBV [Bergström and Forsman, 1973; e.g., Ashagrie et al., 2006], MIKE-SHE [Refsgaard and Storm, 1995; e.g., Im et al., 2009], SWAT [Arnold et al., 1998; e.g., Fohrer et al., 2001], and WaSiM-ETH [Schulla, 1997; e.g., Niehoff et al., 2002]. These models are particularly useful as they can assess past as well as possible future impacts using land use scenarios. The Soil and Water

Assessment Tool [SWAT, Arnold et al., 1998] has proven its suitability for hydrologic impact studies [Gassman et al., 2007], especially under conditions of limited data availability [Ndomba et al., 2008; Stehr et al., 2008]. Hence, it is a suitable model to study the impact of land use changes on water resources in the BSB.

Investigations of the effects of past land use changes on water availability have been carried out in many regional studies worldwide [e.g., Ghaffari et al., 2010: Iran; Im et al., 2009: Korea; Li et al., 2009: China; Miller et al., 2002: USA]. Impacts of land use change on the water resources in Europe were mainly assessed by using scenario analysis. Particularly, agricultural land and forests are a focus of the research in this area [Rounsevell et al., 2006]. Stoate et al. [2009] reviewed ecological impacts of early 21st century agricultural change in Europe. Goetz et al [2001] provided book reviews on agricultural transformation of land use in central and Eastern Europe.

While most of the studies focus on the trend of land use change in Europe, the impact analysis of these changes on the hydrology has been less of a focus. In addition, most of the previous studies were carried out under hypothetical conditions of changes of land use from one class to another one at the time (scenario analysis) rather than assessing realistic historical changes in a system, which is complex with many feedbacks from different processes.

Against this background, the aim of this study was to assess the impact of past land use changes in the BSB on hydrology using SWAT. The study demonstrates the benefits of using land use change dynamically in model applications extending beyond 5 to 10 years. The following research questions were of main interest: (1) What were the key land use changes in a short period of 7 years in the BSB? (2) How did these rather short duration changes impact hydrological fluxes and the water cycle at watershed and sub-watershed level? (3) Would it be necessary to account for historical land use change in a long-term model run? (4) Based on the experiences gained by studying the past land use changes, what are the implications for future land use change studies?

4.2. Material and methods

4.2.1. Study area

Black Sea Basin (Figure 4.1) drains rivers of 23 European and Asian countries (Austria, Belarus, Bosnia, Bulgaria, Croatia, Czech Republic, Georgia, Germany, Hungary, Moldova, Montenegro, Romania, Russia, Serbia, Slovakia, Slovenia, Turkey, Ukraine, Italy, Switzerland, Poland, Albania and Macedonia) from an area of 2.3 million km^2 to the Black Sea. The Basin is inhabited by a total population of around 160 million people [BSEI, 2005]. Major rivers draining into the Black Sea include Danube, Dnieper and Don. The greatest sources of diffuse pollution are agricultural and households not connected to sewer systems. It is mountainous in the east and south, in the Caucasus and in Anatolia, and to the northwest with the Carpathians in the Ukraine and Romania. Most of the rest of the Black Sea's western and northern neighborhood is low lying. Mean annual air temperature shows a distinct north-south gradient from < -3 °C to > 15 °C. Precipitation pattern is characterized by a west-east gradient that is decreasing with distance from the Atlantic Ocean. Areas of high precipitation (> 3000 mm $year^{-1}$) are in the west and areas of low precipitation (< 190 mm $year^{-1}$) are in the north and east [Tockner et al., 2009]. The dominant land use in the basin is agricultural with 65% of coverage according to MODIS Land Cover [NASA, 2001].

4.2.2. SWAT model description

SWAT is a process-based, continuous-time model that operates on a daily time step to predict the impact of management practices on water, sediment and agricultural chemical yields at the catchment scale [Arnold et al., 1998]. The spatial heterogeneity of the watershed in SWAT is preserved by topographically dividing the basin into multiple sub-basins. These subbasins are further subdivided into lumped hydrologic response units (HRUs) comprising homogeneous landscape, soil, and land use characteristic units that are not spatially identified in a given subbasin. The hydrologic cycle as simulated by the model can be separated into the land phase and the routing phase. The land phase simulates runoff and erosion processes, soil water movement, evapotranspiration, crop growth and yield, soil nutrient and carbon cycling, pesticide and bacteria degradation, and thus controls the amount of water, sediment, nutrient and pesticide loadings entering the main channel in each subbasin. A wide range of agricultural practices including tillage, fertilizer and manure application, subsurface drainage, irrigation, ponds and wetlands [Douglas-Mankin et al., 2010] are accounted for in SWAT.

The routing phase controls the movement of water, sediments, nutrients, etc through the channel network to the watershed outlet. SWAT model has undergone continuous development [Arnold et al., 2010; Bosch et al., 2010; Gassman et al., 2007] in the last two decades. In its current version, SWAT2009 [Neitsch et al., 2011] which is used in the present study, several watershed processes can be represented by alternative methods. Table 4.1 gives an overview of the relevant methods used in this study. A detailed description of the model can be obtained from Neitsch et al. [2011].

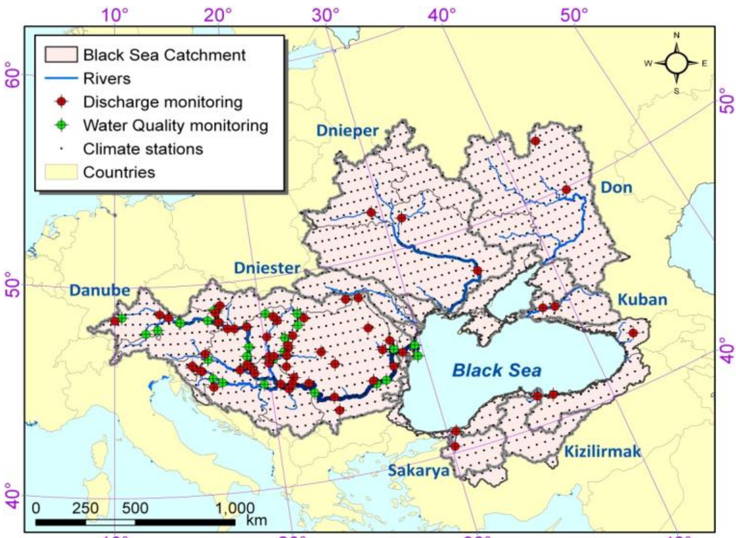

Figure 4.1. Overview of Black Sea Basin depicting major rivers, and measured stations of climate, discharge, and nitrate.

Table 4.1. SWAT processes representation as used in the study.

Processes/components	Method [Neitsch et al., 2011]
Evapotranspiration	Hargreaves
Surface runoff	SCS curve number equation
Erosion	Modified universal soil loss equation
Lateral flow	Kinematic storage model
Groundwater flow	Steady-state response from shallow aquifer
Stream flow routing	Variable storage routing

4.2.3. Model set up

The SWAT model was previously set up for the BSB and calibrated with uncertainty analysis using stream flow, nitrate loads, and crop yield (Figure 4.2) [Rouholahnejad et al., 2013]. In the current study, all the input data remained the same except for the land use data. Table 4.2 presents the input data used in the hydrologic model of BSB. To update land use, we used the dynamic land use update module of SWAT, where the number of HRUs stayed the same as the original model. This way, the temporal changes in a land use class occur as an increment or decrement of the land use in the defined time span. To be able to attribute the changes in model output to land use change, three models were set up and compared. i) a previously calibrated hydrologic model of BSB using MODIS land use 2008 (S-2008), ii) a hydrologic model of BSB using MODIS land use 2001 (S-2001), and iii) a hydrologic model of BSB using MODIS land use 2001 from the beginning of the simulation period and updating its land use to 2008 half way through the simulation time (S-2001-2008).

The Delta approach was used to assess the impact of different land use utilization on three model results and is frequently used in other studies [e.g., Ghaffari et al., 2010; Im et al., 2009; Miller et al., 2002]. In this regard, only model parameters that were defined by the land use maps were different in the three model setups. The HRU fractions in each subbasin of the three models changed between the models based on S-2001 and S-2008 while the total number of HRUs and their combinations were identical.

Table 4.2. Model input data sources and descriptions for the base model

Type	Source	Description
DEM	SRTM [Jarvis et al, 2008]	90 m resolution extracted for BSB
Climate	CRU [2008], [Mitchell and Jones, 2005], Solar Radiation, [Weedon et al., 2011].	0.5° resolution gridded climate data, daily temperature (min., max.), daily precipitation (1970-2006) daily global solar radiation from 6,110 virtual stations (1970-2006)
Stream flow	[GRDC, 2011]	Monthly river discharge data (1970-2006)
River network	ECRINS [2012]	30 m resolution, from European Catchments and RIvers Network System
Soil	FAO [2003]	5 km resolution, from FAO-UNESCO global soil map, provides data for 5000 soil types comprising two layers (0–30 cm and 30–100 cm depth)
Land use	MODIS [NASA, 2001]	500 m spatial resolution, maintained by the NASA Land Processes Distributed Active Archive Center (LP DAAC) at the USGS/Earth Resources Observation and Science Center (EROS)
Management	MIRCA2000 [Portmann et al, 2010], McGill yields data [Monfreda et al., 2008]	5 arc min resolution cropping area and the start and end month of cropping periods, 5 arc min crop yield on three major crop (Wheat, Cory, Barely)

4.2.4. Land use change between 2001 and 2008

The historical analysis of land use changes was based on a comparison between MODIS datasets from 2001 and 2008 (Figure 4.3). In 2001, croplands are the largest class in the BSB (1,725,915 km^2) followed by forest (692,493 km^2), natural vegetation (553,006 km^2) and grassland (535,494 km^2). Compared to land cover in 2001, croplands were still the major land use type in the BSB in 2008 (1,734,497 km^2). However, forest areas increased, most probably due to conversion from natural vegetation. Urban and built-up areas also slightly increased during this period. Forest shows an increment from 19% of total land in BSB in 2001 to 21.3% in 2008. Crops/natural vegetation decreases form 15.1% in 2001 to 13.3% in 2008. Barren or sparsely vegetated areas and permanent wetlands cover less than 1% of the total BSB area in both datasets. The contingency table shows class relations between 2001 and 2008 (Table 4.3) and is the cross-tabulation of land use in 2001 (columns) against land use in 2008 (rows). Where a land use in a row meets the same land use in a column, the value is the area that did not change from 2001 to 2008 (shaded area). The other values represent the areas that changed from one land use class to another between the two years. This matrix is used to analyze the contributions to net change in: forest, grassland and cropland.

Table 4.3. Absolute change among landuse classes

2001 / 2008	Crops/ natural vegetation	Shrubland	Barren or sparsely vegetated	Forest	Grassland	Croplands	Urban and built-up
Crops/natural vegetation	311720	2556	94	34333	25314	110254	0
Shrubland	1376	22223	1227	1042	19958	6320	0
Barren or sparsely vegetated	64	2036	2620	5	1173	141	0
Forest	85378	4611	626	641476	37049	5142	0
Grassland	23183	31394	1531	9043	377929	85795	0
Croplands	129911	12229	63	3034	71212	1517970	0
Urban and built-up	0	0	0	0	0	0	62133

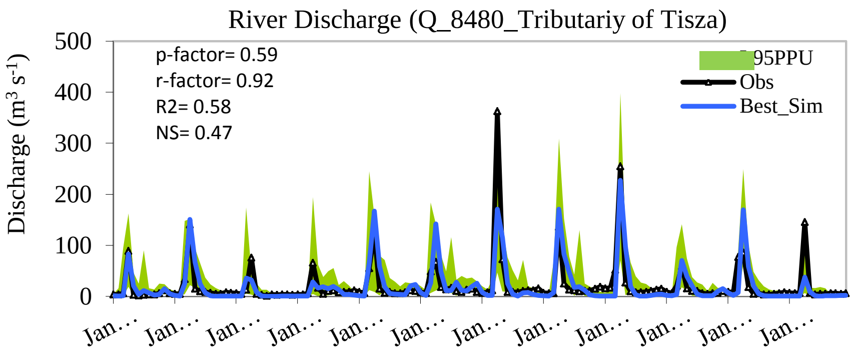

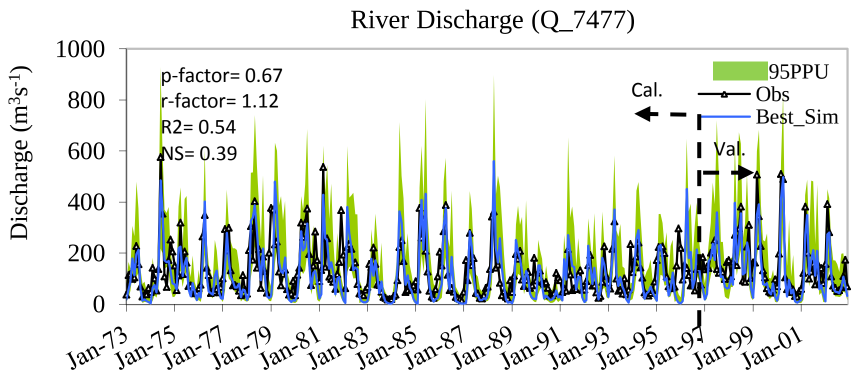

Figure 4.2. Simulated and observed discharges of two rivers in the Black Sea Basin in calibration and validation periods. The shaded region is 95% prediction uncertainty band. These are from the calibrated base model.

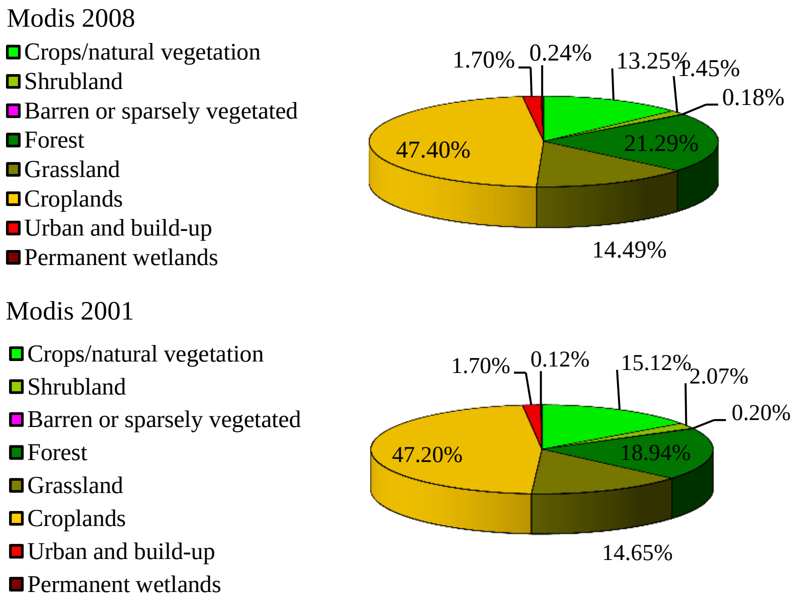

Figure 4.3. Percent share of total area per land use in MODIS 2001 and 2008

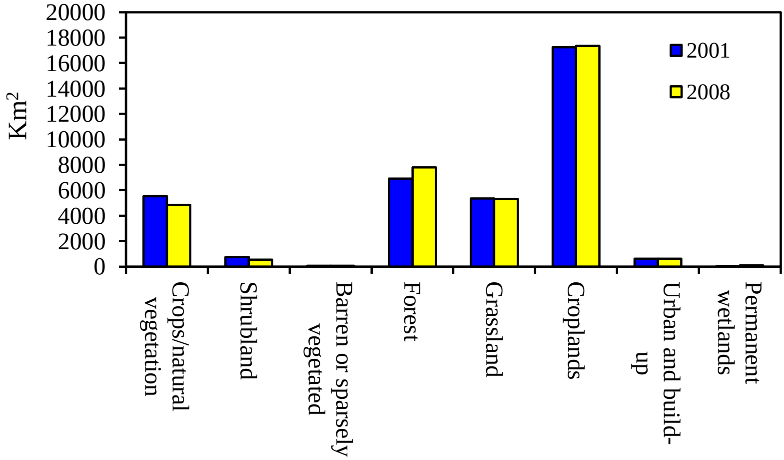

Figure 4.4. Total area per land use class in MODIS 2001 and 2008 (km^2)

The main contribution to the increase of forest areas is from crop and natural vegetation (5,1045ha), followed to a lesser extent by grassland (28,006 ha), shrubland (3,569 ha) and cropland areas (2,108 ha) (Figure 4.5). The abandonment of agriculture is clearly shown during this period with a high percentage of land use conversion to natural vegetation (19,657 ha) and shrubland (5,909 ha). Additionally, some grassland is converted to cropland (14583ha); this is related to intensification and expansion in suitable areas and disappearance in less suitable areas (Figure 4.5). Forest and grassland are very competitive with each other. On one hand, forest areas tend to be converted to grassland (often with cropland as an intermediate step) and grassland to forest. On the other hand, some grassland areas are converted to cropland, in the case of regions experiencing agricultural intensification, or to shrubland, in cases of land abandonment. The largest positive changes during 2001-2008 occurred in the forest class (over 80,000 km^2). Croplands increased by 8,582 km^2. The largest negative change occurred in grassland, which lost more than 5,000 km^2. Analysis of water resources was carried out by comparing the 34-year monthly water balance components using the model results for the three different scenarios. The averages of water balance components in the three model runs were assessed next to analyzing the temporal and spatial variability of the components across the BSB over the 34-year simulation period.

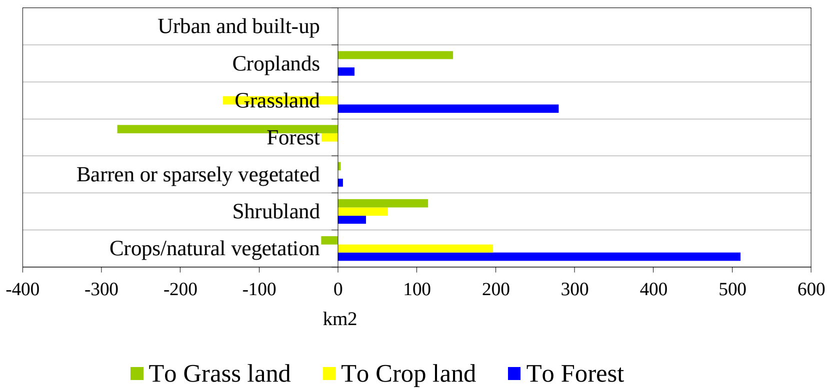

Figure 4.5. Net changes to forest, crop land, and grass land from other land use classes between 2001 and 2008.

4.3. Results

4.3.1. Land use change assessment

The differences within the period 2001–2008 are presented in maps of the BSB regions and adjacent areas (Figure 4.7). These regions are a combination of NUTS (Nomenclature of Territorial Units for Statistics) levels 2 and 3. Four land use classes were analyzed: forest, grassland, croplands and urban/built-up areas. The absolute difference in square kilometers for the forest class shows that significant positive changes in the flow of forest occurred mostly in the northern, extreme western and south-western parts of the BSB. Negative changes occurred in smaller patches along an east-west line across the middle of the BSB (Figure 4.7a). In general terms, grassland flows from 2001 to 2008 show a decreasing trend in the BSB, where the most negative changes were recorded in the mid-west (Romania). To a lesser extent, some positive changes were found in the south (Turkey) and east (Russian Federation) (Figure 4.7b).

Croplands (Figure 4.7c) show a negative absolute difference in the extreme east (Russian Federation) and south (Turkey), as well as in the mid-west (northern Romania). A significant positive trend occurred along the western and northern Black Sea shores and in Belarus, as well as in the western part of the BSB, though to a lesser extent. The absolute difference in the area covered by urban and built-up areas (Figure 4.7d) is less significant than for the rest of the classes. This can be explained by the shortness of the period analyzed. Regions that recorded a negative difference are located close to the Black Sea shore in Romania, Ukraine and Turkey.

To assess the impacts of changes in such a complex system, the impacts are analyzed both at the watershed and sub-watershed level. At sub-watershed level we analyzed the different land use change impacts imposed on the system by first: looking at 4 selected zones (Figure 4.7), second: at subbasin level, and third: at HRU level.

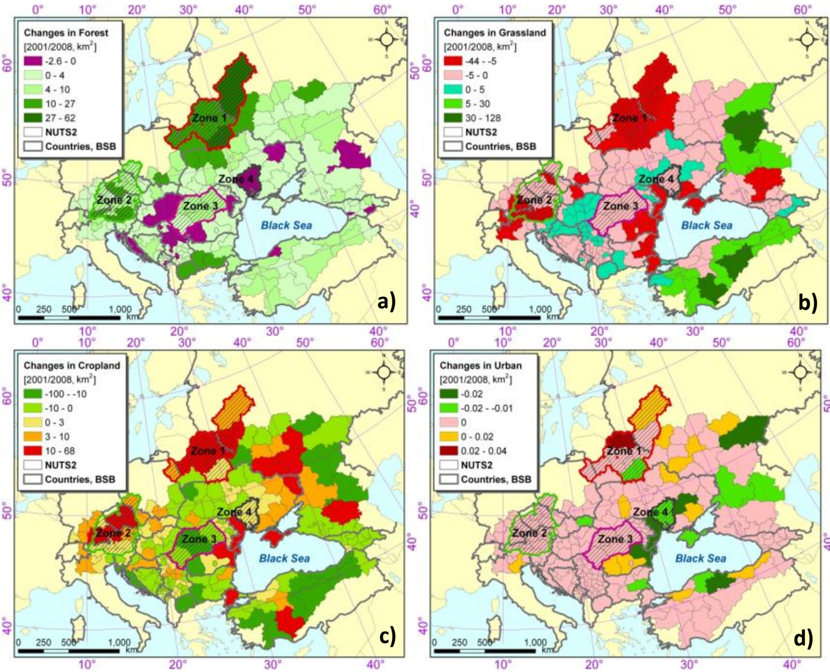

Figure 4.7. Absolute differences in a) forest, b) grassland, c) cropland, d) urban between 2001 and 2008.

4.3.2. Land use change impacts on water resources

Three 37-year model run were performed using S-2001, S-2008, and S-2001-2008. The latter refers to the model with temporal update of land use halfway through simulation time using land use 2001 and 2008 as if the model was built using land use 2001 and updated once to land use 2008 in the middle. The delta approach used does not necessarily provide results that reflect the hydrological observations of the past but illustrates the main changes on the hydrological component [Miller et al., 2002]. On the catchment scale the positive and negative impacts cancel each other out, so that differences in the average long-term water balance components are smaller than 10 mm year^{-1} (Figure 4.8) for the four selected variables: actual evapotranspiration, surface runoff, soil water, and water yields However, more pronounced changes are discernible on long term monthly distribution of the previously mentioned variables (Figure 4.9). The differences are more pronounced in wet seasons from January to May. Figures 4.8 and 4.9 show the spatial variation of long term averages of actual evapotranspiration (AET), water yield (WYLD), soil water (SW), and runoff in 12,982 subbasins of entire BSB model in annual and monthly basis respectively.

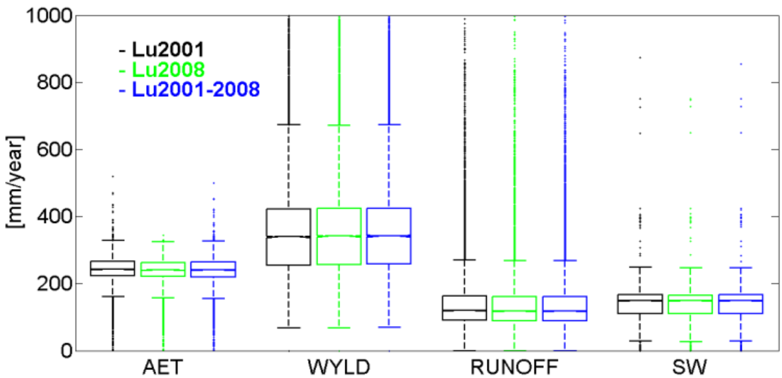

Figure 4.8. Spatial Variation of 34-year averages of water cycle components in BSB, annual distribution.

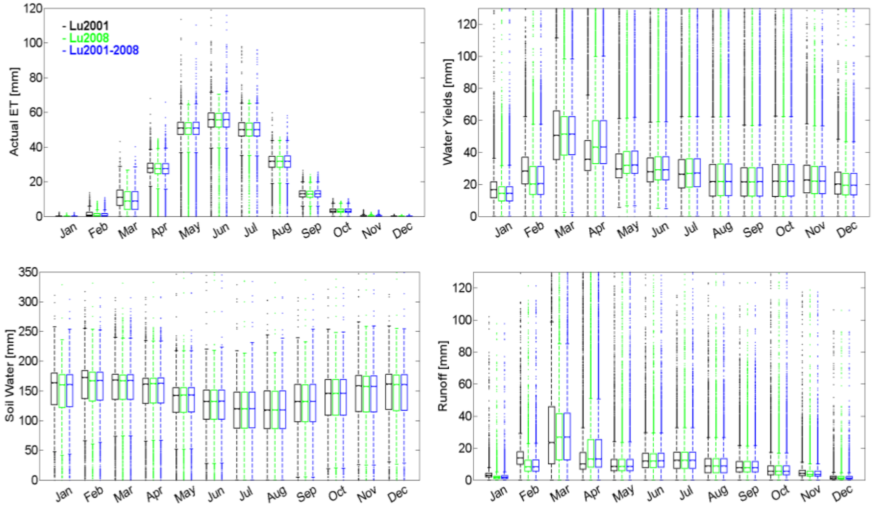

Figure 4.9. Spatial variation of 34-year averages of water cycle components in BSB, monthly distribution.

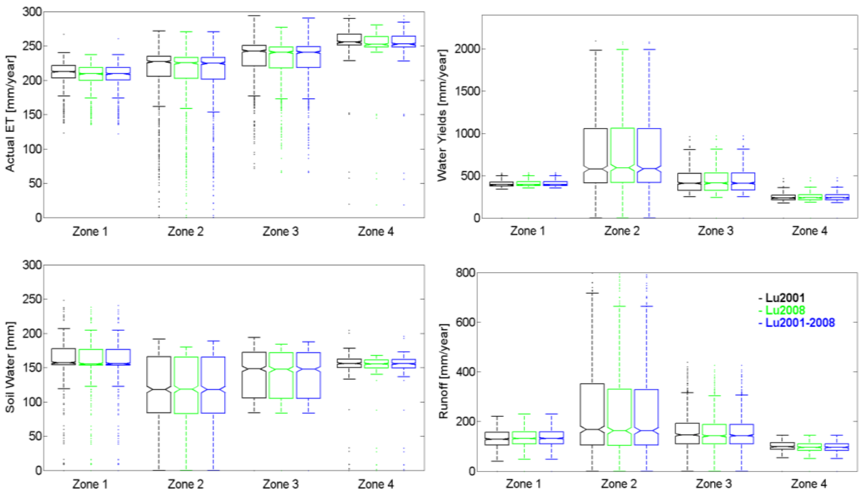

Figure 4.10. Spatial variation of 34 years averages of water cycle components in zones.

To focus more on the different patterns of change, 4 zones were selected and analyzed in more detail in terms of water cycle components. In Zone 1, forest and crop land increased while grassland decreased and urban stayed almost the same. Zone 2 represents areas with growing crop land and less significantly forest expansion while grassland is diminished. In Zone 3 crop land and grass land changed to forest with unvarying urban area. In Zone 4, forest shrinked to cropland while urban and grassland stayed almost the same. The spatial variations of long-term average of selected water cycle components were distinctly different in the four zones (Figure 4.10).

The changes between the three land use scenarios had more significantly impacted on monthly distribution of long term averages of the four water cycle components (Figure 4.11) than yearly distribution (Figure 4.10). While spatial variation of the selected components show only little differences between the three models (Figure 4.10), the monthly distribution of the water cycle components highlights the differences between the three model estimation, especially in wet seasons from Jan to May (Figure 4.11). The differences in model results are more pronounced in zone 1 and Zone 4, where the components do not change spatially if subbasins lie in the corresponding Zones. Although the main idea behind zonal analysis was to find a pattern between a particular land use change in a zone and the corresponding water cycle component change, the analysis couldn't clarify the correlation. This ambiguity is due to the fact that there are multiple land use changes occurring in a zone, and that the estimations are temporally averaged. All these make the attribution difficult.

To quantify what effects changes in land uses exert on water cycle components, we looked at the impact of changes in forest, grassland, and cropland at NUTS 2 level for 215 districts. Furthermore, we quantified the changes in actual evapotranspiration, water yields, surface runoff, and soil water, as a result of changes in different land use scenarios (S-2001 and S-2008) in the 215 districts. As it can be visually seen in the plot of percent changes in land use area versus the percent changes in water cycle components in the 215 districts, there are no significant changes in the variables as a result of land use change (Figure 4.12).

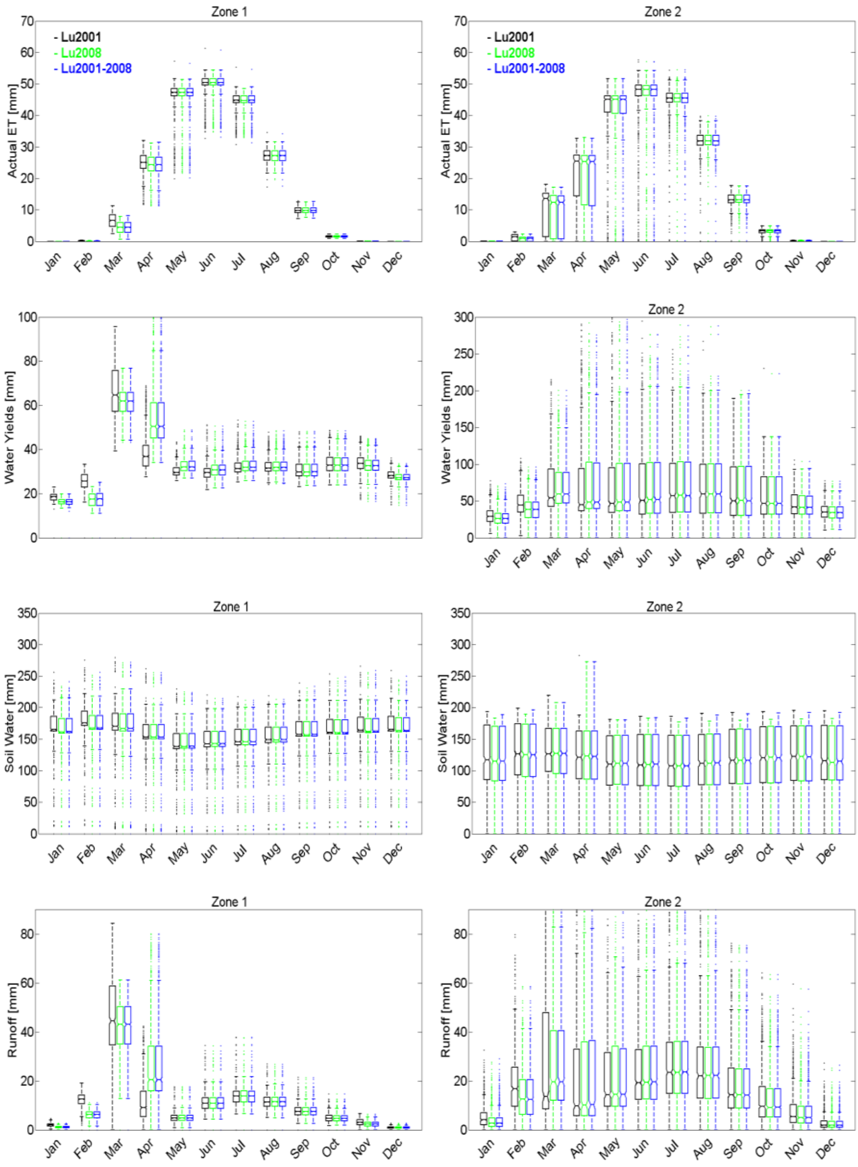
Zone 1
Zone 2
- Lu2001
- Lu2008
- Lu2001-2008
Actual ET [mm]
Water Yields [mm]
Soil Water [mm]
Runoff [mm]
Jan
Feb
Mar
Apr
May
Jun
Jul
Aug
Sep
Oct
Nov
Dec

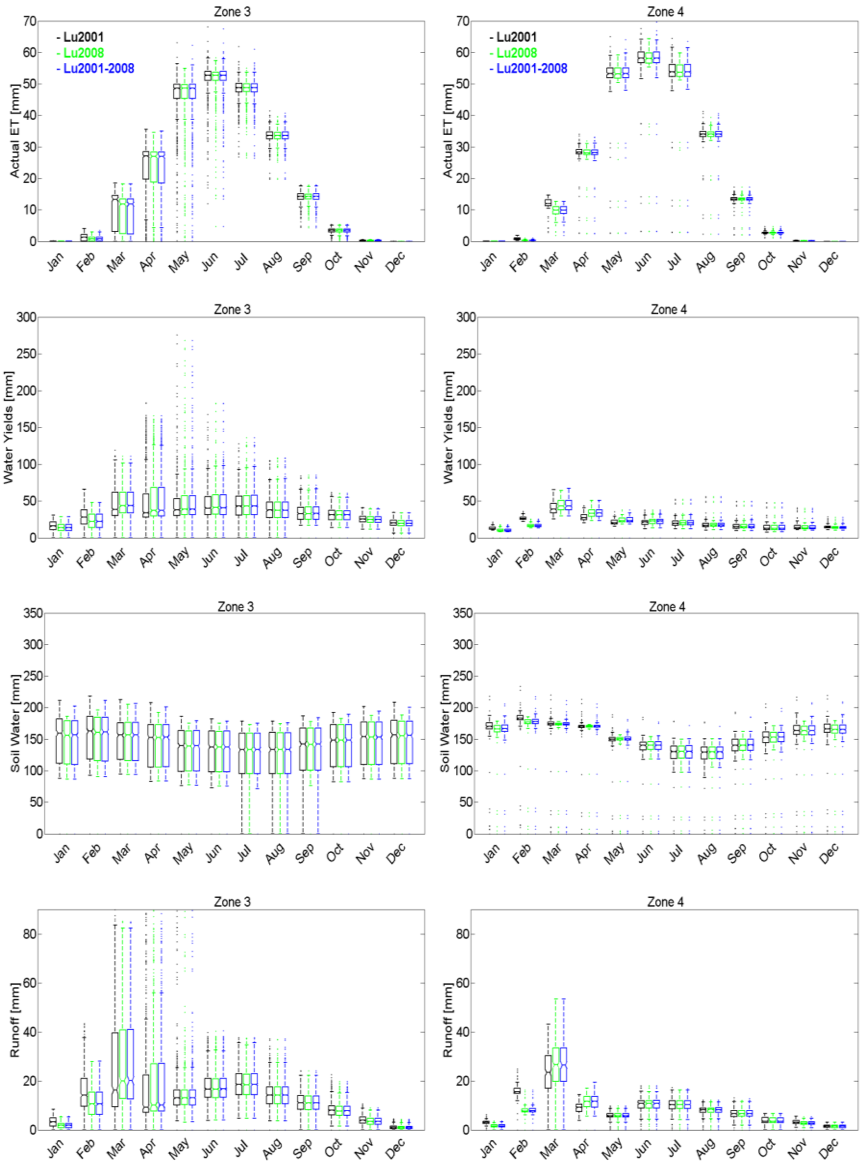

Figure 4.11. 34-year average monthly distributions of water cycle components in different zones.

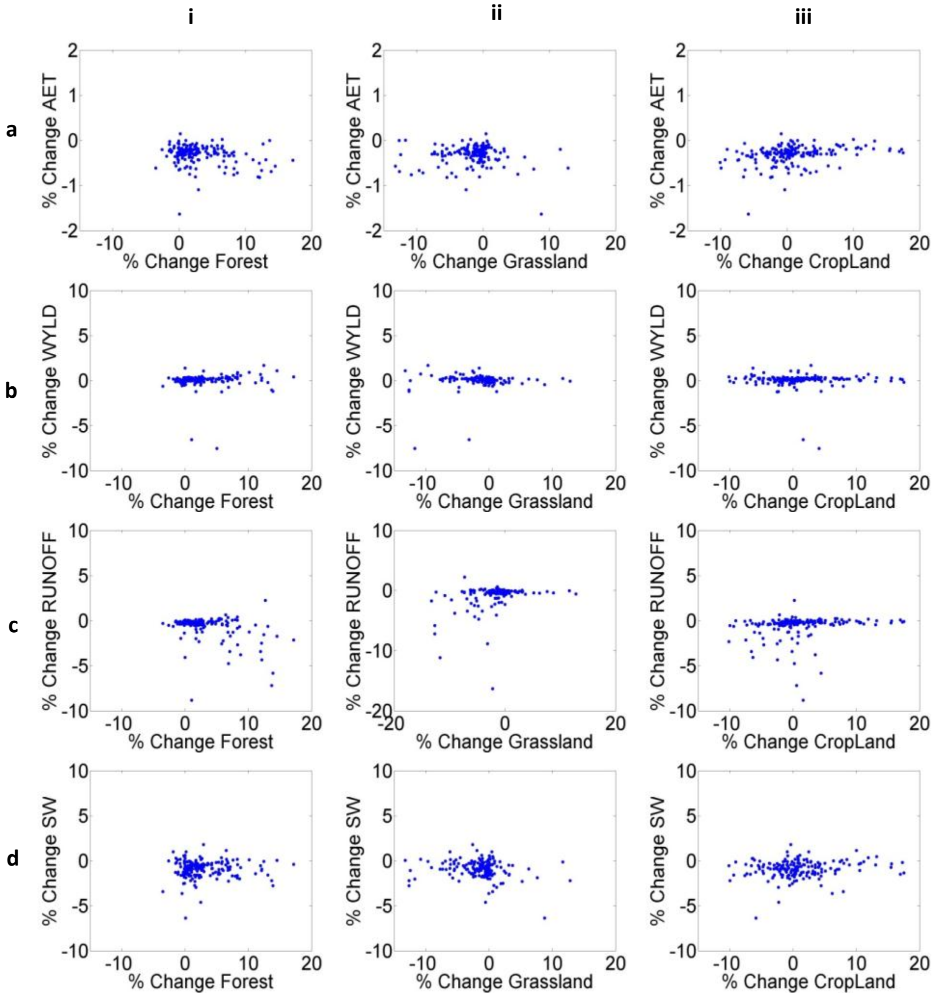

Figure 4.12. Percent changes in a) AET, b) WYLD c) Runoff, and d) SW versus percent changes in i) Forest, ii) Grass land, iii) Crop land at NUTS2 level.

To statistically determine the significance of land use change impacts on water components, we formulated regression equations where water cycle components were treated as dependent variables. The equations were expressed as:

$$Y_i = \beta_1.A + \beta_2.B + \beta_3 C$$

Where Y is the percent change in a water cycle component, β_1, β_2, β_3 are the regression coefficients, A is the percent changes in forest area, B is the percent changes in grassland area, and C is the percent changes in cropland area. AET shows a strong inverse relation to changes in forest area (p-value < 2.2e-16) as it changes by 39% as a result of unit change in forest areas. In this model, changes in other land uses are not as significant to AET.

Table 4.4. Estimates for linear models coefficient for four water cycle components

Y_i	β_1	β_2	β_3	R-squared	P-value
Y_1, %change AET	-0.39	0.025	0.005	0.47	< 2.2e-16
Y_2, %change WYLD	0.037	0.025	0.002	0.0023	0.3307
Y_3, %change RUNOFF	-0.39	0.172	0.048	0.3244	< 2.2e-16
Y_4, %change SW	-0.123	-0.078	-0.02	0.2275	4.064e-11

For runoff, quite the same pattern of change was found with respect to changes in forest, but grassland and cropland also play a significant role. Expectedly, runoff decreases as forest area increases, and increases by increasing grass and cropland areas. Soil moisture is also shown to decrease significantly by decreasing forested areas.

In the next step, to be able to relate more directly the changes in the four water balance variables to changes in land use, we studied the system at the HRU level, which contains a single land use. Contrary to the results given by the linear models, AET shows a higher degree of dependency to changes in agricultural area than forest or grassland where AET significantly increases as agricultural areas grow (Figure 4.13). Changes in forest and grassland had minimum impact on water yields and soil water while the decrease of agricultural area led to a more significant change in water yield and soil water. Decrease of agricultural land led to much more variability in surface runoff with a net decrease in runoff of about 5-7%. Forest and grassland had a more random impact on surface runoff with no discernible pattern (Figure 4.13).

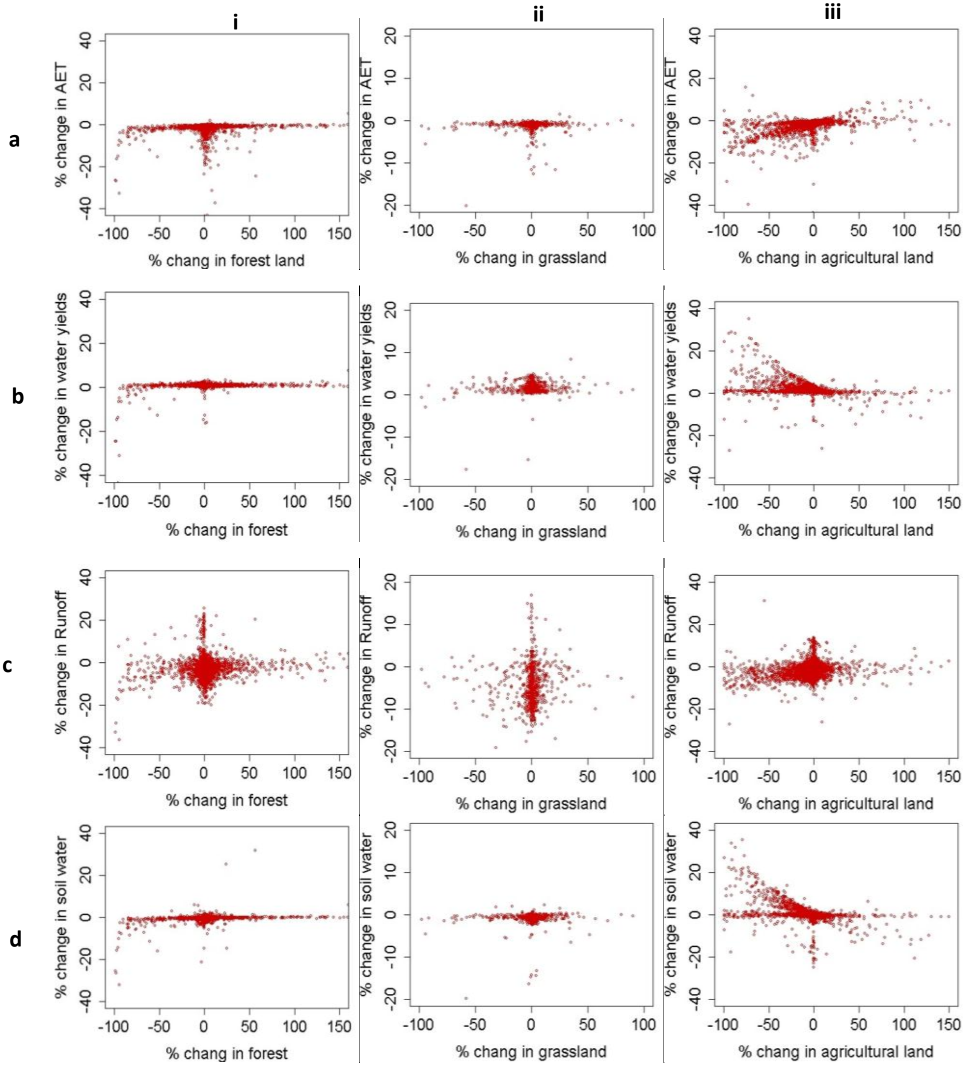

Figure 4.13. Percent changes of a) actual evapotranspiration, b) water yields c) surface runoff, d) soil water versus percent changes in i) forest. ii) grassland, ii) cropland.

4.4. Discussions

According to Hessel et al. [2003], when doing scenario analyses, all scenarios for a watershed are subjected to the same input data uncertainty, so it can be assumed that relative differences in scenario results can in fact be attributed to the applied scenario changes. The results obtained by SWAT depend heavily on the quality of the land use classification. In this study, MODIS land use classifications are paired with the SWAT land classes. Hence this brings the assessment to another level of uncertainty.

Effects of past land use changes in the Black Sea Basin on the water balance components were relatively small. Many authors found that because of compensating effects in complex watersheds with a variety of land use types, impacts of land use changes on hydrology are relatively small at large scales, while they are much more pronounced at smaller scales [Fohrer et al., 2001; Costa et al., 2003; Cao et al., 2009]. This is consistent with the findings in this study.

Analyzing the impact of land use change at larger (watershed, subbasin) and smaller (HRU) levels have their pros and cons. At the larger level changes in water cycle variables are the net results of changes in different land uses, hence not directly attributable to any particular land use change. At the smaller level, however, we only consider the condition where a specific land use is expanding or shrinking, ignoring the fact that the land use in another HRU, which is being converted to the current land use may has different soil and slope characteristics. Nevertheless we suggest analyzing land use change impact at both the HRU level, and the aggregating the results to subbasin level so as to give a better picture of the impact of land use changes.

In the analysis of land use change at the HRU level, models predicted relatively large changes in water cycle components despite minimal changes in land use area. In contrast the spider net analysis of water balance at subbasin level aggregated in larger basins within the BSB and the entire BSB itself, shows insignificant water balance component change due to changes in land use (Figure 4.14). Yet, this may still be used in identifying vulnerable areas where more in depth analysis could be performed.

An important impact of land use change was the increase in soil water and decrease in evapotranspiration due to a decrease in cropland area (Figure 4.13). This was also found in other studies [e.g., Im et al., 2009; Wijesekara et al., 2012]. However, these impacts on runoff and water yields tend not to be very pronounced (<5 %) as compared to the rate of land use change.

It is well known that impacts on the annual water balance of a catchment are relatively small due to compensating effects in a catchment level [e.g., Fohrer et al., 2001]. In a large-scale study on the Meuse River basin, Ashagrie et al. [2006] concluded that the overall impact of land use change was too small to be detected. Wilk and Hughes [2002] argue that the complexity of large river basins could mask many of the impacts of land use changes occuring on smaller scales. Similarly, the FAO [2002] suggests that impacts of land use on hydrology can be studied best in small basins (<1000 km^2). In this study, this effect is underlined by the fact that impacts on the water balance cancel out on the catchment scale, whereas they are observable at the subbasin and HRU scale, and the pattern and attribution of water balance component to specific land use is more distinguishable and pronounced at HRU level.

4.5. Conclusions

Analysis of the current and past land use maps is an important tool for understanding the behavior of land use dynamics in the BSB, in order to establish rules that will reflect this behavior in the future. Our results show that by using SWAT together with available land use map of different dates, land use change impacts on water fluxes can be successfully quantified in the BSB. The main land use categories represented in the BSB are croplands, followed by forest, crops/natural vegetation and grassland, which were found to be more dynamic over time compared to other classes. Our analysis showed that the land use changes had minor impacts on water balance at the watershed scale or the six larger basins within the BSB (Figure 4.14). This is due to compensating effects in catchment scale in large complex watershed and also well reported in literature by other studies. At smaller subbasin scale and at HRU level, the impacts of land use change were quantified using delta method to see the differences in water balance component and finding correlations between land use changes and water cycle component. Nevertheless, at subbasin level as there are multiple land use changes occurring in a subbasin, the changes in water balance cannot be directly attributed to changes of land use. To overcome this, the analyses were carried out at HRU level. Our results on HRU level analysis showed more pronounced changes that could be attributed to land use change alone. However, these results cannot be upscaled to the subbasin or watershed level. Our analyses of water balance at HRU level indicates that an increase in cropland leads to an increase in evapotranspiration up to 20% in some HRUs and decrease in soil water to the same extent. However, these impacts on runoff, water yields tend not to be very pronounced (<5 %) as compared to the rate of land use change. Given that these are only a 7 years land use change impacts and the fact that land use does not change in most hydrologic models, the present study shows the importance of land use update on the accuracy of modeling results especially in long-term modeling work or future analysis. The outcome of this analysis helped to understand the changes in water resources regime due to usage of different land use data in modeling procedures. As a next step, this analysis provides information for considering land use change parameters for future land use change analysis due to the fact that a clear understanding of the behavior of historic land use dynamics in the BSB was needed in order to examine the necessity of such an analysis for future land-climate interaction studies.

Acknowledgments

This project has been funded by the European Commission's Seventh Research Framework through the enviroGRIDS project (Grant Agreement n 226740).

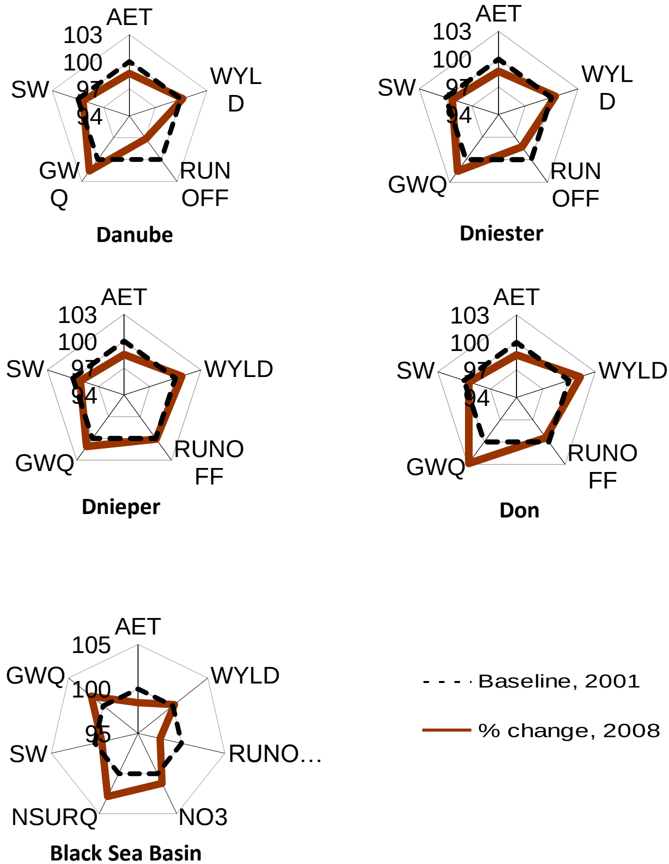

Figure 4.14. Changes in water cycle components in major basins of BSB.

References

Arnold, J. G., R. Srinivasan., R. S. Muttiah., and J. R. Williams (1998), Large area hydrologic modeling and assessment part I: model development. Journal of American Water Resources Association, 34 (1), 73-89.

Arnold, J.G., P. M. Allen, M. Volk, J. Williams, D. D. Bosch, 2010. Assessment of different representations of spatial variability on SWAT model performance. Transactions of the ASABE 53, 1433e1443.

Ashagrie, A. G., P. J. de Laat, M. J. de Wit, M. Tu, and S. Uhlenbrook (2006), Detecting the influence of land use changes on discharges and floods in the Meuse River Basin – the predictive power of a ninety-year rainfall-runoff relation?, Hydrol. Earth Syst. Sci., 10, 691–701, doi:10.5194/hess-10-691-2006.

Bergström, S., and A. Forsman (1973), Development of a conceptual deterministic rainfall-runoff model, Nord. Hydrol., 4, 147–170.

Bieger, K.G. Hörmann, and N. Fohrer (2013), The impact of land use change in the Xiangxi Catchment (China) on water balance and sediment transport, Reg Environ Change, DOI 10.1007/s10113-013-0429-3.

Black Sea Investment Facility (BSEI) (2005), 'Review of the Black Sea Environmental Protection Activities. General review', Black Sea Investment Facility.

Bosch, D.D., J. G. Arnold, M. Volk, P. M. Allen (2010), Simulation of a low-gradient coastal plain watershed using the SWAT landscape model. Transactions of the ASABE 53, 1445e1456.

Bultot F, G. L. Dupriez, and D. Gellens (1990), Simulation of land use changes and impacts on the water balance—a case study for Belgium. J Hydrol 114:327–348. doi:10.1016/0022 1694(90) 90064-5

Climatic Research Unit (CRU) (2008), CRU Time Series (TS) high resolution gridded datasets, University of East Anglia Climatic Research Unit (CRU), NCAS British Atmospheric Data Centre, Available from: http://badc.nerc.ac.uk/view/badc.nerc.ac.uk__ATOM__dataent_1256223773328276.

Douglas-Mankin, K., R. Srinivasan, J. G. Arnold (2010), Soil and water assessment tool (SWAT) model: current developments and applications, Transactions of the ASABE 53, 1423e1431.

Eckhardt K, L. Breuer, and H. G. Frede (2003), Parameter uncertainty and the significance of simulated land use change effects. J Hydrol 273:164–176. doi:10.1016/S0022-1694(02)00395-5

EEA Catchments and Rivers Network System (ECRINS) v1.1 (2012), Rationales, building and improving for widening uses to Water Accounts and WISE applications, Luxembourg: Publications Office of the European Union, ISBN *978-92-9213-320-7*, ISSN *1725-2237*, doi:10.2800/51667.

Fohrer N, D. Moöller, and N. Steiner (2002), An interdisciplinary modelling approach to evaluate the effects of land use change. Phys Chem Earth 27:655–662. doi:10.1016/S1474-7065(02)00050-5

Fohrer N, S. Haverkamp, and H. G. Frede (2005), Assessment of the effects of land use patterns on hydrologic landscape functions: development of sustainable land use concepts for low mountain range areas. Hydrol Process 19:659–672. doi:10.1002/hyp.5623

Fohrer N, S. Haverkamp, K. Eckhardt, and H. G. Frede (2001), Hydrologic response to land use changes on the catchment scale. Phys Chem Earth 26(7–8):577–582. doi:10.1016/S1464-1909(01)00052-1.

Food and Agricultural Organization (FAO) (2003), The digital soil map of the world and derived soil properties, CD-ROM, Version 3.5, Rome, Italy.

Gassman, P. W., M. Reyes, C. H. Green, and J. G. Arnold (2007), The Soil and Water Assessment Tool: Historical development, applications, and future directions, T. ASABE, 50, 1211–1250.

Gassman, P.W., M. Reyes, C. Green, J. G. Arnold (2007), The soil and water assessment tool: historical development, applications, and future research directions. Transactions of the ASABE 50, 1211e1250.

Ghaffari, G., S. Keesstra, J. Ghodousi, and H. Ahmadi (2010), SWATsimulated hydrological impact of land-use change in the Zanjanrood basin, Northwest Iran, Hydrol. Process., 24, 892–903.

Global Runoff Data Centre (GRDC) (2011), Long-Term Mean Monthly Discharges and Annual Characteristics of GRDC Station / Global Runoff Data Centre. Koblenz, Germany: Federal Institute of Hydrology (BfG), http://grdc.bafg.de.

Goetz, S., T. Jaksch, and R. Sibert (Eds.), A. Aldershot (2001), Agricultural transformation of land use in Central and Eastern Europe, Journal of land use policy, xxiv+340pp., ISBN 0 7546 1372 0.

Guo H., Q. Hu, T. Jiang (2008), Annual and seasonal streamflow responses to climate and land-cover changes in the Poyang Lake basin, China, J. Hyrol 355:106–122. doi:10.1016/j.jhydrol.2008.03.020.

He H., J. Zhou, W. Zhang (2008), Modelling the impacts of environmental changes on hydrological regimes in the Hei River Watershed, China. Global Planet Change 61:175–193. doi: 10.1016/j.gloplacha.2007.08.012

Huisman J.A., L. Breuer, and H. G. Frede (2004), Sensitivity of simulated hydrological fluxes towards changes in soil properties in response to land use change. Phys Chem Earth 29:749–758. doi:10.1016/j.pce.2004.05.012

Im, S., H. Kim, C, Kim, and C. Jang (2009), Assessing the impacts of land use changes on watershed hydrology using MIKE SHE, Environ. Geol., 57, 231–239.

Im, S., H. Kim, C. Kim, and C. Jang (209), Assessing the impacts of land use changes on watershed hydrology using MIKE SHE, Environ. Geol., 57, 231–239.

Jarvis, A., H. I. Reuter, A. Nelson, and E. Guevara (2008), Hole-filled SRTM for the globe Version 4, Data access: The CGIAR-CSI SRTM 90m Database: http://srtm.csi.cgiar.org.

Kirchner, J. W (2006), Getting the right answers for the right reasons: Linking measurements, analyses, and models to advance the science of hydrology, Water Resour. Res., 42, W03S04, doi:10.1029/2005WR004362.

Klöcking B, and U. Haberlandt (2002) Impact of land use changes on water dynamics—a case study in temperate meso and macroscale river basins. Phys Chem Earth 27:619–629. doi: 10.1016/S1474-7065(02)00046-3.

Legesse D, C. Vallet-Coulomb, and F. Gasse (2003), Hydrological response of a catchment to climate and land use changes in Tropical Africa: case study South Central Ethiopia. J Hydrol 275:67–85. doi:10.1016/S0022-1694(03)00019-2

Leh M, S. Bajwa, and I. Chaubey (2011), Impact of land use change on erosion risk: an integrated remote sensing, geographic information system and modeling methodology. Land Degrad Dev. doi:10.1002/ldr.1137.

Lenhart T, N. Fohrer, and H. G. Frede (2003), Effects of land use changes on the nutrient balance in mesoscale catchments. Phys Chem Earth 28:1301–1309. doi:10.1016/j.pce.2003.09.006.

Li, Z., W. Liu, X. Zhang, and F. Zheng (2009), Impacts of land use change and climate variability on hydrology in an agricultural catchment on the Loess Plateau of China, J. Hydrol., 377, 35–42.

Lin Y. P., N. M. Hong, P. J. Wu, C. F. Wu, and P. H. Verburg (2007), Impacts of land use change scenarios on hydrology and land use patterns in the Wu-Tu watershed in Northern Taiwan. Landsc Urban Plan 80:111–126.doi:10.1016/j.landurbplan.2006.06.007

Miller, S. N., W. G. Kepner, M. H. Mehaffey, M. Hernandez, R. C. Miller, D. C. Goodrich, K. K. Devonald, D. T. Heggem, and W. P. Miller (2002), Integrating landscape assessment and hydrologic modeling for land cover change analysis, J. Am. Water Resour. As., 38, 915–929.

Mitchell, T. D. and P. D. Jones (2005), An improved method of constructing a database of monthly climate observations and associated high-resolution grids, Int. J. Climatology, 25, 693-712, doi: 10.1002/joc.1181.

NASA (2001), Land Processes Distributed Active Archive Center (LP DAAC), ASTER L1B, USGS/Earth Resources Observation and Science

(EROS) Center, Sioux Falls, South Dakota, Data access: http://lpdaac.usgs.gov.
Ndomba, P., F. Mtalo, and A. Killingtveit (2008), SWAT model application in a data scarce tropical complex catchment in Tanzania, Phys. Chem. Earth, 33, 626–632.
Neitsch S. L., J. G. Arnold , J. R. Kiniry, J. R. Williams (2009), Soil and water assessment tool theoretical documentation version 2009, Texas Water Resources Institute Technical Report No. 406. Texas A&M University System, College Station.
Neitsch, S., J. G. Arnold, J. R. Kiniry, J. Williams (2011), Soil & Water Assessment Tool Theoretical Documentation Version 2009, Texas Water Resources Institute Technical Report No. 406, College Station, Texas, p. 618.
Niehoff, D., U. Fritsch, and A. Bronstert (2002), Land-use impacts on storm-runoff generation: scenarios of land-use change and simulation of hydrological response in a meso-scale catchment in SW-Germany, J. Hydrol., 267, 80–93.
Ouyang W, Skidmore AK, Hao F, Wang T (2010) Soil erosion dynamics response to landscape pattern. Sci Total Environ 408:1358–1366. doi:10.1016/j.scitotenv.2009.10.062.
Refsgaard, J. C. and B. Storm (1995), MIKE SHE, in: Computer Models of Watershed Hydrology, edited by: Singh, V. P., Water Resources Publications, Highlands Ranch, Colorado, 809–846.
RIKS (2005), The Metronamica modelling framework: model descriptions, Model documentation. Maastricht: Research Institute for Knowledge Systems.
Rouholahnejad, E., K. C. Abbaspour, V. Bacu, and A.Lehmann (2013), A high resolution spatiotemporal distribution of water resources quantity and quality in the Black Sea Basin, Water Resources Research.
Rounsevell, M.D.A, I. Reginster, M.B. Arau´jo, T.R. Carter, N. Dendoncker, F. Ewert, J.I. House, S. Kankaanpää, R. Leemans, M.J. Metzger, C. Schmit, P. Smith, and G. Tuck (2006), A coherent set of future land use change scenarios for Europe, Agriculture, Ecosystems and Environment 114 (2006) 57–68.
Sahin V, and M. J. Hall (1996), The effects of afforestation and deforestation on water yields. J Hydrol 178:293–309, doi:10.1016/0022-1694 (95)02825-0
Schulla, J (1997), Hydrologische Modellierung von Flussgebieten zur Abschätzung der Folgen von Klimaänderungen, Zürcher Geographische Schriften, 69, Geographisches Institut ETH, Zürich.
Schuol, J., K. C. Abbaspour, R. Srinivasan, and H. Yang (2008b), Modelling Blue and Green Water Availability in Africa at monthly intervals and

subbasin level, J. Water Resources Research, 44, W07406, doi: 10.1029/2007WR006609.

Stehr, A., P. Debels, F. Romero, and H. Alcayaga (2008), Hydrological modelling with SWAT under conditions of limited data availability: evaluation of results from a Chilean case study, Hydrolog. Sci. J., 53, 588–601.

Stoate C., A. Ba' ldi , P. Beja , N.D. Boatman, I. Herzon, A. van Doorn, G.R. de Snoo, L. Rakosy, and C. Ramwell (2009) Journal of Environmental Management 91 (2009) 22–46.

Stonestrom, D. A., B. R. Scanlon, and L. Zhang (2009), Introduction to special section on Impacts of Land use Change on Water Resources, Water Resour. Res., 45, W00A00, doi:10.1029/2009WR007937.

Tockner, K., U. Uehlinger, and C. T. Robinson (2009), Rivers of Europe, Academic Press, ISBN: *978-0-12-369449-2*.

Tong S. T. Y., and W. Chen (2002), Modeling the relationship between land use and surface water quality. J Environ Manag 66:377–393. doi: 10.1006/jema.2002.0593

Van Rompaey A.J.J., G. Govers , E. Van Hecke, and K. Jacobs (2001), The impacts of land use policy on the soil erosion risk: a case study in central Belgium. Agric Ecosyst Environ 83:83–94. doi:10.1016/S0167-8809(00)00173-0

Verburg P. H., and A. Veldkamp (2001) The role of spatially explicit models in land-use change research: a case study for cropping patterns in China. Agric Ecosyst Environ 85:177–190. doi:10.1016/S0167-8809(01)00184-0

Wagner, P. D., S. Kumar, and K.Schneider (2013), An assessment of land use change impacts on the water resources of the Mula and Mutha Rivers catchment upstream of Pune, India, P. D. Wagner, S. Kumar, and K.Schneider, Hydro. Earth Syst. Sci., 17, 2233-2246, doi: 10.5194/hess-17-2233-2013.

Wang S., S. Kang , L. Zhang, F. Li (2008), Modelling hydrological response to different land-use and climate change scenarios in the Zamu River basin of northwest China, Hydrol Process 22:2502–2510. doi:10.1002/hyp.6846.

Williams J. R., (1969), Flood routing with variable travel time or variable storage coefficients, Trans ASAE 12(1):100–103.

Global Environmental Change, to be submitted

5. Impacts of changing climate and land use on water resources of the Black Sea Basin

Elham Rouholahnejad[1, 2], Karim C. Abbaspour[1], Emanuele Mancosu[3],Raghvan Srinivasan [4], Anthony Lehmann[5]

[1]Eawag, Swiss Federal Institute of Aquatic Science and Technology, Ueberlandstrasse 133, 8600 Duebendorf, Switzerland.

[2] ETH Zürich Institute of Terrestrial Ecosystem, Universitätstr. 16, 8092 Zürich, Switzerland.

[3] UMA - ETCSIA, University of Malaga, European Topic Centre for Spatial Information and Analysis, 29071, Malaga, Spain

[4] Spatial Sciences Laboratory, Texas A&M University, Texas Agricultural, Experimental Station, College Station, Texas, USA

[5] University of Geneva, Climatic Change and Climate Impacts, 7 Route de Drize, CH-1227 Carouge, Switzerland.

Abstract

As water resources become further stressed due to increasing levels of societal demand, understanding the effect of climate change on various components of the water cycle is of strategic importance. A hydrologic model of the Black Sea Basin (BSB) was developed using the Soil and Water Assessment Tool (SWAT) and calibrated for 1970 to 2006 using daily river discharges, river nitrate loads, and annual agricultural crop yield. Future climate scenarios for 2013–2050 were generated from the Danish Regional Climate Model (RCM) (HIRHAM) for IPCC's SRES A2 and B2 scenarios which were downscaled for 1147 climate stations across the BSB using the Delta Method. The two climate scenarios were then applied to the historically calibrated hydrologic model to analyze the effect of future climate on water resources across the BSB The regional climate scenarios were coupled with four land use scenarios based on the IPCC's special report on emissions scenarios (SRES). These included different global socio-economic development pathways described as: BS ALONE, BS COOL, BS COOP, and BS HOT. In general, while the combination of all scenarios showed decreases in water resources in wet areas, A2 generated rainfalls were more frequent with larger intensities. On average, water resources tend to increase in dry areas and decrease in wet areas. Land use changes show less significant impact on water resources as compared to climate change.

KEYWORDS: Hydrology, Land use change, Climate change, SWAT

5.1. Introduction

Observational evidence from all continents and oceans show that natural systems are affected by regional climate changes, particularly by increases in temperature [IPCC, 2007; Mishra and Singh, 2011]. It is virtually certain that increases in the frequency and magnitude of warm daily temperature extremes and decreases in cold extremes will occur in the 21st century at the global scale [IPCC, 2012]. It is likely that the frequency of heavy precipitation will increase in the 21st century over many areas of the globe [IPCC, 2012]. Nearly all regions of the world are expected to experience a net negative impact of climate change on water resources and freshwater ecosystems [IPCC, 2007]. A number of studies have shown that climate change would have significant effects on water availability, water stresses and water demand [Vörösmarty et al., 2000; Abbaspour et al., 2009; Wang et al., 2011].

It is expected that droughts will intensify in the 21st century in some seasons and areas, due to reduced precipitation and/or increased evapotranspiration. This applies to southern and central Europe and the Mediterranean region [IPCC 2012]. Climate change will pose added challenges to the efforts to manage high disaster risk areas.

Changes in the context of increasing vulnerability, will lead to increased stress on human and natural systems and a propensity for serious adverse effects in many places around the world [UNISDR, 2009, 2011]. At the same time, climate change is also expected to bring benefits to certain places and communities, in particular short-term gains in crop yield [Liu et al., 2013].

The Black Sea Basin (BSB) lies in a transition zone between the Mediterranean region in an arid climate of North Africa and the temperate and rainy climate of central Europe and it is affected by interactions between mid-latitude and tropical processes. Because of these features, even relatively minor modifications of the general circulation can lead to substantial changes in the Mediterranean climate [Giorgi and Lionello, 2008]. This makes the BSB a potentially vulnerable region to climatic changes as induced, for example, by increasing concentrations of greenhouse gases [e.g. Lionello et al., 2006; Ulbrich et al., 2006]. Indeed, the Mediterranean region has shown large climate shifts in the past [Luterbacher et al., 2006] and it has been identified as one of the most prominent “Hot-Spots” in future climate change projections [Giorgi 2006].

Giorgi and Lionello [2008] reviewed a few climate change projections over the Mediterranean region based on the most recent and comprehensive ensembles of global and regional climate change simulations. There is also a comprehensive review of climate change projections over the Mediterranean region reported by Ulbrich et al. [2006] based on a limited number of global and regional model simulations performed throughout the early 2000s. A number of papers have reported regional climate change simulations over Europe, including totally or partially the BSB [e.g. Rotach et al., 1997; Jones et al., 1997; Machenhauer et al., 1998; Christensen and Christensen 2003; Semmler and Jacob 2004; Schar et al., 2004; Raisanen et al., 2004; Deque et al., 2005]. Finally, several studies have presented regional evaluations of different generations of global model projections, including the Mediterranean region [Kittel et al., 1998; Giorgi and Bi 2005a, b].

Despite the importance of this region within the global change context, assessments of water resources under different climate change projections are relatively sparse in the literature.

Recent research efforts provide an opportunity to approach the BSB climate change assessment on much stronger grounds than in the past. First, a worldwide effort has been recently carried out by which about 20 research groups around the world completed a large set of global climate simulations for the 20th and 21st century under different greenhouse gas forcing scenarios as a contribution to the fourth Assessment Report (AR4) of the Intergovernmental Panel on Climate Change (IPCC). In addition, the European project Prediction of Regional scenarios and Uncertainties for Defining, EuropeaN Climate change and associated risks and Effects [PRUDENCE, Christensen et al., 2002 and 2007], provides a wide range of global and regional climate models which were used to produce climate change projections over the European region. In the current study, the Danish Regional Climate Model (RCM) HIRHAM, driven by the United Kingdom's Hadley Center HadAM3H GCM was used under the scope of the PRUDENCE project to assess the future climate change projections over the BSB.

On the other hand, the evaluation of the impacts of land use change on water quantity and quality is fundamental to the development of sustainable land use alternatives [Lenhart et al., 2003; Lin et al., 2007] and is an integral component of river basin and water resources management [Eckhardt et al., 2003; Huisman et al., 2004]. A range of models has been developed to better understand and assess changes in land use and land cover in Europe [Veldkamp and Lambin, 2001; Parker et al., 2003; Veldkamp and Verburg, 2004]. However, in spite of progress in integrating biophysical and socio-economic drivers of land use change [Veldkamp and Verburg, 2004], prediction of future land use remains difficult. Scenario analysis provides an alternative tool to assist in explorations of the future. Rounsevell et al. [2005] presented a range of spatially explicit future land use change scenarios for the EU15, Norway and Switzerland, based on an interpretation of the global storylines of the Intergovernmental Panel on Climate Change (IPCC) that are presented in the special report on emissions scenarios (SRES). The scenarios include the major land use/land cover classes: urban, cropland, grassland and forest land as well as introducing new land use classes such as bioenergy crops.

In this study, the quantification of land use scenarios was based on the framework provided by the Integrated Model to Assess the Global Environment [IMAGE, version 2.2: IMAGE team, 2001]. The four land use change scenarios used in the current study comprise a number of plausible alternatives (storylines) based on the IPCC-SRES [Nakicenovic et al., 2000] following four marker scenarios represent different global socio-economic development pathways: i) BS HOT which corresponds to the IPCC's A1FI scenarios (fossil intensive), with high economic development and free-market policies, where environmental issues are not the main concern. ii) BS COOP refers to the B1 climate scenarios, involving strong international cooperation in which environmental concerns are taken seriously. iii) BS ALONE, and iv) BS COOL correspond to the A2 and B2 regional scenarios, respectively.

For a long-term strategic planning of a country's water resources in the face of the evolving climate and land use change impacts, it is important that these effects be quantified with a high spatial and temporal resolution. However, few publications have focused on the long-term evaluation of a basin's water balance due to combination of climate and land use change impacts on regional hydrologic processes in

BSB. Yet this may be the most beneficial application of hydro-climatology to support long-term water resources management and planning [Serrat-Capdevila et al., 2007].

An integrated hydrologic model coupled with scenarios of changes could help to study the net effect of climate and land use change in a region. Models often used to assess impacts of land and climate changes on water resources include: HBV [Bergström and Forsman, 1973; e.g., Ashagrie et al., 2006], MIKE-SHE [Refsgaard and Storm, 1995; e.g., Im et al., 2009], SWAT [Arnold et al., 1998; e.g., Fohrer et al., 2001], and WaSiM-ETH [Schulla, 1997; e.g., Niehoff et al., 2002] among many others. These models are particularly useful as they can assess past as well as possible future impact scenarios. The Soil and Water Assessment Tool [SWAT, Arnold et al., 1998] has proven its suitability for hydrologic impact studies [Gassman et al., 2007], especially under conditions of limited data availability [Ndomba et al., 2008; Stehr et al., 2008]. Hence, it is a suitable model to study the impact of climate and land use changes on water resources in the BSB.

In this study we used a previously calibrated SWAT model [Rouholahnejad et al., 2013] to assess the impact of climate and land use change on the water resources of the BSB for 2013-2050. In addition the impacts of climate change without considering land use change is also addressed for this period. We specifically looked at the changes in various components of the water balance including precipitation and evapotranspiration distribution, soil moisture, and aquifer recharge. These variables were then used to quantify the changes in water resources with respect to blue water (river discharge plus aquifer recharge) and green water (soil moisture and evapotranspiration).

5.2. Material and Methods

5.2.1. Study area

The Black Sea Basin drains rivers of 23 European and Asian countries (Austria, Belarus, Bosnia, Bulgaria, Croatia, Czech Republic, Georgia, Germany, Hungary, Moldova, Montenegro, Romania, Russia, Serbia, Slovakia, Slovenia, Turkey, Ukraine, Italy, Switzerland, Poland, Albania and Macedonia) from an area of 2.3 million km^2 into the Black Sea (Figure 5.1). The Basin is inhabited by a total population of around

160 million people [BSEI, 2005]. Major rivers draining into the Black Sea include Danube, Dniester, Dnieper, Don, Kuban, Sakarya, and Kizirmak. The greatest sources of diffuse pollution in the basin are agriculture and households not connected to sewer systems. The BSB is mountainous in the east and south, in the Caucasus and in Anatolia, and to the northwest with the Carpathians in the Ukraine and Romania. Most of the rest of the Black Sea's western and northern neighborhood is low lying. The mean annual air temperature shows a distinct north-south gradient from <-3 °C to >15 °C. The precipitation pattern is characterized by a west-east gradient that is decreasing with distance from the Atlantic Ocean. Areas of high precipitation (>3000 mm $year^{-1}$) are in the west and areas of low precipitation (< 190 mm $year^{-1}$) are in the north and east [Tockner et al., 2009]. The dominant land use in the basin is agricultural land with 65% of coverage according to MODIS Land Cover [NASA, 2001].

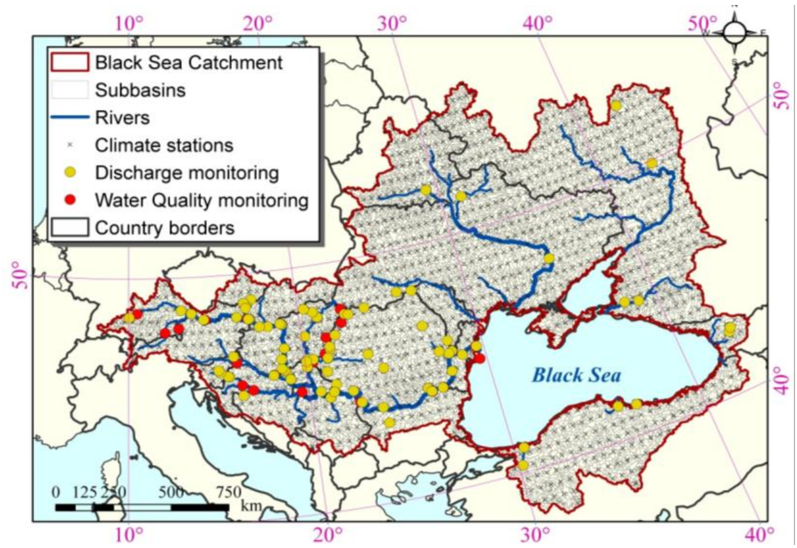

Figure 5.1. General map of study area presenting geographic distribution of major rivers, subbains, countries political boundaries, observation stations of climate, river discharge and nitrate loads.

5.2.2. Soil Water Assessment Tool (SWAT)

The Soil and Water Assessment Tool [Arnold et al., 1998] was used to simulate hydrology, water quality, and vegetation growth in BSB. SWAT is a process-based, semi-distributed hydrologic model which is developed to quantify the impact of land management practices on water, sediment and agricultural chemical yields in large complex watersheds with varying soils, land uses and management conditions over long periods of time. SWAT has been used for the assessment of land use and management impacts on water quantity and quality in many studies worldwide [Guo et al., 2008; He et al., 2008; Ouyang et al., 2008; Wang et al., 2008]. Hydrology, climate, nutrient cycling, soil temperature, sediment movement, crop growth, agricultural management, and pesticide dynamics are the main components of SWAT. The spatial heterogeneity of the watershed is preserved by topographically dividing the basin into multiple sub-basins. The subbasins are further subdivided into hydrologic response units (HRU). These are lumped areas within a subbasin with a unique combination of slope, soil type and land use and enable the model to reflect differences in evapotranspiration for various crops and soils. Simulation of the hydrologic cycle is separated into a land phase and a water phase [Neitsch et al., 2009]. The simulation of the land phase is based on the water balance equation, which is calculated separately for each HRU. Runoff generated in the HRUs is summed up to calculate the amount of water reaching the main channel in each subbasin [Neitsch et al., 2009]. The water phase of the hydrologic cycle describes the routing of runoff in the river channel, using the variable storage coefficient method by Williams [1969]. A detailed description of the model can be obtained from Neitsch et al. [2009].

5.2.3. Land use scenarios

The land use scenarios which are used in the current study are developed within the European Union 7th research framework through EnviroGrids project. The developed scenarios comprise a number of plausible alternatives (storylines) based on a coherent set of assumptions, key relationships and driving forces, to create a set of quantitative, internally consistent and spatially explicit scenarios of future land use covering the entire BSB.

The scenario storylines are based on the IPCC's special report on emissions scenarios (SRES) [Nakicenovic et al., 2000]. Four marker scenarios representing different global socio-economic development pathways as shown in Figure 5.2, were chosen for this study. In the vertical axis, 'A' represents economically oriented scenarios and 'B' is environmentally and equity oriented one. In the horizontal axis, '1' represents the globalized and '2' the regionalized scenario. The research group [Mancosu et al., 2012] partially used other related global scenario studies, such as World Water Vision [Cosgrove and Rijsberman, 2000], Global Scenario Group [Kemp-Benedict et al., 2002] and Four Energy Futures [Bollen et al., 2004], as well as European studies such as ATEAM [Rickebusch et al., 2011], EUruralis [Klijn et al., 2005] and Prelude [EEA, 2005] in the scenario development.

The four localized scenarios particularly defined for land use scenarios of changes in the BSB are characterized as follows:

(i) BS HOT – In this scenario the highest economic growth is assumed, with low population increase, free-market policies, very large increase in greenhouse gas emissions, and consequently global climate change. This also implies very high environmental pressures in the areas of the BSB, which could be partially alleviated by rapidly emerging technological developments. In general, agricultural areas will decline in the BSB due to strong urbanization. Abandoned land tends to turn into urban areas or natural vegetation and forest. Forest areas will increase in all countries initially, but afterwards will decrease in western countries and increase in eastern countries.

Urbanization rates will increase due to population movement from rural to urban areas and consequently there will be an expansion of built-up areas. Urban areas are expected to increase in highly populated regions as a result of high rates of economic development and population growth. As a result of high population growth, high economic growth leads to a larger use of space per person and consequently growth in the industry and services sectors. Meanwhile, in sparsely populated areas, natural areas associated with agricultural abandonment are expected to increase.

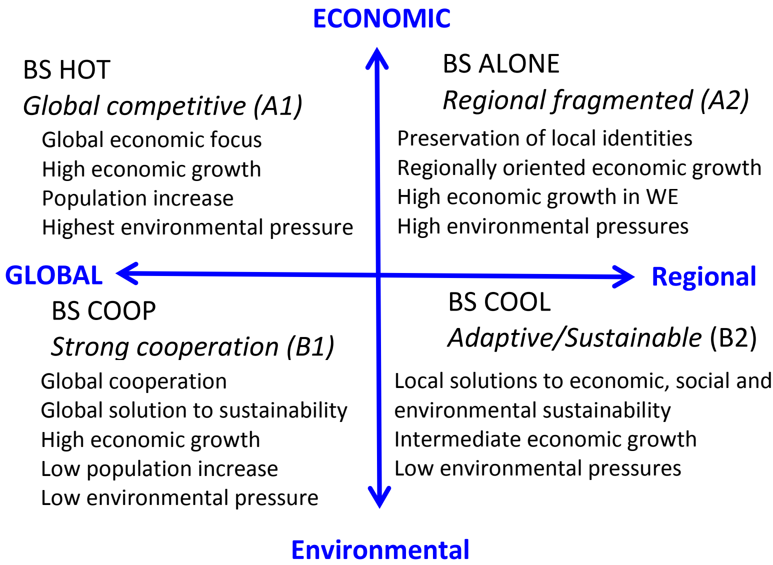

Figure 5.2. Black Sea Basin Scenarios – BS HOT, BS COOP, BS ALONE and BS COOL

(ii) BS ALONE – The BS ALONE scenario is characterized by lower levels of trade and regionally oriented economic growth. In the eastern countries high economic growth and population growth are expected to decrease, while in the western countries economic growth will be lower and population growth will increase. In general, this scenario shows the highest increase in agricultural areas over the whole BSB, due to strong regional policies and production incentives. In this scenario there is strong competition between agriculture and urban areas, deforestation is highly apparent, especially in Western European countries, and nature conservation continues only within existing protected areas. The increase of urban areas is mostly due to the increase in prosperity. These new urban areas will therefore include both sprawl around existing urban areas and an increase in urban areas in tourist regions.

(iii) BS COOP – In the BS COOP scenario economic growth will be high and population growth will be low. Some regions are expected to lose population, mainly during the first period (2000-2025), and afterwards the population will remain stable. Economic growth rates are certainly lower than in BS HOT, but with less pronounced differences between countries. Lower growth is also foreseen during the second period (2025-2050). The emphasis is on globalization of both economic and environmental concerns. In the BS COOP scenario, strong emphasis is placed on the implementation of global environmental policies in order to cut the rise in greenhouse gases and decrease the effects of climate change in the BSB. Afforestation is strongly supported and consequently agricultural areas tend to decline, mainly in less suitable areas. Abandoned lands are expected to be converted to natural protected areas. Urban areas are expected to increase; however, this increment will be very compact (no change in size) due to the strictness of spatial policies, in particular in the western countries. In the eastern countries the planning policies are less strict and the urban areas experience stronger growth; however, this growth is lower than in the BS HOT (global economic) scenario.

(iv) BS COOL – This combines intermediate economic growth with medium population growth. However, a small group of countries in the BSB are expected to increase. Generally this scenario displays the most heterogeneous patterns of development in the BSB countries. In this scenario no major changes in land use are expected to happen. Urbanization is very low and consequently agricultural and forest areas are not expected to change. In this scenario the most important change to emphasize is the conversion to cropland from grassland, especially in the western countries. Table 5.1 summarizes the general trends for the four scenarios.

Table 5.1. Summary of land use trends and driving forces in the Black Sea Basin's scenarios

	Scenarios			
Driving forces	***BS HOT***	***BS ALONE***	***BS COOP***	***BS COOL***
Population growth	low	very high	low	medium
Urban population	increase	increase	slight Increase	slight increase
GDP growth	very high	slow	high	medium
Forest area	increase	decrease	increase	decrease
Grassland area	increase	decrease	increase	decrease
Cropland area	increase	increase	decrease	increase
Built-up area	increase	increase	increase	stable
Protected areas	stable	stable	increase	stable
Climate change	high	high	lower	low

Quantification of land use scenarios

The quantification of land use scenarios was based on the framework provided by the Integrated Model to Assess the Global Environment [IMAGE, version 2.2: IMAGE team, 2001], which is an improved version of the model that was used for the implementation of IPCC-SRES by Alcamo et al. [1998]. The IMAGE framework links the Energy-Industry System (EIS), the Terrestrial-Environmental System (TES), and the Atmosphere-Ocean System (AOS). The land use model simulates changes for 17 regions instead of the 13 regions proposed for the original SRES exercise and also calculates not only the contribution of different sources to greenhouse gas emissions, but also the resulting concentrations, climate change and interactions among individual components [IMAGE team, 2001; Strengers, 2004]. The model provides a large amount of data covering the IPCC-SRES scenarios from 1970 to 2100. The land use model used in IMAGE 2.2 is a rule-based cellular automaton model combining physical and human factors. The output is a spatially explicit description of global land use dynamics at 0.5 degree resolution for 17 regions of the world. The land use model inputs are the land use from the previous time step, the demand for food, feed, biofuel crops and timber products, and potential vegetation [Alcamo et al., 1998; IMAGE team, 2001].

The BSB land use change scenarios used in this study deployed the demand provided by the IMAGE 2.2 model for the selected IPCC-SRES scenarios. Land use changes in the BSB are disaggregated to the regional level and used as input to the regional/local land allocation model (Metronamica). This land use model requires the forest, cropland, grassland and urban areas for each of the 214 regions in the BSB. These regions are a combination of NUTS (Nomenclature of Territorial Units for Statistics) levels 2 and 3.

The land use change scenarios were quantified as yearly changes in land uses on a 1 km x 1 km grid cells, in two time steps 2025 and 2050 for four scenarios, covering the whole BSB. The land use scenarios were developed for cropland, grassland, forest, and urban areas for the BSB countries while the input data were derived from the MODIS land cover datasets for 2001 and 2008.

The land use demand for each of the three IMAGE 2.2 regions lying in the Black Sea Basin, the OECD (Organisation for Economic Cooperation and Development) region of Europe: Austria, Germany, Italy, Switzerland, Turkey, the REF EE (REF Eastern Europe, countries undergoing economic reform): Albania, Bosnia and Herzegovina, Bulgaria, Croatia, Czech Republic, Hungary, Macedonia, Montenegro, Romania, Serbia, Slovakia, Slovenia), and the Former USSR (Belarus, Georgia, Moldova, Russia, Ukraine) were disaggregated at the NUTS2 level assuming that all NUTS2 regions have the same growth rate as the larger, more inclusive unit. The disaggregated land use to the regional level was used as a demand for the land use demand module in the Metronamica model. More details are presented by Mancosu et al. [2012].

5.2.4. Climate change scenarios

Climate projections performed with Global Climate Model (GCM) outputs are used to obtain the necessary data driving the Regional Climate Model (RCM). However, RCM outputs, such as temperature, precipitation, winds, pressure, etc., may not be readily appropriate for use due to systematic errors that could bias the inputs of any subsequent study. A simple approach developed for bias removal which is still popular today is the Delta Method (DM). The DM has been used in various studies as a downscaling technique, as it is known to give reasonable results for the mean characteristics of future temperature and precipitation [Fowler et al., 2007; Lenderink et al., 2007]. The DM is also known for bias removal, since it is based on differences and ratios between current and simulated future climates, assuming that biases are systematic [Lenderink et al., 2007; Bosshard et al., 2011].

In this study, Regional Climate Model (RCM) outputs are used to determine future change in climate with respect to the present-day climate, typically a difference in temperature and a percentage change of precipitation. Then, these changes are applied to observed historical climate data. The mounting data are then used as input to SWAT. The assumption behind this method is that future model bias for both mean and variability will be the same as for present-day simulations. A number of studies have exploited this method [e.g. Quilbé et al. 2008; Wood et al., 2004].

Regional Climate Model outputs

The RCM outputs used in this study were simulated with the Danish RCM HIRHAM, driven by the United Kingdom's Hadley Center HadAM3H GCM outputs. This model had been used under the scope of the Fifth Research Framework Program of the European Union, the PRUDENCE project [Christensen and Christensen, 2007].

Two future climates were simulated for the period of 2013 to 2100 (HS and HB), representing two IPCC's SRES green house gas emission scenarios [Nakicenovic et al., 2000]. The HS scenario corresponds to the IPCC's SRES A2 scenario, while the HB scenario represents the SRES B2 scenario. In this study we used precipitation, and minimum and maximum air temperature at 2 meters above the surface (respectively RCM Pcp, RCM Tmin and RCM Tmax). These data were downloaded from the PRUDENCE website in netCDF format.

A gridded climate dataset created by the Climate Research Unit (CRU), covering the period from 1901 to 2006 with 0.5° grid resolution [CRU, 2008] was used as input data for future climate scenario development.

5.2.5. Model set up, calibration, and validation

To assess the impacts of climate and land use changes on the water resources of the BSB, a previously calibrated and validated hydrological model of the Basin, was used as base model. SWAT was used to model the hydrology, water quality, and crop yields. For calibration and uncertainty analysis, we used the Sequential Uncertainty Fitting program SUFI-2 [Abbaspour et al., 2004, 2007], which is a tool for sensitivity analysis, multi-site calibration, and uncertainty analysis. SUFI-2 is linked to SWAT in the SWAT-CUP software [Abbaspour, 2010]. Details of the model setup and calibration are published elsewhere [Rouholahnejad et al., 2013]. Here we only present a brief summary of input data and model parameterization. These include a digital elevation model (DEM) with a spatial resolution of 90 m [SRTM, Jarvis et al, 2008], a river network dataset [European Catchments and RIvers Network System, ECRINS, 2012], a soil map [FAO, 2003], and climate data [CRU, 2008; Mitchell and Jones, 2005] at 0.5 ^{o} resolution for the period from 1970 to 2006 including daily minimum and maximum temperature, and daily precipitation. MODIS land cover for years 2001 and 2008 with spatial resolution of 500 m [NASA, 2001], and monthly river discharges data for model calibration and validation was mainly obtained from the Global Runoff Data Center [GRDC, 2011]. Nitrate concentrations in rivers were taken from 37 observation stations obtained from the International Commission for the Protection of the Danube River (ICPDR). Cropping area and the start and end month of cropping periods in the BSB were derived from MIRCA2000 database on global monthly irrigated and rainfed cropping areas around the year 2000 (5-year average), at a spatial resolution of 5 arc min [Portmann et al, 2010]. Crop yield data was obtained from McGill University [Monfreda et al., 2008] in NetCDF and ArcGIS ASCII format at 5 arc min resolution. The simulation period was 1970–2006 using SWAT 2009 and Arc SWAT interface for model set up and run. Table 5.2 gives an overview of the relevant methods used in model set up.

Table 5.2. SWAT processes representation as used in the study.

Processes/components	Method [Neitsch et al., 2011]
Evapotranspiration	Hargreaves
Surface runoff	SCS curve number equation
Erosion	Modified universal soil loss equation
Lateral flow	Kinematic storage model
Groundwater flow	Steady-state response from shallow aquifer
Stream flow routing	Variable storage routing

The two climate change scenarios (HB1 and HS1) were paired with the four land use change scenarios (BS ALONE, BS COOL, BS COOP, and BS HOT) leading to 8 combinations of climate-land use scenarios and applied as inputs to the calibrated hydrologic model of the Basin in 8 separate set ups. In addition, two model set ups were designed to look at the climate change only without changing land use. The latter models used MODIS land use in the historical hydrologic model while the other 8 combinations of land use-climate scenarios used a dynamically updating algorithm where land uses were updated yearly up to the end of simulation period.

Table 5.3. List of parameters and their initial ranges used for model calibration

Parameter name	Definition	Initial range
r__CN2.mgt	SCS runoff curve number for moisture condition II	-0.35 - 0.35
r__ALPHA_BF.gw	Base flow alpha factor (days)	-0.8 – 0.8
r__GW_DELAY.gw	Groundwater delay time (days)	-0.8 – 0.8
r__GWQMN.gw	Threshold depth of water in shallow aquifer for return flow (mm)	-0.8 – 0.8
r__GW_REVAP.gw	Groundwater revap. coefficient	-0.4 – 0.4
r__REVAPMN.gw	Threshold depth of water in the shallow aquifer for 'revap' (mm)	-0.4 – 0.4
r__RCHRG_DP.gw	Deep aquifer percolation fraction	0.3 – 0.5
r__CH_N2.rte	Manning's n value for main channel	-0.8 – 0.8
r__CH_K2.rte	Effective hydraulic conductivity in the main channel (mm hr^{-1})	-0.8 – 0.8
r__ALPHA_BNK.rte	Baseflow alpha factor for bank storage (days)	-0.6 – 0.6
r__SOL_AWC().sol	Soil available water storage capacity (mm H2O/mm soil)	-0.5 – 0.5
r__SOL_K().sol	Soil conductivity (mm hr^{-1})	-0.8 – 0.8
r__SOL_BD().sol	Soil bulk density (g cm^{-3})	-0.4 – 0.4
r__SFTMP().sno	Snowfall temperature (°C)	-0.4 – 0.4
r__SMTMP().sno	Snow melt base temperature (°C)	-0.4 – 0.4
r__SMFMX().sno	Maximum melt rate for snow during the year (mm°C^{-1} day^{-1})	-0.4 – 0.4
r__SMFMN().sno	Minimum melt rate for snow during the year (mm°C^{-1} day^{-1})	-0.4 – 0.4
r__SLSUBBSN.hru	Average slope length (m)	-0.4 – 0.4
r__OV_N.hru	Manning's n value for overland flow	-0.4 – 0.4
r__HRU_SLP.hru	Average slope steepness (m m^{-1})	-0.4 – 0.4
r__CMN.bsn	Rate factor for humus mineralization of active organic nitrogen	-0.4 – 0.4
r__NPERCO.bsn	Nitrogen percolation coefficient	-0.4 – 0.4
r__N_UPDIS.bsn	Nitrogen uptake distribution parameter	-0.4 – 0.4
r__RCN.bsn	Concentration of nitrogen in rainfall (mg N L^{-1})	-0.4 – 0.4
r__SHALLST_N.gw	Concentration of nitrate in groundwater to streamflow (mg N L^{-1})	-0.4 – 0.4

5.3. Results and discussion

5.3.1. Impacts of climate change on temperature and precipitation

The BSB base hydrologic model was calibrated for 1973 to 1996, and validated for 1997- 2006. The calibrating parameters are as shown in Table 5.3. The simulated stream flow along with the uncertainty band and observation for two rivers in the BSB are presented in Figure 5.3 as an example.

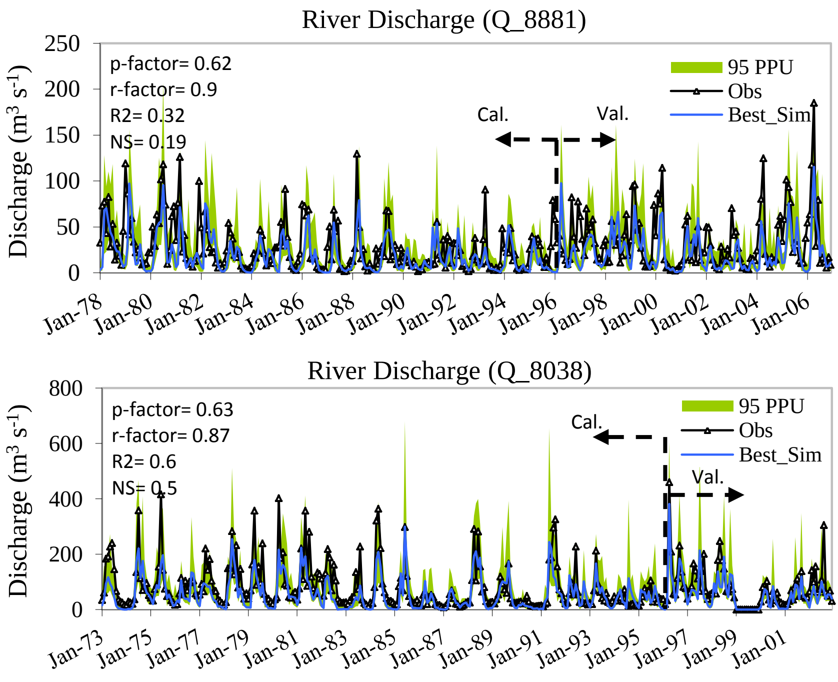

Figure 5.3. Simulated and observed discharges of two rivers in the Black Sea Basin in calibration and validation periods. The shaded region is 95% prediction uncertainty band. These are from the calibrated base model.

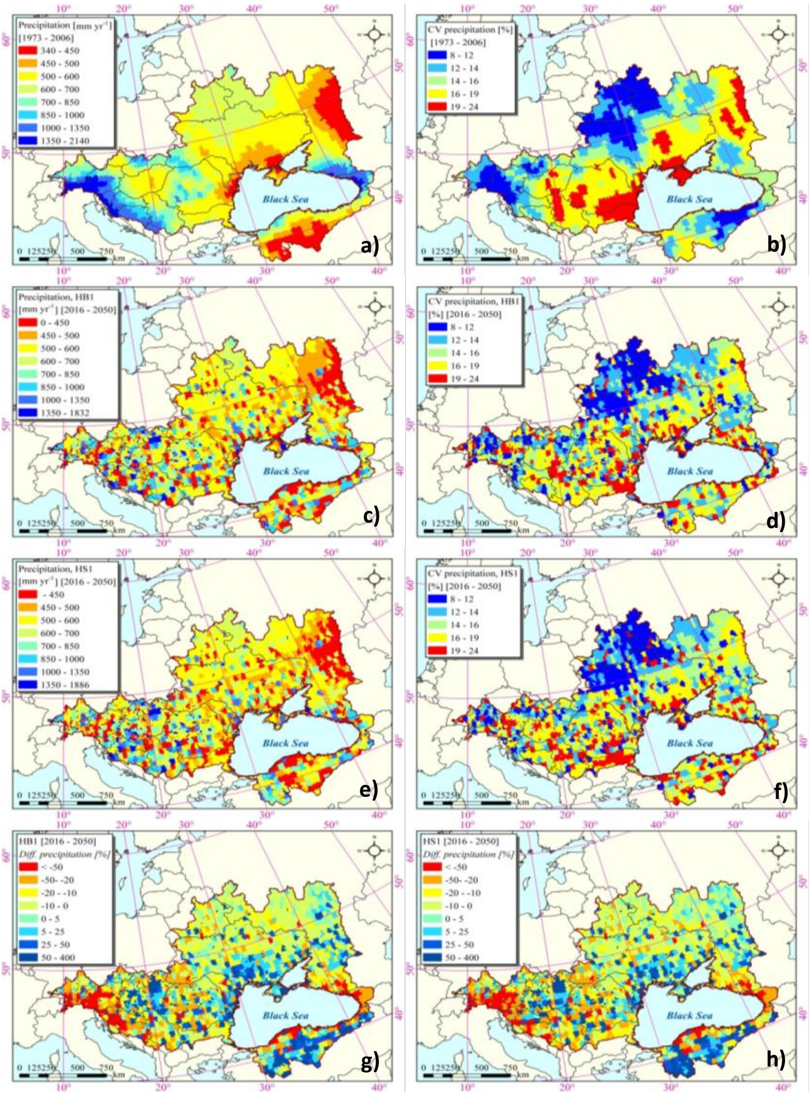

Figure 5.4. Precipitation distribution in Black Sea Basin: a) historic, b) coefficient of variation of historic precipitation (1973-2006), c) precipitation, HB1 scenario, d) coefficient of variation of precipitation, HB1 scenario (2013-2050), e) precipitation, HS1 scenario, f) coefficient of variation of precipitation, HS1 scenario (2013- 2050), g) percent deviation of HB1 precipitation scenario from historic, h) percent deviation of HS1 precipitation scenario from historic.

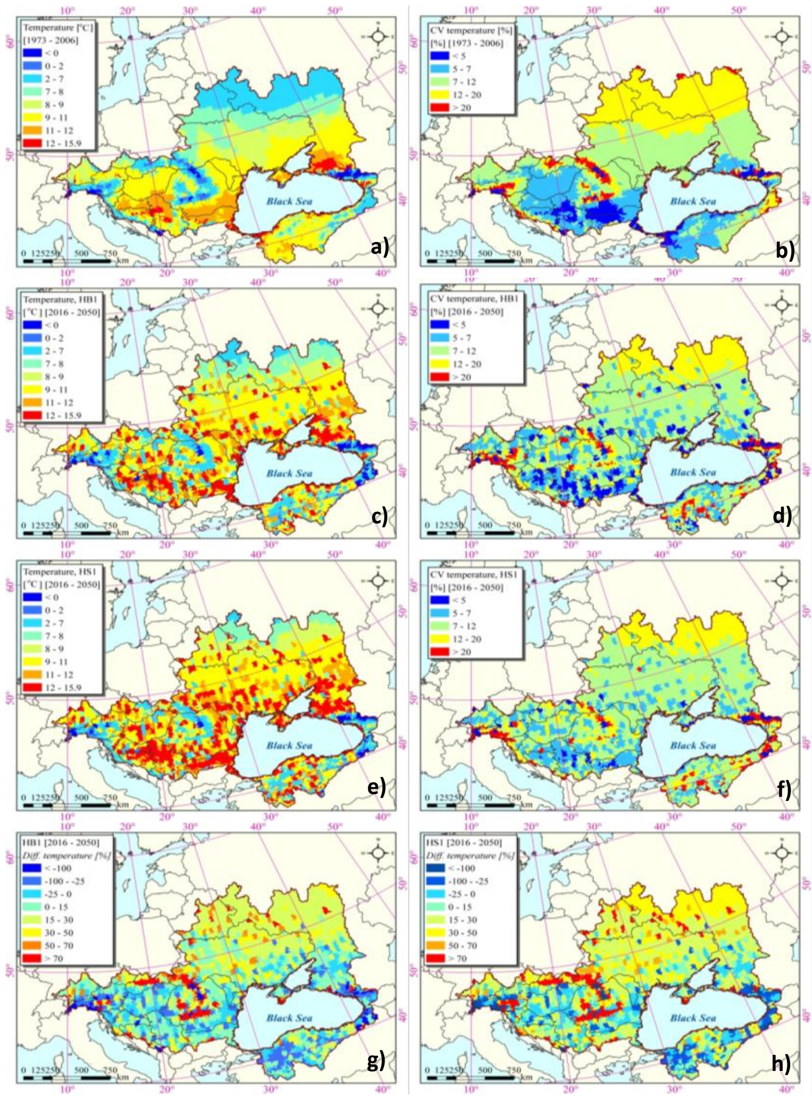

Figure 5.5. Temperature distribution in Black Sea Basin: a) historic, b) coefficient of variation of historic temperature (1973-2006), c) temperature, HB1 scenario, d) coefficient of variation of temperature, HB1 scenario (2013-2050), e) temperature, HS1 scenario, f) coefficient of variation of temperature, HS1 scenario (2013- 2050), g) percent deviation of HB1 temperature scenario from historic, h) percent deviation of HS1 temperature scenario from historic.

Figure 5.4 and 5.5 show the distributions of long term average precipitation and temperature at the subbasin level for the entire BSB, respectively. Shown in the figures are the historic and future climate scenarios along with their coefficient of variation over time (1973-2006 for historic and 2006-2050 for future) besides the percent deviation of the two future climate scenarios from historic.

The historical distribution of precipitation along with its coefficient of variation over time (1973-2006) marks distinct precipitation distribution patterns in BSB with significant temporal variation around the sea, and in Danube, Dnieper, and Don river basins (Figure 5.4a, b). Historically, the upper western part of the catchment in alpine region receives rain of about 1300 $mmyr^{-1}$ on average, which is much higher than in other parts of the catchment where Ukraine, Russia and Turkey lie. The regions with smaller historical range of precipitation tend to show higher variation in precipitation over time (Figure 5.4b).

The precipitation distributions of the two future climate scenarios are depicted in Figure 5.4 along with their coefficient of variations (Figure 5.4c,d,e,f). The two scenarios demonstrate similar patterns of long-term annual average distribution except that in HS1 scenario regions with small precipitation will expand. This is true for subbasins where average precipitation is less than 450 mm $year^{-1}$.

The HB1 scenario in general suggests higher annual averages for precipitations in subbasins with low initial rate of rainfall. The regions with mid-range precipitation (500-800 $mmyr^{-1}$) keep the same pattern in both scenarios. It should be noted that these observations are true for the long term averages of the two climate scenarios. Daily distributions may be quite different. In Figure 5.4g and 5.4h, the precipitation anomaly maps depict percent deviation from historic data for the two climate scenarios for the entire basin. The differences are calculated between the averages of 2016-2050 with those of the 1973-2006 periods. While the two scenarios show an increase in the precipitation in Turkish part, middle Danube and south Ukraine, the HS1 scenario, suggests more decrease in precipitation in the upper catchment subbasins. The increase in precipitation in south of the catchment in Turkey is also more pronounced in the HS1 scenario compared to HB1.

5.3.2. Impacts of land use and climate change on fresh water resources

The term "blue water" is widely used in the literature as the summation of the water yields and deep aquifer recharge. Falkenmark and Rockstorm [2006] introduced "green water flow" as the evapotranspiration and "green water resource" as the soil moisture. The latter refers to the renewable resources that can potentially generate economic growth as it is the source of rain-fed agriculture. Figure 5.6a shows the long-term average of blue water (mm yr^{-1}) based on the historic simulation (1973-2006). The coefficient of variation of blue water in BSB during these 34 years shows significant variation in central and east part of the catchment as well as in the Turkish part, where the historic annual average of blue water is (< 100 mm yr^{-1}). The projected effects of climate change on blue water is shown in Figure 5.6c as an anomaly map based on the deviation from historic blue water averaged over 10 scenarios. Generally, blue water increases by 75% in areas of scarce blue water, but this might not bring a significant increase in terms of blue water resources availability as the historical values are quite small. The variations between the 10 models show significant differences in blue water estimation in the Danube Basin and in the far-east and southern parts of the catchment in Turkey (Figure 5.6d). Historical and future variations of blue water indicate high reliability of blue water resources in Ukraine (Figure 5.6b) and Belarus (Figure 5.6d) while other parts are subject to large temporal changes.

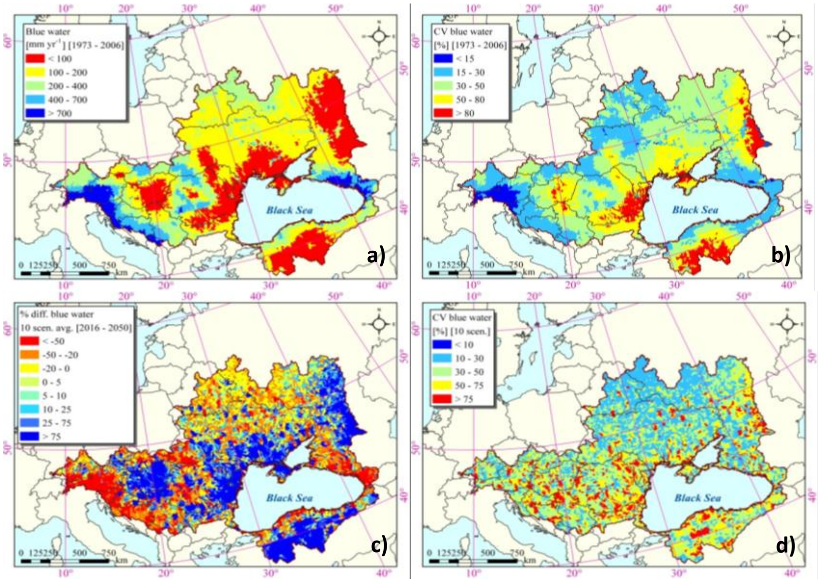

Figure 5.6. spatial distribution of blue water in black Sea Basin: a) historical (1973-2006), b) temporal variation of blue water (1973-2006), c) percent deviation of future blue water (20016-2050) from historic (1973-2006), d) average of predictions of 10 scenarios.

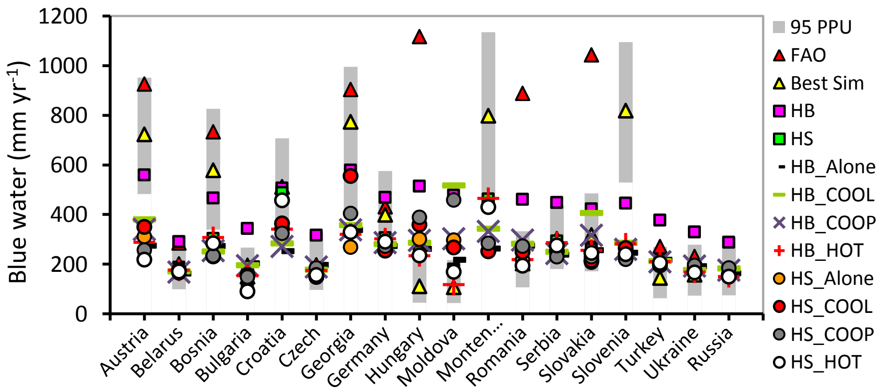

Figure 5.7. Comparison of predicted blue water (mm yr^{-1}) by 10 scenarios for the period of 2016-2050 with that of historical 95PPU and the best estimate for the period of 1973-2006 in Black Sea Basin countries.

The estimated blue water resources by the 10 different land use-climate scenarios were aggregated at the country level along with best simulation and 95% prediction uncertainty (95PPU) of the historical data (Figure 5.7). For most countries, the average future prediction of blue water is larger than the lower band of the historic prediction uncertainty. The future blue water resources are smaller than the historic best estimates in all countries of BSB except for Hungary and Turkey as predicted by all scenarios. In these two countries, all scenarios show increases in blue water compared to the best historical estimate. In addition, scenarios with HB1 tend to systematically predict higher blue water as compared to HS1 scenarios.

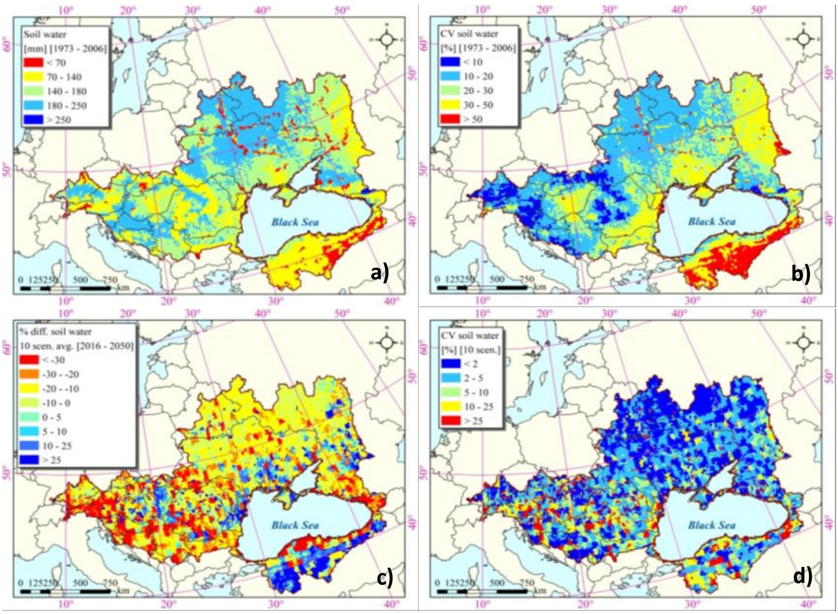

Figure 5.8. Spatial distribution of green water storage (soil water) in Black Sea Basin: a) historical (1973-2006), b) temporal variation of green water storage (1973-2006), c) percent deviation of future green water storage (20016-2050) from historic (1973-2006), d) average of predictions of 10 scenarios.

The spatial variation of long-term average annual green water storage (soil moisture) (Figure 5.8a) shows that most of the Basin lies in the range of 70-250 mm of soil moisture. However the variation over time shows a distinct east-west pattern suggesting different levels of reliability for soil water in the region. The southern parts of the catchment in Turkey tend to have smaller soil water with more variation over time (Figure 5.8 b), which makes the region less reliable in terms of green water resources.

The anomaly map of soil water (Figure 5.8c) is the average of 10 scenarios estimation deviation from historic. It shows up to 30% reduction in soil water in the Danube Basin and northern BSB upstream of Dnieper and Don, in Ukraine and Russia as suggested by the average of the 10 scenarios. There are some signs of soil water increase in the middle Danube, south Ukraine and the Turkish part of the BSB. The coefficient of variation of the 10 scenarios indicates that there is a good agreement between the scenarios with less than 2 percent variation in the prediction of soil water (Figure 5.8d).

The 10 scenarios didn't show a significant change in the estimation of evapotranspiration across the BSB (Figure 5.9d). This is true for all regions except for middle Danube and Turkey, where scenarios show 10-25 percent variation among their predictions. The average deviation from historic values, suggests that evapotranspiration decreased by 30 percent in historically water abundant areas in the far west of the catchment and in coastal regions in Turkey, while other areas are predicted to have higher evapotransoiration based on the scenarios averages. The variation between predictions in models using four different land use scenarios shows limited impacts of land use changes on predicted evapotranspiration and soil water between scenarios for a given climate scenario (Figure 5.10). The variations between scenarios are more pronounced in blue water predictions (Figure 5.10 e, f).

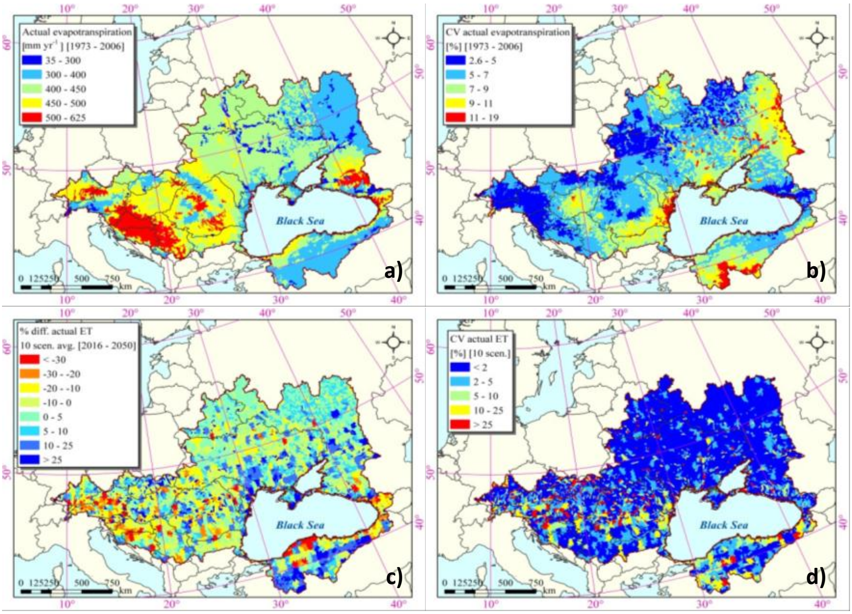

Figure 5.9. spatial distribution of green water flow (evapotranspiration) in Black Sea Basin: a) historical (1973-2006), b) temporal variation of green water flow (1973-2006), c) percent deviation of future green water flow (20016-2050) from historic (1973-2006), d) average of predictions of 10 scenarios.

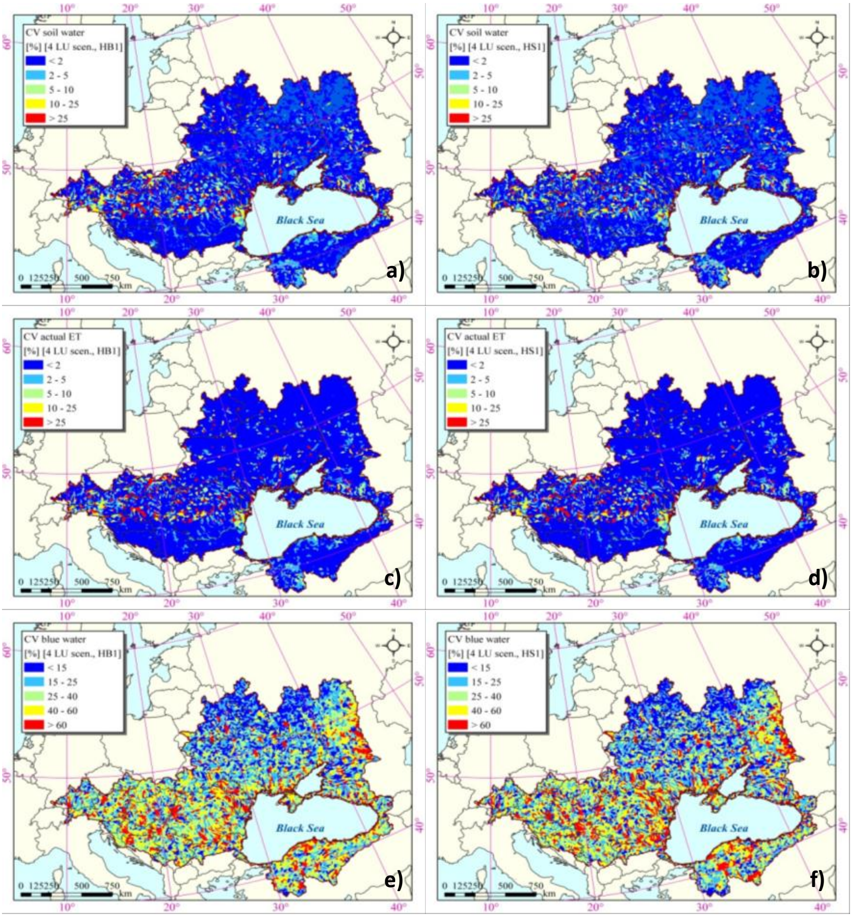

Figure 5.10. Coefficient of variation between model predictions using four land use scenarios (BS ALONE, BS COOL, BS COOP, and BS HOT): a) CV soil water using HB1 as climate scenario, b) CV soil water using HS1 as climate scenario, c) CV actual ET using HB1 as climate scenario, d) CV actual ET using HS1 as climate scenario, e) CV blue water using HB1 as climate scenario, d) CV blue water using HS1 as climate scenario.

5.3.3. Impacts of climate change on extreme events

In the next step we compared the frequency of wet days occurrence with precipitation thresholds >2 and >10 mm d^{-1} in five selected subbasins in different climatic regions across the BSB (Figure 5.11). In a subbasin in the Eastern part of the BSB in Russia, the two climate scenarios predicted almost the same pattern as the historical climate. This is a region with low annual rainfall (350-450 mm yr^{-1}). There are few rainfall events exceeding 10 mm d^{-1} throughout the year. In a subbasin in the Southern Ukraine, however, the frequency of wet days are largest for both thresholds (Figure 5.11 c,d). This subbasin lies in an area with 450-500 mm yr^{-1} average annual precipitation. The next subbasin highlights an interesting discrepancy between the two climate scenarios in the Alpine region in the middle of the Danube Basin. Precipitation in this region ranges between 1000-1350 mm yr^{-1} (Figure 5.11e,f). Here, HS1 predicts large increases in the number of wet days with a threshold of >2 mm d^{-1}, while HB1 predicts smaller wet-day frequencies than historic. The same pattern is true for the wet-day threshold of >10 mm, although with less pronounced increases. The increases in the frequencies of rainfalls >10 mm d^{-1} may indicate larger flooding frequencies.

The next subbasin was chosen in Austria with rainfall rate of 1000-1350 mm $year^{-1}$. In this subbasin the frequencies of wet-days decreases as compared with the historical data. The decreases at the threshold of <2 mm d^{-1} may indicate more prolonged drought days, while decreases at the <10 mm d^{-1} rainfall events indicate smaller groundwater recharge, hence a largest chance of groundwater depletion and associated problems such as land subsidence.

Finally, in the subbasin in Turkey, the climate models behave differently from the Alpine region, as HB1 predicts larger frequencies of rainfall events than HS1, while HS1 stays in the range of historic distribution throughout the year, except for July to September where HS1 predicts distinctly higher than historic.

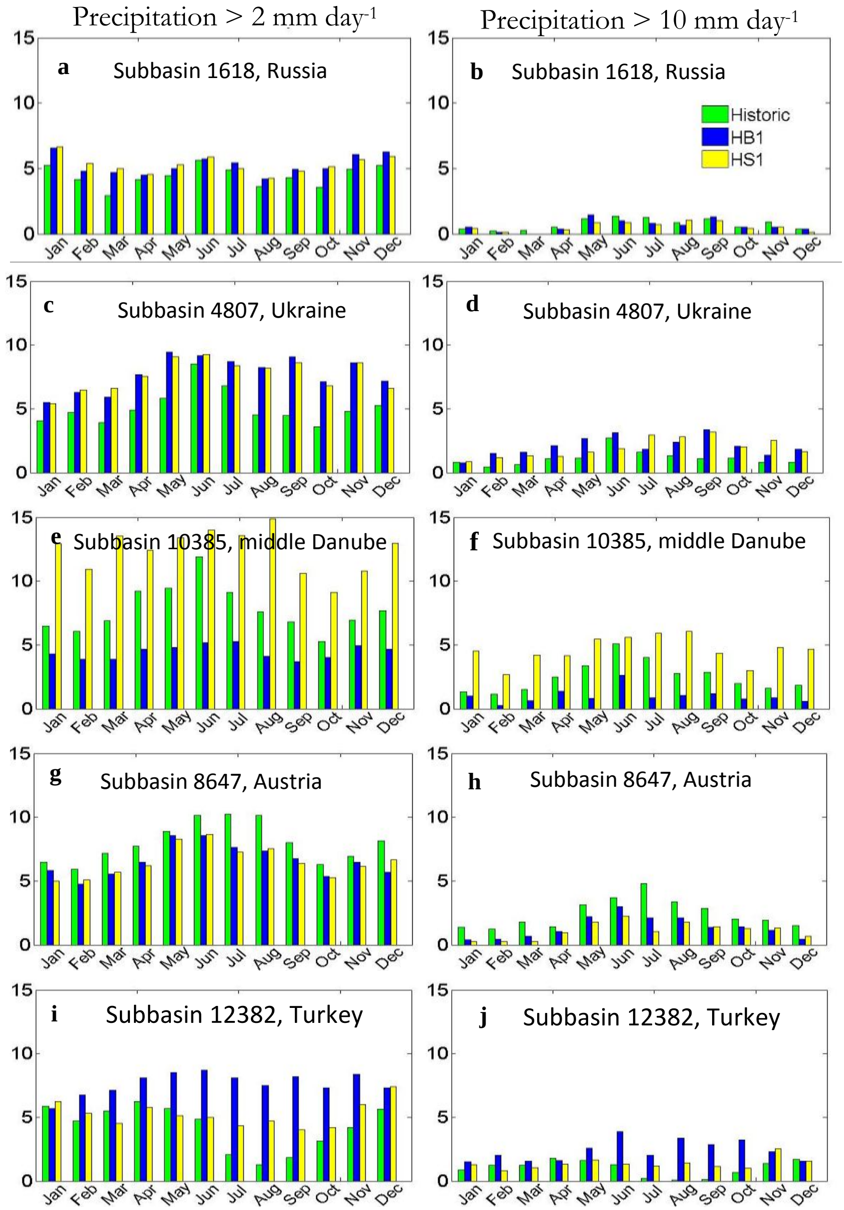

Figure 5.11. Comparison of the number of wet days(>2 mm d^{-1} left column and >10 mm d^{-1} right column) between the historical (1980-2006) and future scenarios (HB1 and HS1, 2016-2030) for five selected subbasins.

5.4. Summary and conclusions

Combinations of two regional climate scenarios and four regional land use scenarios were defined to study possible future impacts of climate and land use changes in the BSB. The land use scenarios were based on the IPCC’s special report on emissions scenarios (SRES) corresponding to four marker scenarios represent different global socio-economic development pathways. Climate scenarios were generated from the Danish Regional Climate Model (RCM) (HIRHAM) for IPCC's SRES A2 and B2 scenarios. On average the scenarios suggested increases in long-term average annual future precipitation by 50-400% in the middle and downstream of Danube, downstream of Dniester and Dnieper, and the Turkish part of the catchment. As these regions are low precipitation areas, these increases are not considered as being significant. According to the two climate scenarios, the western part of the catchment, which is a wet region, will experience a decline in precipitation by 50%. As the initial values are large, this expected to have large impacts on the water resources of the entire catchment and leaves the catchment experiencing a net decrease of precipitation. Temperature tends to increase in the northern part of the catchment by 15-25% and decrease in the west and southern part. However the extent of changes is more severe in HS1 scenario as compared to HB1.

We also quantified the impacts of combined climate and land use changes on freshwater distribution in Black Sea Basin. As suggested by all scenarios, on average, the regions with larger historical fresh water resources (blue water, green water flow, and green water storage) are expected to experience up to 50% decrease in their water resources while areas with lower historic water resources will gain up to 75% of their historical record in water resources but this might not bring a significant increase in terms of blue water resources availability as the historical values are quite small. For the whole basin the gain is less than loss. In addition, historical and future variations of blue water indicate high reliability of blue water resources in Ukraine and Belarus while other parts are subject to large temporal changes. In terms of green water resources, the average deviation of scenario prediction from historic, suggests decrease in evapotranspiration by 30 percent in historically water abundant areas while other regions are subjected to have higher evapotranspiration.

The effect of climate change is more pronounced on water resources, especially blue water while the impact of land use change was less significant. To see the detailed effect of land use change on water resources component, it is beneficial to look at the water cycle at HRU level where land uses are identical. This will give a true measure of land use change impacts on water resources. The strength of the current work is the application of combined land use and climate change scenarios. However the study neglects the future changes in soil parameters over time, which accompanies changing land uses. Accounting for these changes will increase the confidence on projected results and needs to be further investigated.

An additional concern is the use of two regional climate models (RCM, HS1 and HB1) in model prediction while pursuing a thorough investigation based on combined effect of other Global Climate Models (GCMs) or Regional Climate Models (RCMs) might result in different outcomes and hence is recommended.

Acknowledgment

This project has been funded by the European Commission's Seventh Research Framework through the enviroGRIDS project (Grant Agreement n 226740). The authors are especially grateful to Envirogrid partners for contributing climate and land use scenarios of changes in this study. Special thanks Anna Silvia from University of Geneva for fruitful discussions and to Prof. Dr. Rainer Schulin from ETH Zurich University for the valuable comments and discussions for this work.

References

Abbaspour KC, Yang J, Maximov I, Siber R, Bogner K, Mieleitner J, Zobrist J, Srinivasan R., 2007. Modelling hydrology and water quality in the pre-Alpine/Alpine Thur watershed using SWAT. Journal of Hydrology 333: 413–430.

Abbaspour KC, 2010. User Manual for SWAT-CUP, SWAT Calibration and Uncertainty Analysis Programs. Swiss Federal Institute of Aquatic Science and Technology, Eawag, Duebendorf, Switzerland. 93 pp.

Abbaspour, K.C., Johnson, C.A., van Genuchten, M.T., 2004. Estimating uncertain flow and transport parameters using a sequential uncertainty fitting procedure. Vadose Zone J. 3, 1340–1352.

Alcamo, J., Leemans, R. and Kreileman, E., 1998. Global Change Scenarios of the 21st century: Results from the IMAGE 2.1 model. London: Pergamon & Elseviers Science.

Ashagrie, A. G., de Laat, P. J., de Wit, M. J., Tu, M., and Uhlenbrook, 2006. S.: Detecting the influence of land use changes on discharges and floods in the Meuse River Basin – the predictive power of a ninety-year rainfall-runoff relation?, Hydrol. Earth Syst. Sci., 10, 691–701, doi:10.5194/hess-10-691-2006

Barbosa, Ana; Mancosu, Emanuele; Gago da Silva, Ana; Bono, Andrea; Lehmann, Anthony; Mierla, Marian; Hanganu, Jenica); Littkopf, Andreas, 2012. Proposed land use scenario analysis, model input parameters and allocation rules, enviroGirid sfinal Report D3.7

Bergström, S. and Forsman, A.: Development of a conceptual deterministic rainfall-runoff model, 1973. Nord. Hydrol., 4, 147–170.

Bollen, J.C., Manders, A.J.G. and Mulder, M., 2004. Four Futures for Energy Markets and Climate Change. The Hague: CPB Netherlands Bureau for Economic Policy Analysis, National Institute for Public Health and the Environment RIVM.

Bosshard T., Kotlarski, S., Ewen,T. and Schar, C., 2011. Spectral representation of the annual cycle in the climate change signal. Hydrology and Earth System Sciences

BSEI, Black Sea Investment Facility. 2005. 'Review of the Black Sea Environmental Protection Activities. General review', Black Sea Investment Facility.

Christensen, J. H. and Christensen, O. B., 2007. A summary of the PRUDENCE model projections of changes in European climate by the end of this century. Climatic Change, vol. 81, p. 7-30

Christensen, J.H., Carter, T.R., Giorgi, F., 2002. PRUDENCE employs new methods to assess European climate change. EOS 83, 147.

Christensen, J.H., Christensen, O.B., 2003, Climate modeling: severe summertime flooding in Europe. Nature 421, 805–806.

Climatic Research Unit (CRU), 2008. CRU Time Series (TS) high resolution gridded datasets, University of East Anglia Climatic Research Unit (CRU), NCAS British Atmospheric Data Centre, Available from: http://badc.nerc.ac.uk/view/badc.nerc.ac.uk__ATOM__dataent_1256223773328276.

Cosgrove, W.J. and Rijsberman, F.R., 2000. World Water Vision: Making Water Everybody's Business*.* London: Earthscan Publications.

Deque, M., et al., 2005. Global high resolution vs. regional climate model climate change scenarios over Europe: quantifying confidence level from PRUDENCE results. Clim. Dyn. 25, 653–670.

Eckhardt K, L. Breuer, and H. G. Frede, 2003. Parameter uncertainty and the significance of simulated land use change effects. J Hydrol 273:164–176. doi:10.1016/S0022-1694(02)00395-5

EEA Catchments and Rivers Network System (ECRINS) v1.1, 2012. Rationales, building and improving for widening uses to Water Accounts and WISE applications, Luxembourg: Publications Office of the European Union, ISBN *978-92-9213-320-7*, ISSN *1725-2237*, doi:10.2800/51667.

European Environment Agency, 2005. The European Environment, State and Outlook 2005. Luxembourg: Office for Official Publications of the European Communities.

Falkenmark, M., J. Rockström, 2006. The new blue and green water paradigm: Breaking new ground for water resources planning and management. J. Water Resour. Plann. Manage.: ASCE 132 (3), 129–132.

Fohrer, N., Haverkamp, S., Eckhardt, K., and Frede, H.-G., 2001, Hydrologic response to land use changes on the catchment scale, Phys. Chem. Earth Pt. B, 26, 577–582.

Food and Agricultural Organization (FAO) (2003), The digital soil map of the world and derived soil properties, CD-ROM, Version 3.5, Rome, Italy.

Fowler, H. J., Blenkinsop, S. and Tebaldi, C., 2007. Linking climate change modelling to impacts studies: recent advances in downscaling techniques for hydrological modelling. International Journal of Climatology

Gassman, P. W., Reyes, M., Green, C. H., and Arnold, J. G., 2007, The Soil and Water Assessment Tool: Historical development, applications, and future directions, T. ASABE, 50, 1211–1250.

Ghaffari, G., Keesstra, S., Ghodousi, J., and Ahmadi, H., 2010 SWATsimulated hydrological impact of land-use change in the Zanjanrood basin, Northwest Iran, Hydrol. Process., 24, 892–903.

Giorgi, F., 2006. Climate change Hot-spots. Geophys. Res. Lett. 33, L08707.

Giorgi, F. and P. Lionello, 2008. Climate change projections for the Mediterranean region, Global and Planetary Change, 63 (2008) 90–104.

Giorgi, F., Bi, X., 2005a. Regional changes in surface climate interannual variability for the 21st century from ensembles of global model simulations. Geophys. Res. Lett. 32, L13701.

Giorgi, F., Bi, X., 2005b. Updated regional precipitation and temperature changes for the 21st century from ensembles of recent AOGCM simulations. Geophys. Res. Lett. 32, L21715.

Global Runoff Data Centre (GRDC), 2011. Long-Term Mean Monthly Discharges and Annual Characteristics of GRDC Station / Global

Runoff Data Centre. Koblenz, Germany: Federal Institute of Hydrology (BfG), http://grdc.bafg.de.
Guo H., Q. Hu, T. Jiang, 2008. Annual and seasonal streamflow responses to climate and land-cover changes in the Poyang Lake basin, China, J. Hyrol 355:106–122. doi:10.1016/j.jhydrol.2008.03.020.
He H., J. Zhou, W. Zhang, 2008. Modelling the impacts of environmental changes on hydrological regimes in the Hei River Watershed, China. Global Planet Change 61:175–193. doi: 10.1016/j.gloplacha.2007.08.012
http://www.eawag.ch/organisation/abteilungen/siam/software/swat/index_EN
Huisman J.A., L. Breuer, and H. G. Frede, 2004. Sensitivity of simulated hydrological fluxes towards changes in soil properties in response to land use change. Phys Chem Earth 29:749–758. doi:10.1016/j.pce.2004.05.012
Im, S., Kim, H., Kim, C., and Jang, C., 2009, Assessing the impacts of land use changes on watershed hydrology using MIKE SHE, Environ. Geol., 57, 231–239.
IMAGE team, 2001. The IMAGE 2.2 implementation of the SRES scenarios: a comprehensive analysis of emissions, climate change and impacts in the 21st century. RIVM CD-ROM Publication 481508018, Bilthoven: National Institute of Public Health and the Environment RIVM. Available at: http://www.rivm.nl/image
IPCC, 2007: Climate Change 2007: Mitigation. Contribution of Working Group III to the Fourth Assessment Report of the Intergovernmental Panel on Climate Change [B. Metz, O.R. Davidson, P.R. Bosch, R. Dave, L.A. Meyer (eds)], Cambridge University Press, Cambridge, United Kingdom and New York, NY, USA., XXX pp.
IPCC, 2012: Managing the Risks of Extreme Events and Disasters to Advance Climate Change Adaptation. A Special Report of Working Groups I and II of the Intergovernmental Panel on Climate Change [Field, C.B., V. Barros, T.F. Stocker, D. Qin, D.J. Dokken, K.L. Ebi, M.D. Mastrandrea, K.J. Mach, G.-K. Plattner, S.K. Allen, M. Tignor, and P.M. Midgley (eds.)]. Cambridge University Press, Cambridge, UK, and New York, NY, USA, 582 pp.
Jarvis, A., H. I. Reuter, A. Nelson, and E. Guevara, 2008. Hole-filled SRTM for the globe Version 4, Data access: The CGIAR-CSI SRTM 90m Database: http://srtm.csi.cgiar.org.
Jones, R.G., Murphy, J.M., Noguer, M., Keen, A.B., 1997. Simulation of climate change over Europe using a nested regional climate model. II: comparison of driving and regional model responses to a doubling of carbon dioxide. Q. J. R. Meteorol. Soc. 123, 265–292.

Kemp-Benedict, E., Heaps, C. and Raskin, P., 2002. Global Scenario Group Futures. Technical notes. Stockholm Environment Institute.

Kittel, T.G.F., Giorgi, F., Meehl, G.A., 1998. Intercomparison of regional biases and doubled CO2 sensitivities of coupled atmosphere–ocean general circulation model experiments. Clim. Dyn. 14, 1–15.

Klijn, J.A., Vullings, L.A.E., van den Berg, M., van Meijl, H., van Lammeren, R., van Rheenen, T., Veldkamp, A., Verburg, P.H., Westhoek, H. and Eickhout, B., 2005. The EURURALIS study: Technical document. Wageningen: Alterra. Available at: http://www.EURURALIS.nl /background.htm

Lenderink, G., Buishand, A. and van Deursen, W., 2007. Estimates of future discharges of the river Rhine using two scenario methodologies: direct versus delta approach. Hydrology and Earth System Sciences

Lenhart T, N. Fohrer, and H. G. Frede, 2003. Effects of land use changes on the nutrient balance in mesoscale catchments. Phys Chem Earth 28:1301–1309. doi:10.1016/j.pce.2003.09.006.

Lin Y. P., N. M. Hong, P. J. Wu, C. F. Wu, and P. H. Verburg, 2007. Impacts of land use change scenarios on hydrology and land use patterns in the Wu-Tu watershed in Northern Taiwan. Landsc Urban Plan 80:111–126.doi:10.1016/j.landurbplan.2006.06.007

Lionello, P., P. Malanotte-Rizzoli, and R. Boscolo, 2006. The Mediterranean climate: an overview of the main characteristics and issues, Mediterranean Climate Variability, Elsevier, Amsterdam, pp. 1–26.

Liu J, Folberth C, Yang H, Röckström J, Abbaspour K, Zehnder AJ., 2013. A global and spatially explicit assessment of climate change impacts on crop production and consumptive water use. PLoS One. 2013;8(2): e57750. doi: 10.1371/journal.pone.0057750.

Luterbacher, J., et al., 2006. Mediterranean climate variability over the last centuries. A review. In: Lionello, P., Malanotte-Rizzoli, P., Boscolo, R. (Eds.), Mediterranean Climate Variability. Elsevier, Amsterdam, pp. 27–148.

Machenhauer, B., et al., 1998. Validation and Analysis of Regional Present-day Climate and Climate Change Simulations over Europe. . MPI Report No, 275. MPI, Hamburg, Germany.

Mishra Ak, Singh VP, 2011. Drought modeling- A review. Journal of hydrology 357 (3-4)349-367.

Mitchell, T. D. and P. D. Jones. 2005. An improved method of constructing a database of monthly climate observations and associated high-resolution grids, Int. J. Climatology, 25, 693-712, doi: 10.1002/joc.1181.

Monfreda, C., N. Ramankutty, and J. A. Foley, 2008. Farming the planet: 2. Geographic distribution of crop areas, yields, physiological types, and

net primary production in the year 2000, J. Global Biogeochemical Cycles, 22, GB1022, doi:10.1029/2007GB002947.
Nakicenovic, N., Alcamo, J., Davis, G., de Vries, B., Fenhann, J., Gaffin, S., Gregory, K., Grübler, A., Jung, T.Y., Kram, T., La Rovere, E., Michaelis, L., Mori, S., Morita, T., Pepper, W., Pitcher, H., Price, L., Riahi, K., Roehrl, A., Rogner, H.H., Sankovski, A., Schlesinger, M., Shukla, P., Smith, S., Swart, R., van Rooyen, S., Victor, N. and Dadi, Z., 2000. Special Report on emissions scenarios. Cambridge: Cambridge University Press.
NASA, 2001. Land Processes Distributed Active Archive Center (LP DAAC), ASTER L1B, USGS/Earth Resources Observation and Science (EROS) Center, Sioux Falls, South Dakota, Data access: http://lpdaac.usgs.gov.
Ndomba, P., Mtalo, F., and Killingtveit, A. 2008. SWAT model application in a data scarce tropical complex catchment in Tanzania, Phys. Chem. Earth, 33, 626–632.
Neitsch S. L., J. G. Arnold , J. R. Kiniry, J. R. Williams, 2009. Soil and water assessment tool theoretical documentation version 2009, Texas Water Resources Institute Technical Report No. 406. Texas A&M University System, College Station.
Neitsch, S., J. G. Arnold, J. R. Kiniry, J. Williams, 2011. Soil & Water Assessment Tool Theoretical Documentation Version 2009, Texas Water Resources Institute Technical Report No. 406, College Station, Texas, p. 618.
Niehoff, D., Fritsch, U., and Bronstert, A., 2002. Land-use impacts on storm-runoff generation: scenarios of land-use change and simulation of hydrological response in a meso-scale catchment in SW-Germany, J. Hydrol., 267, 80–93.
Ouyang W, Skidmore AK, Hao F, Wang T., 2010. Soil erosion dynamics response to landscape pattern. Sci Total Environ 408:1358–1366. doi:10.1016/j.scitotenv.2009.10.062.
Parker, D.C., Manson, S.M., Janssen, M.A., Hoffmann, M.J., Deadman, P., 2003. Multi-agent systems for the simulation of land use and land use change: a review. Ann. Assoc. Am. Geogr. 93, 314–337.
Portmann, F. T., S. Siebert, and P. Döll, 2010. MIRCA2000 Global monthly irrigated and rainfed crop areas around the year 2000: A new high resolution data set for agricultural and hydrological modeling, J. GLOBAL BIOGEOCHEMICAL CYCLES, 24, GB1011, doi:10.1029/2008GB003435.
Quilbé,R., Rousseau, A., N., Moquet,J., Trinh,N. B., Dibike, Y., Gachon, P. and Chaumont, D., 2008. Assessing the effect of climate change on river flow using general circulation models and hydrological modeling

application to the Chaudière River, Quebec, Canada. Canadian Water Resources Journal, vol. 33, p. 73-93

Raisanen, J., et al., 2004. European climate in the late twenty-first century: regional simulations with two driving global models and two forcing scenarios. Clim. Dyn. 22, 13–31.

Refsgaard, J. C. and Storm, B.: MIKE SHE, in: Computer Models of Watershed Hydrology, edited by: Singh, V. P., Water Resources Publications, Highlands Ranch, Colorado, 809–846, 1995.

Rickebusch, S., Metzger, M.J., Xu, G., Vogiatzakis, I.N., Potts, S.G., Stirpe, M.T. and Rounsevell, M., 2011. A qualitative method for the spatial and thematic downscaling of land-use change scenarios. *Environmental Science and Policy*, 14: 268–278.

Rotach, M.W., et al., 1997. Nested regional simulation of climate change over the Alps for the scenario of doubled greenhouse gas forcing. Theor. Appl. Climatol. 57, 209–227.

Rouholahnejad, E., K. C. Abbaspour, V. Bacu, and A.Lehmann (2013), A high resolution spatiotemporal distribution of water resources quantity and quality in the Black Sea Basin, Water Resources Research.

Rounsevell,M.D.A., Ewert, F., Reginster, I., Leemans, R., Carter, T.R., 2005. Future scenarios of European agricultural land use. II. Projecting changes in cropland and grassland. Agric. Ecosyst. Environ. 107, 117–135.

Schar, C., et al., 2004. The role of increasing temperature variability in European summer heatwaves. Nature 427, 332–336.

Schulla, J.: Hydrologische Modellierung von Flussgebieten zur Abschätzung der Folgen von Klimaänderungen, Zürcher Geographische Schriften, 1997. 69, Geographisches Institut ETH, Zürich.

Semmler, T., Jacob, D., 2004. Modeling extreme precipitation events — a climate change simulation for Europe. Glob. Planet. Change 44, 119–127.

Serrat-Capdevila, A., J. B. Valdes, J. G. Perez, K. Baird, L. J. Mata, and T. Madock III, 2007. Modeling climate change impacts—and uncertainty— on the hydrology of a riparian system: The San Pedro Basin (Arizona/ Sonora), J. Hydrol., 347(1 – 2), 48 – 66, doi:10.1016/j.jhydrol.2007. 08.028.

Stehr, A., Debels, P., Romero, F., and Alcayaga, H., 2008. Hydrological modelling with SWAT under conditions of limited data availability: evaluation of results from a Chilean case study, Hydrolog. Sci. J., 53, 588–601.

Strengers, B., Leemans, R., Eickhout, B., de Vries, B. and Bouwman, L., 2004. The land-use projections and resulting emissions in the IPCC SRES scenarios as simulated by the IMAGE 2.2 model. GeoJournal, 61(4),

381–393. Available at: http://www.springerlink.com/content/p7j26720j7892r11
Tockner, K., U. Uehlinger., and C. T. Robinson., 2009. Rivers of Europe., ISBN: 978-0-12-369449-2.
Ulbrich, U., et al., 2006. The Mediterranean climate change under global warming. In: Lionello, P., Malanotte-Rizzoli, P., Boscolo, R. (Eds.), Mediterranean Climate Variability. Elsevier, Amsterdam, pp. 398–415.
UNISDR, 2009. Global Assessment Report on Disaster Risk Reduction: Risk and Poverty in a Changing Climate – Invest Today for a Safer Tomorrow. United Nations International Strategy for Disaster Reduction, Geneva, Switzerland, 207 pp.
UNISDR, 2011. Global Assessment Report on Disaster Risk Reduction. Revealing Risk, Redefining Development. United Nations International Strategy for Disaster Reduction, Geneva, Switzerland.
Veldkamp, A., Lambin, E.F., 2001. Predicting land use change. Agric. Ecosyst. Environ. 85, 1–6.
Veldkamp, A., Verburg, P.H., 2004. Modelling land use change and environmental impact. J. Environ. Manage. 72, 1–3
Vörösmarty Cj, Green Pj, Salisbury J, Lammers RB, 2000, Global Water Resources: vulnerability from climate change population growth, Science 289: 284-288.
Wang J, Wang E, Liu DL, 2011, modeling the impacts of climate change on wheat yields and field water balance over the Murray-Darling Basin in Australia. Threshold and applied climatology 104: 285-300
Wang S., S. Kang , L. Zhang, F. Li, 2008, Modelling hydrological response to different land-use and climate change scenarios in the Zamu River basin of northwest China, Hydrol Process 22:2502–2510. doi:10.1002/hyp.6846.

6. General conclusions, study limitations, and outlook

6.1. General conclusion

The general goal of this study was to assess the impacts of land use and climate change on water resources of Black Sea Basin (BSB) at high spatial and temporal resolution and more generally, to investigate the possibility of building a high-resolution large-scale model and then calibrating it. As we become more aware of the intricate nature of the problems facing our environment, and interconnectedness of processes and issues such as: upstream-downstream problems, water transfers across borders, shares of countries in producing pollutants, water rights and transfers, etc, we are taking a more and more holistic look at the problems. To address these issues, there is a need for having a clearer picture of the whole watershed as well as its parts.

To lay the basis for this major goal, a systematic analysis of water availability was necessary. The semi-distributed, physically- and process-based hydrologic model SWAT in combination with the sequential uncertainty fitting program SUFI-2 were used to build a hydrologic model of the BSB. A careful calibration, validation, as well as sensitivity and uncertainty analysis were performed to improve the reliability of the model results. A parallel processing scheme was developed to improve calibration computation time. SUFI-2 was used to calibrate the model with a large number of parameters and measured data from many gauging stations. The calibration was based on river discharge, crop growth, and river nitrate load at multiple sites. As there are often no data on soil moisture, evapotranspiration, or aquifer recharge, we used crop yield as a surrogate to add confidence on the distribution of the components of the infiltrated water. The calibration and validation results were quite satisfactory for a large number of outlets for both discharge and nitrate loads. As a consequence, our confidence on the estimated water resources is high. However, as nitrate data was only available for the Danube Basin, nitrate load estimation at other areas should be considered as less reliable. Model results were presented as 95% prediction uncertainty band (95PPU) showing that inherent uncertainties need to be considered, before general conclusions are drawn.

Using the calibrated model results, we were able to quantify various components of water balance including blue water flow (water yield plus deep aquifer recharge), green water flow (evapotranspiration), and green water storage (soil moisture) and their respective uncertainty bounds at subbasin level and monthly time steps. This information is very useful for developing an overview of the actual water resources status and helps to spot regions where an in-depth analysis may be necessary.

We identified water scarce regions, and showed how the model could provide information on transboundary water issues such as natural flows and pollution loads. Regions in Ukraine and Romania bordering the Black Sea and parts of Turkey and Russia in the Basin experience the highest water deficit. Model outputs could be used to establish environmental goals, planning of remedial measures and development of monitoring strategies. Much more results and analysis could be obtained with the model developed in this study, such as calculation of freshwater and nutrient fluxes in to the Sea.

Based on the widely used water scarcity indicators, our analysis showed that severe water scarcity exists in about 30% of the Basin area. Given that the major land cover of the Basin is agriculture with 65% coverage, the vulnerable situation of water resources availability has serious implication for the Basin's available water resources reliability and food security. This may even be further intensified under the expected future climate change and land use change impacts. The future climate change and land use change analysis in Black Sea Basin indicated up to 50% reduction in fresh water availability in regions with larger water resources. This may lead to added pressures on the water resources of the BSB and needs to be addressed well in advance.

A comprehensive database of the BSB was created within the framework of the current study and the Meta database became available in the Global Earth Observation (GEO) platform to contribute to fill the existing gaps in water resources data in the Black Sea Basin.

6.2. Study limitations

Like many other large scale modeling works, this study is subject to certain limitations in the context of data quality and quantity. The available data generally allowed obtaining satisfactory results; however inclusion of more discharge and water quality data (nitrate, phosphate, sediment, etc.) and higher resolution crop yield data for model calibration could provide more confidence in the model result.

Our results show that parallel SUFI-2 is able to achieve reasonable speedup on real-world computation-intensive calibration applications, while significantly exceeding the performance of non-parallelized packages. However larger time savings can be achieved with multiple CPUs and larger RAM memory. Furthermore, computations based on GPU technology hold the promise of achieving greater speed ups in execution of hydrologic models [Kalyanapu, et al., 2011; Singh, et al., 2011].

The current study lacks the inclusion of dams and reservoirs although their inclusion could have a significant effect on model results. Including other water management practices (e.g. water transfer infrastructure, irrigation systems, etc.) would undoubtedly have increased confidence on model results.

Lacking detailed observational data on management practices such as irrigation, fertilizer application, planting and harvesting dates led to simplified assumptions on these factors. This could yet be further improved.

Due to the large scale of the study area, incorporation of global data was inevitable. Thus, there were some mismatches between the data collected from different sources. In some cases, it was the first use of the globally available data. The conflicts were taken care of to the extent possible but incorporated data are not error free.

The study on climate and land use change neglects the future changes in soil parameters over time, which accompanies changing land uses. Accounting for these changes will increase the confidence on the projected results and needs to be further investigated.

An additional concern is the use of two regional climate models (RCM, HS1 and HB1) in model prediction while pursuing a thorough investigation based on combined effect of other Global Climate Models (GCMs) or Regional Climate Models (RCMs) might result in different outcomes and hence is recommended.

6.3. Outlook

Next to land use and climate change analyses, many more applications of the hydrologic model developed in this study could be foreseen such as calculating cross-boundary water transfers as well as transfer of pollutant loads from upstream, and calculation of nitrogen load entering the Sea, etc. Furthermore, sediment and phosphorus modeling, which were left out from this study because of data availability limitations, are nevertheless of great importance in the Black Sea Basin and need careful modeling work.

There are a few parameters in SWAT that are not treated as spatially distributed, but are spatial and of great importance. These include concentration of nitrate in the atmospheric and crop related parameters. Treating these parameters as spatially distributed could further help model regionalization and allow more in-depth analysis.

Large-scale hydrological model set up at high spatial and temporal resolution still needs high performance computers and a lot of patience. Reading and writing hundreds of thousands of SWAT input files imposes an unnecessary overhead on computational time of a model run. Therefore, it is highly recommended that this very useful tool undergo some structural changes to achieve better performance.

The results of this project provides useful information on current and future status of water resources in BSB to support decision makers to meet the challenges posed by water scarcity and climate change across the region as well as regional policies. The developed methodology is fully transferable to other regions of the world. This work provides the basis for more sustainable water resources management by investigating strategies to determine the best management practices in agricultural and water resources management in particular. The resulting tools and data will allow local experts, stakeholders, and decision makers to better analyze river basin pressures and their impacts on human and ecosystem well-being.

References

Kalyanapu, A. J., Shankar, S., Pardyjak, E. R., Judi, D. R., Burian, S. J., 2011. Assessment of GPU computational enhancement to a 2D flood model. Environmental Modelling and Software, 26, 1009-1016.

Singh, B., Pardyjak, E. R., Norgren, A., Willemsen, P., 2011. Accelerating urban fast response Lagrangian dispersion simulation using inexpensive graphics processor parallelism. Environmental Modelling and Software, 26, 739-750.